Hydrodynamics of Viscous Oil-Water Flow through Undulated pipelines

Anand Babu Desamala

Hydrodynamics of viscous oil-water flow through undulated pipelines

THESIS

Submitted in Partial Fulfillment of the Requirements for the Degree of

Doctor of Philosophy
in
Engineering
by

Anand Babu Desamala

Under the supervision of

Dr. Tapas Kumar Mandal

and

Dr. Ashok Kumar Dasmahapatra

DEPARTMENT OF CHEMICAL ENGINEERING

INDIAN INSTITUTE OF TECHNOLOGY GUWAHATI

GUWAHATI-781039, INDIA

March, 2014

DEDICATED TO MY BROTHER

AND

MY PARENTS

INDIAN INSTITUTE OF TECHNOLOGY GUWAHATI
GUWAHATI - 781039, ASSAM, INDIA

DEPARTMENT OF CHEMICAL ENGINEERING

CERTIFICATE

This is to certify that the thesis entitled "***Hydrodynamics of viscous oil-water flow through undulated pipelines***" submitted by **Anand Babu Desamala** in fulfillment of the requirement of the *Degree of Doctor of Philosophy in Engineering*, is a record of bonafide research work carried out by him, in the Department of Chemical Engineering, Indian Institute of Technology, Guwahati, under our guidance and supervision. In our opinion, the thesis has reached the standard fulfilling the requirements of the Ph. D. degree as prescribed in the regulations of this institute.

(Dr. Tapas Kumar Mandal)
Associate Professor
Department of chemical Engineering
Indian institute of Technology Guwahati
Guwahati-781039, India
Email: tapasche@iitg.ernet.in

(Dr. Ashok Kumar Dasmahapatra)
Assistant Professor
Department of chemical Engineering
Indian institute of Technology Guwahati
Guwahati-781039, India
Email: akdm@iitg.ernet.in

Acknowledgement

Words fail to express my sincere gratitude to my thesis supervisors Dr. Tapas Kumar Mandal and Dr. Ashok Kumar Dasmahapatra for their encouragement, patience, insightful advice, guidance and sustained interest in successful completion of my dissertation. In addition, their philosophical guidance has built up a momentum inside me.

I wish to acknowledge my respectful thanks to Prof. Prabirkumar Saha, former-HOD, and Prof. Vijay S. Moholkar, present-HOD for extending all the necessary facilities for carrying-out my research work. I am also grateful to all the professors in the department for their sincere cooperation.

I am thankful to Mr. S. Guha and Mr. V. Choudary for their great help and sincere cooperation during fabrication of the experimental setup and its runs.

I would like to thank my co-researchers Mr. Vinayak Vijayan, Mrs. Anjali Dasari, Mr. Rambhupal Naidu, Mr. Bharat Kumar Goshika and Ravi Thej Pilla for their enormous help and encouragement during research work.

If I forget to mention the help render by my friends Sivaiah (Late), Leela, Rajasekhar, Praveen, Rajesh, Harsha, Anil, Chinna, Yadav, Murali, Swamy, Kamal, Ravi, Santhi, Rajeev, Ashish, I will be doing a great injustice.

I am always thankful to Mr. Srinivasarao Jallepalli, Mrs. Archana, and Mr. Suresh for their continuous support and encouragement during the course of my research work.

I am thankful to my dad and mom, who have not only supported me in the completion of my Ph.D. but also have stood by me throughout my life. They have patiently supported me at all instances in my research work. I am also thankful to all my family members for their encouragement and support.

I am indebted to my wife Sujana Priya Darshini, whose constant encouragement, patience in looking after the whole family problems and motivation, made me to achieve this endeavor in a peaceful and cheerful manner.

Last but not the least; I am grateful to my three year old Anusree (Cherry). Her constant smile in all odds is a source of inspiration for me.

Date:

Place: IIT Guwahati (Anand Babu Desamala)

Abstract

The flow of two immiscible liquids occurs commonly in petroleum industry, where crude oil and water produced from wells, are transported over long distances for subsequent separation and processing. In such cases, undulation of pipelines comprising of interconnected horizontal, upward and downward inclined sections are inevitable due to different elevation of the earth surface. Therefore, it is necessary to understand the different flow patterns and their transition boundaries for proper designing and sizing of a downstream separation and other unit of processing facilities. The majority of the past studies are confined to horizontal, inclined and vertical pipes of uniform cross-section. Not much is known about liquid–liquid flow across pipe network, although these are common occurrences in cross-country transportation. So an interest was felt to study the hydrodynamics of moderately viscous oil-water flow through a pipe network. Two networks have been selected in the present study: peak and valley configuration (Single unit of undulation is selected in both the cases). Due to the complexity of the undulated pipeline, first, experiments have been conducted in a simple horizontal pipeline to understand the hydrodynamics and the results are simulated using CFD. The objectives of the present work are as follows.

- ✓ CFD simulation and experimental validation of flow pattern transition during viscous oil-water flow through a horizontal pipeline.
- ✓ Study of hydrodynamics (flow pattern, pressure drop, and holdup) of viscous-oil water flow through undulated pipeline in peak configuration experimentally.

- ✓ CFD simulation of hydrodynamics of viscous oil-water flow through an undulated pipeline in peak configuration.
- ✓ Investigation of effect of valley on hydrodynamics during viscous oil-water flow through an undulated pipeline by experimental and CFD simulation.

In the present study, experiments have been conducted to study the hydrodynamics of liquid-liquid two-phase flow through an undulated pipe line (both in peak and valley configuration) by using lubricating oil and water as test fluids. All flow patterns except wispy annular flow are identified by visual and imaging technique while conductivity probe technique is used to detect the wispy annular configuration. Seven different flow patterns (viz., plug flow, slug flow, stratified wavy flow, stratified mixed flow, wispy annular flow, dispersion of oil in water flow and dispersion of water in oil flow) have been observed at all the four sections (Upstream, uphill, downhill and downstream). These flow patterns of all four sections are presented in the form of flow pattern maps and compared among them. Comparison across the sections shows that small undulation (5°) has a marginal effect on the flow behavior of viscous oil-water mixture.

Computational fluid dynamics study has also been conducted to predict different flow patterns of viscous oil-water two-phase flow through the undulated pipe. For this purpose, first simulation is carried out for a simple horizontal pipeline and validated with the experimental results. Then it is adopted for undulated pipeline. Based on the grid independent study 47037 (horizontal), 45682 (peak configuration), 50117 (valley

configuration) numbers of cells are selected as optimum number of cells for simulation. Using VOF (volume of fluid) method with k-ε turbulence model, intermittent flow (viz., plug, slug) along with other separated flow patterns (viz., stratified wavy, stratified mixed and wispy annular flow), and their transition boundaries are simulated successfully. Simulation results show a good agreement with experimental results in predicting of volume fraction, flow patterns and transition boundaries. Annular flow and its region is also simulated (not all the boundaries related to the wispy annular flow) with an appreciable accuracy. VOF also predicts the volume fraction, pressure and velocity profile of the separated flow. The present findings also reveal the ability of VOF to predict the hydrodynamics of viscous oil-water two-phase flow.

List of Contents

Nomenclature

A	Cross sectional area of the pipe, (m^2)
A_O	Area of oil phase, (m^2)
$A_{oil\ wave}$	Cross sectional area of the oil wave, (m^2)
A_W	Area of water phase, (m^2)
C_d	Drag coefficient (-)
D	Diameter of pipe, (m)
EO	Eotvos number (-)
f	Friction factor (-)
F_s	Surface tension force, (Kg/m s^2)
F_d	Drag force acting on a wave crest, (Kg/m s^2)
F_g	Gravity force acting on wave, (m/s^2)
Fr	Froude number (-)
g	Acceleration due to gravity, (m/s^2)
G	Mass flow rate, (kg/s)
k	Turbulent kinetic energy, (J/kg)
L	Length in deformed wave, (m)
L	Length of the pipe, (m)
m	Mass velocity, (kg m^2/s)
p	phases (-)
Q	Volumetric flow rate, (m^3/s)
Q_O	Volumetric flow rate of oil, (m^3/s)
Q_W	Volumetric flow rate of water, (m^3/s)

Re	Reynolds number (-)
Re_m	Mixture Reynolds number (-)
S	Slip ratio (-)
Si	Interface length, (m)
S_O	Wall perimeter of oil phase, (m)
S_W	Wetted perimeter of water phase, (m)
t	time, (s)
U	Superficial velocity, (m/s)
Um	Mixture velocity, (m/s)
U_O	In-situ oil velocity, (m/s)
U_{SO}	Superficial oil velocity, (m/s)
U_{SW}	Superficial water velocity, (m/s)
U_W	In-situ water velocity, (m/s)
We	Weber number (-)
X	Mass fraction (-)

Greek Letters

a	Wave amplitude, (m)
β	Inclination angle (^{o})
ΔP/L	Pressure gradient (Pa/m)
ε	Pipe roughness factor (-)
ε	Turbulent dissipation rate, (J/kg s)
θ	Angle between the surface tension force and the horizontal, (°)
κ	Curvature (1/m)

λ	Wavelength, (m)
μ	Viscosity, (Pa s)
μ_t	Turbulent viscosity, (Pa s)
ρ	Density, (Kg/m^3)
ρ_m	Mixture density (Kg/m^3)
μ_m	Mixture viscosity (Kg/m-s)
σ	Interfacial tension, (N/m)
τ_i	Interfacial shear stress, (Kg/ms^2)
τ_O	Oil phase shear stress, (Kg/ms^2)
τ_W	Water phase shear stress, (Kg/ms^2)

Subscripts

c	Continuous phase
d	Dispersed phase
g	Gas
l	Liquid
M	Mixture
O	Oil phase
SO	Superficial oil
SW	Superficial water
t	turbulence
tp	Two phase
W	Water phase

Abbreviations

A	Wispy Annular flow
B_O	Bubbly flow (oil)
B_W	Bubbly flow (water)
C	Churn flow
CFD	Computational fluid dynamics
$D_{O/W}$	Dispersion of oil in water
$D_{O/W\&W}$	Dispersion of oil in water and water
$D_{W/O}$	Dispersion of water in oil
LED	Light emitting diode
P	Plug flow
R	Rivulet flow
S	Slug flow
SM	Stratified mixed
SS	Smooth stratified
ST	Stratified flow
SW	Wavy stratified
TL	Three layer flow
VOF	Volume of fluid

List of Figures

List of Tables

Chapter 1

Introduction and Literature review

1.1 Introduction

Flows of two immiscible liquids are commonly encountered in chemical and petroleum industry. In oil exploration industries, a small amount of water is often injected into the transportation line to reduce frictional pressure drop during transportation of oil from oil fields to processing units. The presence of water in the pipeline along with oil makes the hydrodynamics more complex. The pipeline geometry may not contain just a straight pipe but also fittings such as, bends, valves, junctions and others which make the pipe geometry more and more complicated as shown in Fig. 1.1.

Fig. 1.1. Pipe network (Wang et al. 2008)

The transportation of more than one phases through such complex pipe networks and prediction of its hydrodynamics are major challenging task to a process engineer. Two fluids always try to minimize their total energy, and they distribute themselves at different interfacial configurations depending upon their superficial velocities, fluid properties, conduit geometry and orientation. Therefore, there is a need of in-depth

understanding of such flow characteristics to an engineer for optimizing the configuration of the pipeline and downstream processes to achieve the most economic and reliable design. A major part of all chemical engineering process and operations is concerned with liquid-liquid two-phase flows like solvent extraction, emulsification, oil exploration, cross-country transportation of crude oil and reaction between liquid-liquid two immiscible phases (for example bio diesel production). Two phase flow is more complicated than single phase flow. In addition to the usual inertia, viscous and pressure forces present in single-phase flow, two-phase flows are also affected by interfacial tension forces, the wetting characteristics of the liquid on the tube wall, exchange of momentum between the two phases during the flow. In two phase flow, the phases can distribute themselves into different interfacial configuration called flow patterns or flow regimes depending on the operational variables, physical properties of the fluids and geometrical variables of the system. Some commonly observed flow regimes in a complicated pipe network (peak configuration) are shown in Fig. 1.2. The following section elaborates the physic behind the hydrodynamics of multiphase flow.

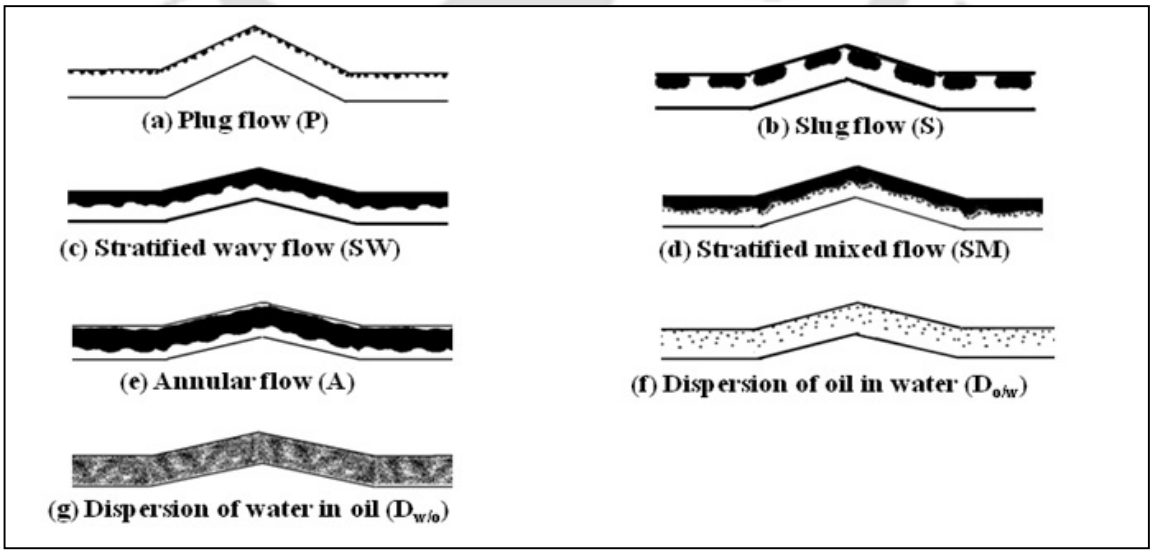

Fig. 1.2. Various multiphase flow regimes

1.2 Hydrodynamics

Hydrodynamics (study of liquids in motion) of multiphase flow is governed by physical properties of fluids, conduit geometry, conduit orientations and flow rates of both the phase. Physical properties of water and gas does not vary widely while oil properties can be quite diverse, and the oil-water viscosity ratio can vary from more than a million to less than one and its rheological behavior can be Newtonian or non Newtonian. Hence, hydrodynamic parameters like flow pattern, holdup, and pressure drop of a particular fluid pair cannot match with other set of fluids. Knowledge of the hydrodynamics of such two-phase flow (liquid-liquid) is essential for the design of extractor, mixture-settlers, transportation pipeline, downstream separators and emulsifier etc.

The presence of water in pipelines affects the transport of oil from the reservoir to the processing unit in the sense that when two immiscible liquids flow together in a pipe, the mixture behaves different from single-phase flow. Depending on the mixture velocity and the water cut several flow configurations, known as flow patterns, or flow regimes are formed. According to literature, oil-water flow patterns are broadly classified into three categories namely intermittent flow (Chakrabarti et al. 2005; Raj et al. 2005; Charles et al. 1961), separated flow (Yusuf et al. 2012; Trallero 1997; Nadler and Mewes, 1997) and dispersed flow (Rodriguez et al. 2006; Zhao et al. 2006; Lum et al. 2004). Intermittent flows consist of relatively large oil bubbles separated by water slugs (viz., plug flow and slug flow). Separated flows comprise core-annular flow (oil in the core, water in the annulus) and stratified flow patterns (viz., stratified smooth, wavy and mixed flow).

Dispersed flow includes oil bubbles in water, water drops in oil, and also water-in-oil and oil-in-water emulsions. The physics behind the flow patterns occurring during two-phase flow in pipeline is described briefly:

In two-phase flow (gas-liquid/liquid-liquid) phenomena, there are several forces acting on the fluid mixture, each of which has some impact on the overall flow configuration. These forces include those due to inertia, buoyancy, gravity, drag, viscous and interfacial forces (viz., interfacial tension and drag). The flow pattern is determined by a delicate balance of all these forces.

At low phase velocities (of both the fluids), inertia force is less as compared to surface force. So the ratio of inertial to surface force know as Weber number (*We*), is small in magnitude and expressed by following equation,

$$We = \frac{\rho U^2 D}{\sigma} = \frac{inertial\ force}{surface\ force} \tag{1.1}$$

The dominated surface force obliges (forces/coerces) the oil phase to make a lenticular shape. These lenticulating oil masses try to float up due to its buoyancy and flow axially in the conduit. This interfacial configuration is known as plug flow. The size of lenticulated oil mass (oil plugs) goes on increasing with oil superficial velocities. After a certain velocity level, the lenticular bodies are transformed into big oil droplets or oil Taylor bubbles and this flow pattern is known as slug flow. Most interesting is that the surface force gradually dominates over the gravitational force with decreasing pipe

diameters because Eotvos number ($Eo = \frac{\Delta \rho g D^2}{\sigma}$) decreases with decreasing in pipe diameter. Hence, lower pipe diameter always favors the slug flow (Beretta et al. 1997; Mandal et al. 2007). This plug and slug flow show a periodicity depending upon velocity magnitude of the fluid pair and the hydrodynamics is transient in nature. This flow pattern brings trouble in operation and designing of transportation line and other equipments (as pump; Brown 1965, Maron et al. 1991) because it always gives a pulse (of pressure, mass, etc.) on a system. So fully analytical analysis to predict the hydrodynamics (prediction flow pattern, pressure drop and holdup) of such flow is very difficult and no such work is reported in the literature till date (as per best of author's knowledge). All the reported work on hydrodynamics of intermittent flow is semi-empirical type (Andreussi and Bendiksen 1989; Wallis, 1969). Most popular theory applied for this flow is the drift-flux model developed based on relative motion of the individual phases (Wallis, 1969, Hasan and Kabir, 1992; Shi et al. 2005) to predict void fraction, which is used in calculation of mixture properties like density, viscosity etc. This void fraction value gives a better prediction of two-phase pressure drop.

The length of water bridge between two successive oil slugs decreases with further increasing of oil flow rate, and finally it disappears and forms a continuous oil layer. Then, there are two continuous fluid layers in the conduit. One is made of oil and another is of water. A continuous stream of oil flows over the continuous water layer in horizontal or inclined pipeline due to the difference in density. This flow pattern is known as stratified flow (as in Fig. 1.3) and shape of the interface is determined by balancing the drag and surface force. This type of flow is analyzed by the well know two-

fluid model in which two momentum equations are written separately for each phase and combined them as follows.

Water phase: $$-A_w\left(\frac{dP}{dz}\right) + \tau_w S_w - \tau_i S_i + \rho_w A_w g sin\beta = 0 \quad (1.2)$$

Oil phase:

$$-A_o\left(\frac{dP}{dz}\right) + \tau_o S_o + \tau_i S_i + \rho_o A_o g sin\beta = 0 \quad (1.3)$$

Where 'A_O' and 'A_W' are the oil and water cross-section areas; 'τ_i', 'τ_w' and 'τ_o' are the interfacial, water and oil wall shear stresses, 'S_i', 'S_w' and 'S_o' are the interfacial, water and oil wetted perimeters, 'β' is pipe inclination, 'ρ_o' and 'ρ_w' are densities of oil and water respectively. The main difficulty in this approach is in the calculation of interfacial shear (τ_i) and interfacial length (S_i) from interfacial morphology. Various methods (Bannwart, 2001; Brauner, 1990; Chakrabarti et al. 2005; Yipping et al. 2008; Poesio et al. 2009) may be combined together with the two-fluid model to account for the above parameters. Correlation based approaches are also widely used in literature (Rodriguez and Baldani, 2012; Sun and Mishima, 2009) largely based on gas-liquid flow. To account for the pressure jump across the interface due to interfacial tension, Laplace–Young equation (Eq. 1.4) is also incorporated as a source term in above equations. (Rodriguez and Bannwart, 2008; Rodriguez and Castro, 2014). It is shown in Eq. (1.4)

$$\frac{dP}{dz} = \sigma\left[\frac{1}{R_1} + \frac{1}{R_2}\right] \quad (1.4)$$

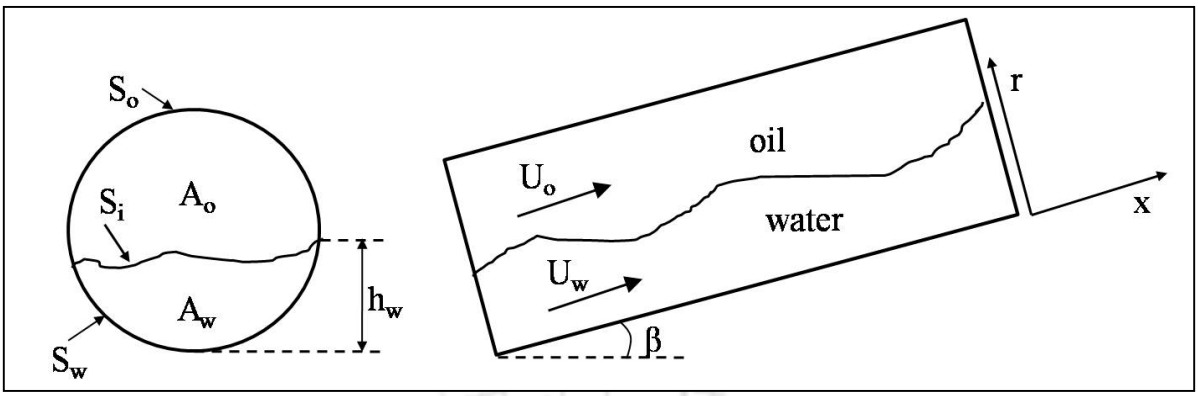

Fig. 1.3. Schematic description of stratified flow configuration (Rodriguez and Castro, 2014) ('U' is the average axial velocity; 'A_O' and 'A_W' are the oil and water cross-section areas; 'hw' is water phase height, β is the pipe inclination, 'S_i', 'S_w' and 'S_o' are the interfacial, water and oil wetted perimeters).

By introducing the interfacial tension during this flow configuration, the interface can be smooth/wavy/mixed based on magnitude of drag (F_d), gravity and surface (F_σ) forces at the interfaces. The flow remains stratified smooth till gravity and surface forces are dominating over the others. Interfacial shear and interface starts to oscillate with increasing the phase velocities (either of the phases or both the phases) and flow becomes stratified wavy (Brauner and Maron, 1992a, 1992b). Interfacial shear and drag forces are always trying to destabilize the wave at interface and their magnitudes gradually increase due to continuous increasing of phase velocities (Govindarajan and Sahu, 2014). Velocity difference under the range of stratified wavy flow is not enough to overcome the stabilizing effect of gravity and surface tension (Al-Wahaibi and Angeli, 2007). At a certain velocity, drag force (F_d) acting on wave crest (either oil or water) becomes greater than surface force (F_σ) acting on interface as shown in Fig. 1.4. Then ($F_d \geq F\sigma$) the wave

crest is converted into oil droplets at oil-water interface. Now there are three distinct layers, - 1) a continuous water layer at bottom, 2) a continuous oil layer at top and 3) a mixed layer of oil droplets in continuous water in between continuous layer of oil and water- it is termed as SM (Al-Wahaibi and Angeli, 2007, 2009; Brauner and Maron, 1992; Al-Wahaibi et al. 2007).

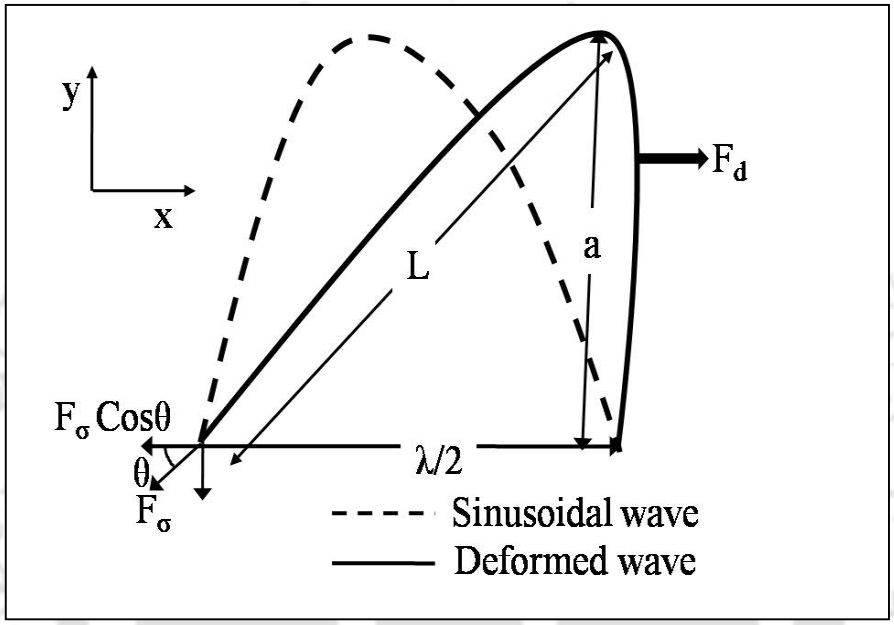

Fig. 1.4. Force balance on a deformed wave at the oil–water interface (Al-Wahaibi et al. 2007) (where 'F_σ' and 'F_d' are surface and drag forces; 'a' is wave amplitude; 'λ' is wave length and 'L' is the length of the deformed wave)

On the other hand, resultant force of interfacial tension (F_σ) and drag forces (F_d) counterbalances the buoyancy force (F_b) at moderate velocities as drag force is sufficiently high. At this condition "$F_d + F_\sigma \geq F_b$" (Al-Wahaibi and Angeli, 2007) oil flows along the center of the pipe as a continuous core and water occupies inner pipe wall and

flows through an annulus between oil core and pipe wall as shown in Fig. 1.5. The configuration is known as annular flow or core annular flow (CAF).

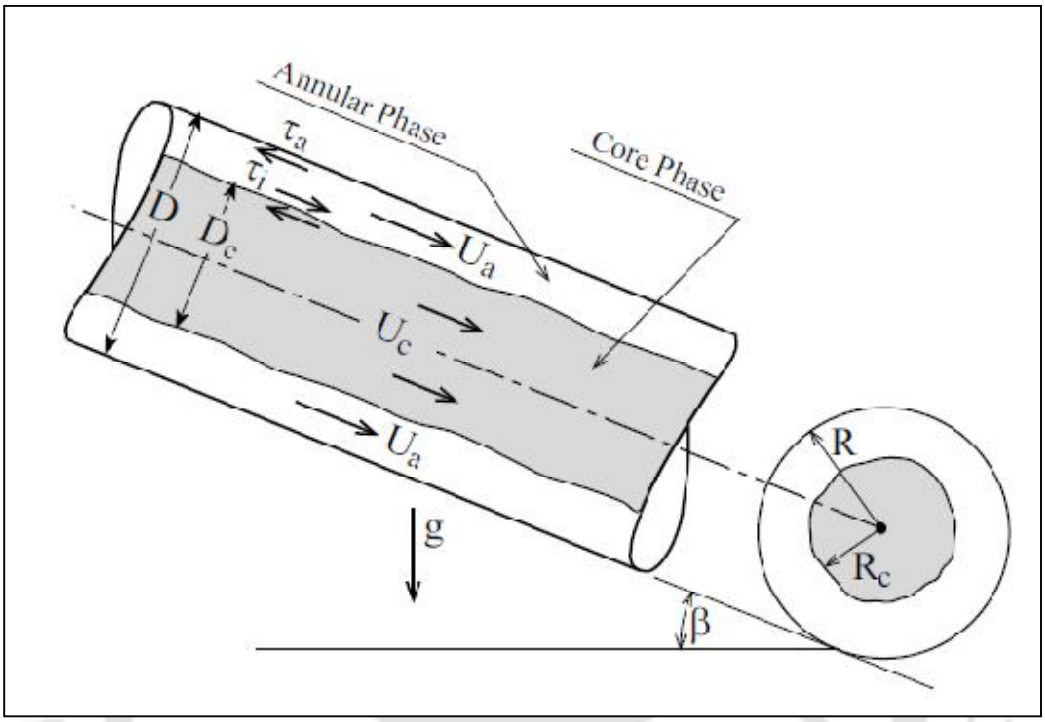

Fig. 1.5. Schematic description of core-annular configuration (Brauner, 1991) (where 'U_a', 'U_c' are velocities of annular and core phases; 'Rc' is the core radius; 'D' is the diameter; 'τ_a', and 'τ_i' are wall and interfacial shear stresses respectively)

Since the oil does not come in contact with the wall, the wall shear is comparable to the shear encountered during the flow of water only through the pipe. This reduces the pumping power and its cost drastically. This concept (reduction of pumping cost) can be implemented in transportation of viscous oil via pipe network. Although this technique appears to be very attractive for heavy oil transportation, there are several problems like limited range of fluid velocities and water fraction (Hasson et al. 1970; Parda and Bannwart, 2001; Bensakhria et al. 2004), fouling on the pipe wall by oil (Arney et al.

1996; Santos et al. 2004; Silva et al. 2006), stability of annular flow in horizontal and inclined pipes, etc (Bannwart, 1998; Rodriguez and Bannwart, 2008; Chen et al. 1990; Grassi et al. 2008; Strazza et al. 2011; Redapangu et al. 2012a, 2012b and 2013). The hydrodynamics of such flow (holdup, pressure drop, stability, etc) can be predicted with the help of extended two-fluid model (Brauner, 1991; Rodriguez and Bannwart, 2006, 2008).

Dispersed flow can broadly be classified into two categories, - 1) oil dispersed in water ($D_{O/W}$) and 2) water dispersed in oil ($D_{W/O}$). $D_{O/W}$ and $D_{W/O}$ start at higher velocity of water and oil respectively. In $D_{O/W}$ flow, inertial force of water (turbulence in the water) phase is high enough to disperse the oil phase as small droplets in water and it reverses during $D_{W/O}$. At the onset of dispersion (either one), maximum drop size (d_{max}) should be less than the critical diameter (d_{crit}) of droplet (d_{max} < dcrit; Brauner, 2001). This flow favors mixing, heat transfer, mass transfer, etc. Homogenous flow theory is applied to predict the hydrodynamics of such flow within acceptable range of errors (Wallis, 1969; Brauner and Maron, 1992a).

A unique phenomenon popularly known as phase inversion occurs at certain conditions. The phase inversion mechanism is probably influenced by several parameters such as operating conditions, fluids physical properties, geometry of the pipe (diameter, inclination angle, mixing unit) and pipe material (Elseth, 2001). According to Angeli (1997), the phase inversion of two immiscible liquids can be defined as the transition of one phase from being dispersed to being continuous. It results a dispersed phase into a

continuous phase and vice versa. Due to this, pressure drop is changed drastically because total pressure drop is highly influenced by viscosity of the continuous phase (Piela et al. 2009; Xu et al. 2010).

In the next section, a brief literature review about pipe network has been carried out to extract lacuna of the past researcher work. Flow through pipe network represents a complex situation. So prior to this, some selective literature on horizontal, inclined and vertical flow has also been discussed in this section. Following section describes about experimental work on horizontal, inclined, vertical and undulated flow followed by analytical developments on it and then a comprehensive review of computational fluid dynamics (CFD) work.

1.3 Literature review

Various experimental works have been performed in literature to enhance the understanding of liquid-liquid flow since 1950. Clark et al. (1949) in their pioneering work have developed a method of transportation of viscous oil by injecting small amount of water to reduce pressure drop during flow. Russell et al. (1959) proposed a classification of the observed flow patterns in horizontal pipeline after conducting a series of experiments systematically on oil-water flow. In 1960s and 1970s, most of the researchers mainly focused on improving pumping requirements during viscous oil transportation by introducing water in the pipeline (Charles et al. 1961; Hasson et al. 1970). Charles et al. (1961) have conducted experiments of equal density oil-water mixtures in a 1 inch pipe with oils of three different viscosities and investigated different flow patterns which are quite similar to the flow patterns reported by Russell et al.

(1959). Hasson et al. (1970) performed a systematic study of liquid–liquid annular flow by using distilled water and kerosene-perchlor-ethylene solution as the test liquids. They used an annular nozzle to inject the liquids into the pipeline and measured the film thickness at the wall by analyzing the trajectory of the core fluid in a horizontal pipe.

In recent years, hydrodynamics (in particular on flow patterns and transition characteristics) of oil-water two-phase flow have received considerable attention by various researchers (Lum et al. 2006; Rodriguez and Oliemans, 2006; Nalder and Mewes, 1997; Angeli and Hewitt, 2000; Trallero et al. 1997 ; Oddie et al. 2003; Fujii et al. 1994; Angeli and Hewitt, 1998). Researchers identified several flow patterns of oil-water two-phase flow through horizontal (Charles et al., 1961; Fujii et al., 1994; Trallero, 1997; Nadler and Mewes, 1997; Mandal et al., 2007; Cai et al., 2012), vertical (Jana et al., 2006; Du et al., 2012; Zhao et al., 2013) and inclined (Zavareh et al., 1988; Oddie et al., 2003; Rodriguez et al., 2006; Grassi et al., 2008; Zong et al., 2010; Strazza et al., 2011) pipes. A comprehensive review on oil-water flow patterns in horizontal pipe can be found in Trallero et al. (1997). Horizontal flow is mostly dominated by stratified and dispersed flow (Trallero, 1997; Nadler and Mewes, 1997; Cai et al., 2012) whereas annular and dispersed flow are the major flow patterns in vertical pipes (Jana et al., 2006; Ghosh et al., 2010; Du et al., 2012). Fujii et al. (1994) studied oil-water flow in acrylic pipe with diameter 2.5 cm with viscosity ratio of 61.5 and density ratio 0.98. They have observed the flow patterns such as bubble flow, large elongated bubbly flow, slug flow and annular flow. These flow patterns are quite similar to the flow patterns observed by Charles et al. (1961). Lum et al. (2006) have investigated the effect of upward ($+5^o$, $+10^o$) and

downward (-5^o) pipe inclinations on flow patterns, holdup and pressure gradient during oil-water flows at mixture velocity, 0.7 to 2.5 m/s. It has been observed that the frictional pressure gradient in both upward and downward flow is lower than that of horizontal flow. The frictional pressure drop becomes minimum for all inclinations at high mixture velocities, where transition from dispersed water-in-oil to dual continuous flow takes place. Rodriguez et al. (2006) have reported experimental results on oil–water flow in different pipe inclinations (-5^o, -2^o, -1.5^o, 0^o, 1^o, 2^o and 5^o), and observed a stable wavy flow in downward inclined pipe and higher water recirculation in upward inclined pipes. They have also observed that stratified smooth flow disappears and replaced by stratified wavy flow. Inclination in the pipe line along the flow introduces instability at the interface (Zong et al., 2010; Grassi et al., 2008; Lum et al., 2004) between two phases. Therefore, stratified wavy, stratified mixed and dispersed flows are the dominating flow in an inclined pipeline (Rodriguez et al., 2006). Due to the buoyancy, annular flow is most stable in vertical pipe and least stable in horizontal pipe (Yusuf et al. 2012; Ghosh et al. 2009).

Inclination also strongly influences the slip velocity and it (slip velocity) increases with higher inclination, either downward or upward (Rodriguez et al., 2006, Abduvayt et al., 2006). Flow patterns are strongly influenced by the pipe diameter, entry geometry and fluid properties (Beretta et al. 1997). It has been observed that a smaller pipe diameter promotes slug and annular flow (Mandal et al., 2007). High viscous fluids compared to low viscous one, favor annular flow (Grassi et al., 2008 and Strazza et al., 2011). The stability of a particular flow pattern depends on the balance between various forces. For

example, Ooms et al. (2007) have shown that the balance between the hydrodynamic force and buoyancy force on the core establishes an eccentric core annular flow in a horizontal pipe. Core annular flow among the all is more significant because of low pressure drop and hence, minimum pumping power is needed for transportation of oil. This core-annular configuration is attained when viscous oil phase is surrounded by water annulus (Bensakhira et al. 2004; Ooms et al. 2007; Grassi et al. 2008; Sotgia et al. 2008; Balakhrisna et al. 2010; Poesio et al. 2012).

Hydrodynamics of multiphase flow through complicated geometry like undulated pipelines, hilly terrain pipelines are poorly understood. Most studies have focused on gas-liquid (air-water) two-phase flow through these complex pipe networks (Zheng et al., 1994, 1995; Henau et al., 1995; Al-Safran et al., 2005; Mandal et al., 2008). Zheng et al. (1994) have presented a model for slug tracking and simulating slug behavior in elbows). Their results showed that slugs can be generated at low elbows, dissipate at top elbows, and shrink or grow in length as they travel along the pipe. Al-Safran et al. (2005) experimentally investigated slug initiation mechanism at valley (lower dip) and they observed five flow categories of slug flow patterns in valley configuration of a hilly-terrain pipeline. They observed that the slug flow is enhanced due to such geometry. They also investigated the effect of valley on slug length distribution at uphill and downhill sections. Mandal et al. (2008) have estimated slug characteristics, dissipation, slug velocity and slug length in different sections of undulated pipeline from conductivity probe signals applying cross-correlation technique.

Beside the gas-liquid flow, a limited number of studies have focused to understand the phenomena of liquid-liquid flow through undulated pipeline (Abduvayt et al., 2006; Mandal 2007). Abduvayt et al. (2006) have described the experimental result of flow pattern, pressure drop, water holdup and slip of the phases in hilly terrain pipeline (in peak configuration) for oil-water (oil viscosity = 1.88 ± 0.19 mPa s) flow. They have reported that the stratified smooth flow was totally absent at $+3^{o}$ uphill and -3^{o} downhill sections of the hilly terrain pipeline and slip increased with increasing the pipe inclination. Mandal (2007) have estimated the flow patterns of oil-water flow (oil viscosity = 1.2 mPa s) through an undulated pipeline at peak and valley configuration using optical probe. A marginal influence of undulation on transition boundaries of stratified wavy to three-layer flow and three layer to disperse flow at different section have been reported.

Experimental observations are complemented with the help of analytical models (Brauner and Maron, 1992; Rodriguez and Bannwart, 2006, 2008; Brauner et al., 1998) and computer simulations (Kaushik et al., 2012; Al-Yaari et al., 2011; Ekambara et al., 2008). Analytical models are applicable to a set of selective flow patterns rather than a complete picture. For example, Brauner and Maron (1992) have proposed models based on the stability analysis of flow patterns, to predict the transition boundaries from stratified flow pattern to annular and intermittent. Later on Brauner et al. (1998) have modified their models with the help of two fluid model, to predict the shape of an interface for a stratified wavy flow as a function of system parameters like velocities, fluid properties, etc. In stratified flow, flow dynamics is influenced by entrainment of one phase into

another, which has not been incorporated in the above model. Al-wahaibi and Angeli (2009) have successfully predicted the entrainment fraction of a horizontal stratified flow in a circular pipeline by balancing "rate of drop entrainment" and "rate of drop deposition" methods, which have been derived from two-fluid model.

CFD simulations are also being done to intricately understand the hydrodynamics in multiphase flow with both gas-liquid (Parvareh et al. 2010; Ekambara et al. 2010; Frank, 2005 and Huang et al. 1994) and liquid-liquid (Kaushik et al. 2012; Al-Yaari et al. 2011 and Ghosh et al. 2010) systems. Parvareh et al. (2010) have investigated two-phase (gas-liquid) flow regimes in vertical and horizontal tubes, using VOF to account for the interfacial phenomena between two phases. They have successfully predicted plug flow, slug flow, stratified wavy flow and annular flow using CFD and validated with experimental results. Ekambara et al. (2010) have simulated bubbly two-phase flow in horizontal pipes using two different models - k–ε with constant bubble size and k–ε with population balance model. The model predictions show that the population balance gives a better agreement with the experimental data than the constant bubble size model. Their results indicate that the volume fraction has a maximum near the upper pipe wall, and the profiles tend to flatten with increasing liquid flow rate. They have also found that increasing the gas flow rate at fixed liquid flow rate increases the local volume fraction; and the axial liquid mean velocity showed a relatively uniform distribution except near the upper pipe wall. Huang et al. (1994) have used K- ε turbulence model to study the effect of eccentricity on friction factor and holdup for both laminar and turbulent flows. They have noticed that, the friction factor increases with eccentricity. Ko et al. (2002)

have found that, shear stress transport model is better than the K-ω turbulence model, to solve the kinetic energy and dissipation equations of turbulent wavy core flow. Ghosh et al. (2011) have simulated the core annular down flow using Eulerian–Eulerian based VOF technique in FLUENT. They have validated the simulated flow patterns with experimental results and noticed a good agreement. They have also noted the constant change in oil volume fraction for higher L/D ratio (L/D > 22), and the core characteristics also changes to thin wavy core as water velocity increases. Al-Yaari and Abu-sharkh (2011) have performed 3D simulation to investigate the stratified wavy and mixed flow patterns using RNG K- ε multiphase model. They have predicted stratified wavy flow and validated with experimental results. VOF has also successfully applied to investigate core-annular flow through a pipeline with a sudden expansion and contraction (Kaushik et al. 2012) and the simulated results are well matched with the experimentally observed flow behavior. In addition to these, there are few studies those determine the velocity, void fraction and pressure drop profiles of two phase flow in pipes (Ghorai et al., 2006; Sidi-Ali et al., 2010). Ghorai et al. (2006) have performed extensive numerical simulations to predict the flow field characteristics like gas velocity, volume fraction of liquid. They have also developed a correlation between interfacial friction factor and wall friction factor for stratified wavy flow. Sidi-Ali et al. (2010) have performed 3D simulations to investigate interfacial friction factor of horizontal stratified two phase flow using Fluent. They have noticed good agreement with experimental results.

From the literature it is evident that there are large numbers of publications to understand the flow mechanism of liquid-liquid two-phase flow in straight pipes (i.e. horizontal,

inclined and vertical pipes). In these days, the interest goes beyond it to include interconnected pipe networks like hilly terrain, undulated pipeline, road crossing, divergence network, etc. In this case, the flow may take place through one or several interconnected horizontal, inclined and vertical pipes. This type of pipe network commonly appears in transportation of heavy/light oils from oil fields to processing units.

1.4. Aims and objectives

Based on the above discussion, the primary aim of the dissertation work is directed towards a detail study of hydrodynamics of viscous oil-water flow through pipe network. Two networks have been selected in the present study for the sake of simplicity: peak and valley configuration as shown in Fig. 1.6a and 1.6b respectively. Single unit of undulation is selected in both the cases. Here undulation comprises of an interconnected uphill and a downhill sections between two horizontal portions (Fig. 1.6). **Detailed dimensions of the undulated pipeline are shown in Fig. 2.1, Chapter 2.**

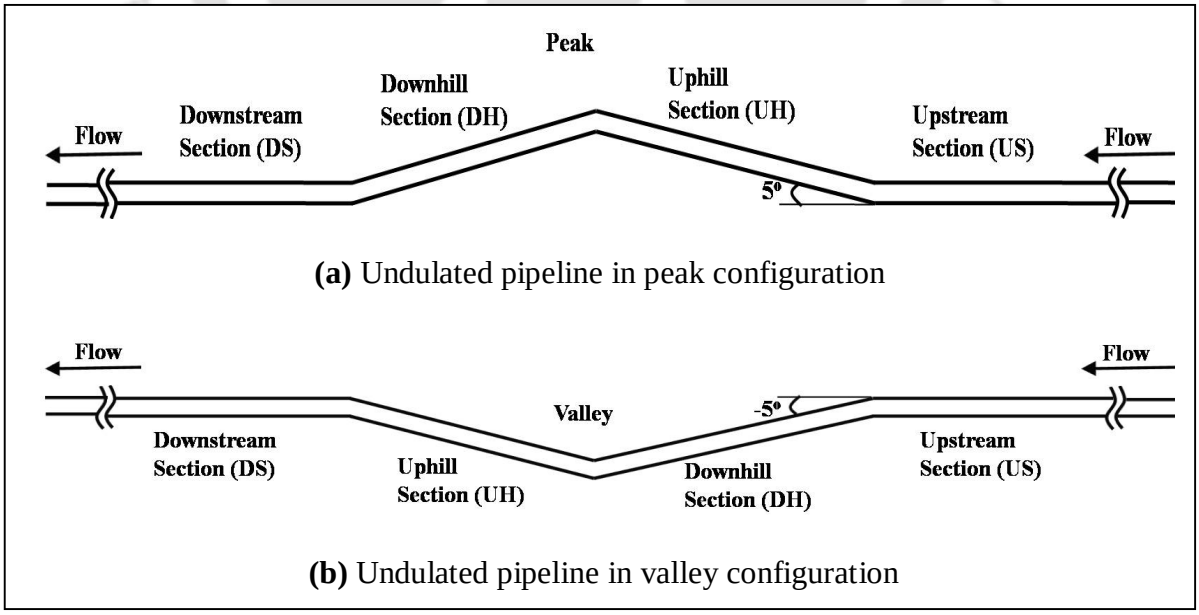

(a) Undulated pipeline in peak configuration

(b) Undulated pipeline in valley configuration

Fig. 1.6. Different configuration of undulated pipeline

It seems that hydrodynamics in such complex system will be more complicated than that in a straight horizontal pipe. So, hydrodynamics of the same fluid pair in horizontal pipeline has been studied prior to the investigation of viscous oil-water flow through the undulated pipes. In the present study, hydrodynamics (flow patterns, pressure drop and holdup) of viscous oil-water flow through horizontal and undulated pipes has experimentally been studied first, then simulation is done for the same. In experiments, flow patterns have been identified by visual, photographic and probe techniques. The flow patterns observed in all the cases (horizontal, undulation pipe in peak and valley configuration) have been represented in the graphical form called flow pattern map. The flow pattern maps observed at different sections (upstream, uphill, downhill and downstream) is compared for both the configurations to get the effect of undulation on flow patterns. Further flow pattern maps have been compared with the available literature data to know the effect of viscosity on flow patterns.

Hydrodynamics of the same as experiments (flow patterns, oil volume fraction, total pressure and velocity profiles) has been predicted using 2D simulation in Fluent 6.3 software. For this, Volume of the Fluid (VOF) method with k-ε turbulence model is adopted to predict the flow patterns and their transitions. Further this model is used to understand the profiles of volume fraction, pressure and velocity for separated (viz., stratified wavy, stratified mixed and annular) flow. This information is extremely helpful in understanding the hydrodynamics of two–phase flow and industrial design such as, pipe network for oil transportation.

1.5. Structure of the thesis

The dissertation has been organized as follows. Chapter 1 deals with introduction, a brief literature review, importance and scope of the present work. Then objectives of the present work are mentioned in the present chapter1.

Chapter 2 depicts the details of the experimental setup and experimental procedure used in the present study. The different identification and measurement techniques used have also been discussed in this chapter 2. Further, CFD methodology followed in the present work has been discussed in this chapter.

The results in the present study have been discussed in chapter 3 to 6. Chapter 3 presents the investigation of different flow patterns of oil-water flow in horizontal pipeline especially wispy annular flow using conductance probe. Next, transitional boundaries of flow patterns are predicted using CFD simulation. Simulated results have been validated with experimental results.

Chapter 4 describes the hydrodynamics of moderately viscous oil-water flow through undulated pipe in peak configuration with an angle of 5°, which is relevant to oil refineries.

Chapter 5 presents detail analysis on oil-water two-phase flow by applying VOF in an undulated pipeline in peak configuration. The simulation results have been compared

with experiments to find out the acceptability for flow patterns. Further, model is used to understand the wispy annular flow characteristics in peak configuration.

Chapter 6 describes the investigation of flow patterns during viscous oil-water flow through undulated pipe in valley configuration with an angle of -5°. Subsequently, flow patterns are simulated using VOF model and efforts have been put-up to understand the profiles of volume fraction, pressure and velocity of separated flow.

Chapter 7 presents the salient conclusions drawn from the present study as well as the recommendations for future work.

References

Abduvayt, P.,Manabe, R., Watanabe, T.,Arihara, N., 2006.Analysis of oil/water-flow tests in horizontal, hilly terrain, and vertical pipes. SPE Prod. Oper., SPE 90096, 123–133.

Al-Safran, E., Sarica, C., Zhang, H. -Q., Brill, J., 2005.Investigation of slug flow characteristics in the valley of a hilly-terrain pipeline, Int. J. Multiphase Flow 31, 337–357.

Al-Wahaibi, T., Smith, M., Angeli, P., 2007. Transition between stratified and non-stratified horizontal oil–water flows. Part II: Mechanism of drop formation, Chem. Eng. Sci. 62, 2929-2940.

Al-Wahaibi, T., Angeli, P., 2007. Transition between stratified and non-stratified horizontal oil–water flows. Part I: Stability analysis. Chem. Eng. Sci. 62, 2915-2928.

Al-wahibi, T., Angeli P., 2009. Predictive model of the entrained fraction in horizontal oil-water flows. Chem. Eng. Sci. 64, 2817-2825.

Al-Yaari, M. A., Abu-Sharkh, B. F., 2011. CFD prediction of stratified oil-water flow in a horizontal pipe. Asian Trans. Eng. 01, 68–75.

Andreussi, P., Bendiksen, K., 1989. An investigation of void fraction in liquid slugs for horizontal and inclined gas-liquid pipe flow. Int. J. Multiphase Flow 15, 937–946.

Angeli, P. and Hewitt, G. F., 2000. Flow structure in horizontal oil-water flow. Int. J. Multiphase Flow 26, 1117 – 1140.

Angeli, P. and Hewitt, G.F., 1998. Pressure gradient in horizontal liquid-liquid flows. Int. J. Multiphase Flow 24, 1183 – 1203.

Angeli, P., 1997. Liquid-liquid dispersed flows in horizontal pipes, Ph.D. thesis. Imperial College, University of London.

Arney, M. S., Ribeiro, G. S., Bai, R., Joseph, D.D., 1996. Cement lined pipes for water lubricated transport of heavy oil. Int. J. Multiphase Flow 22, 207–21.

Balakhrisna, T.,Ghosh, S., Das, G., Das, P. K., 2010. Oil–water flows through sudden contraction and expansion in a horizontal pipe-phase distribution and pressure drop. Int. J. Multiphase flow 36, 13–24.

Bannwart, A.C., 1998. Wave speed and volumetric fraction in core annular flow. Int. J. Multiphase Flow 24, 961–974.

Bannwart, A.C., 2001. Modeling aspects of oil-water core-annular flows. J. Pet. Sci. Eng. 32, 127-143.

Bensakhria, A., Peysson, Y., Antonini, G., 2004. Experimental study of the pipeline lubrication for heavy oil transport. Oil Gas Sci. Technol. -Rev. IFP 59, 523–533.

Beretta, A., Ferrari, P., Galbiati, L., Andreini, P. A., 1997. Horizontal oil-water flow in small diameter tubes. Flow patterns. Int. Comm. Heat Mass Transfer 24, 223−229.

Brauner, N. and MoalemMaron, D., 1992a. Flow pattern transitions in two-phase liquid-liquid flow in horizontal tubes. Int. J. Multiphase Flow 18, 123 – 140.

Brauner, N., Moalem Maron, D., 1992b. Analysis of stratified/non-stratified transitional boundaries in inclined gas-liquid flows. Int. J. Multiphase Flow 18, 541–557.

Brauner, N., 1990. On the relation between two-phase flow under reduced gravity and earth experiment. Int. Comm. Heat Mass Transfer 17, 271-282.

Brauner, N., 1991. Two-phase liquid-liquid annular flow. Int. J. Multiphase Flow 17, 59–76.

Brauner, N., 2001. The prediction of dispersed flows boundaries in liquid-liquid and gas-liquid systems. Int. J. Multiphase Flow 27, 885 – 910.

Brauner, N., Maron, D. M., Rovinsky, J., 1998. A two fluid model for stratified flows with curved interfaces. Int. J. Multiphase Flow 24, 975-1004.

Brown, R. A. S., 1965. The mechanics of large gas bubbles in tubes. I. Bubble velocities in stagnant liquids. The Can. J.Chem. Eng. 43, 217-223.

Cai, J., Li, C., Tang, X., Ayello, F., Richter, S., Nesic, S., 2012.Experimental study of water wetting in oil–water two phase flow—Horizontal flow of model oil. Chem. Eng. Sci. 73, 334−344.

Chakrabarti, D. P., Das, G., Ray, S., 2005. Pressure drop in liquid-liquid two phase horizontal flow: Experiment and prediction. Chem. Eng. Technol. 28, 1003-1009.

Charles, M. E., Govier, G. W., Hodgson, G. W., 1961. The horizontal flow of equal density oil-water mixtures. Can. J. Chem. Eng. 39, 27–36.

Chen, K. P., Bai, R., Joseph, D. D., 1990. Lubricated pipelining. Part 3. Stability of core-annular flow in vertical pipes. J. Fluid Mech. 214, 251–86.

Clark, A. F. and Shapiro, A., 1949. Method of pumping petroleum. U. S. patent No. 2, 533, 878 (1949).

Du, M., Jin, N., Gao, Z., Wang, Z., Zhai, L., 2012. Flow pattern and water holdup measurements of vertical upward oil–water two-phase flow in small diameter pipes. Int. J. Multiphase flow 41, 91–105.

Ekambara, K., Sanders, R. S., Nandakumar, K. and Masliyah, J. H., 2008. CFD simulation of bubbly two-phase flow in horizontal pipes. Chem. Eng. J. 144, 277 – 288.

Elseth, G., 2001. An experimental study of oil–water flow in horizontal pipes. Ph.D. thesis. The Norwegian University of Science and Technology, Porsgrunn.

Frank, T., 2005. Numerical simulation of slug flow regime for an air-water two-phase flow in horizontal pipes. NURETH – 11, Oct 2-6, Popes' Palace conference center, France.

Fujii, T., Otha J., Nakazawa, T., Morimoto, O., 1994.Thebehavior of an immiscible equal–density liquid–liquid two–phase flow in a horizontal tube. JSME Int. J. Series B 37(1), 22–29.

Ghorai, S. and Nigam, K. D. P., 2006. CFD modeling of flow profiles and interfacial phenomena in two-phase flow in pipes. Chem. Eng. Process. 45, 55 – 65.

Ghosh, S., Das, G. and Das, P. K., 2011. Simulation of core annular in return bends – comprehensive CFD study. Chem. Eng. Res. Des. 89, 2244 – 2253.

Ghosh, S., Das, G., Das, P. K., 2010. Simulation of core annular downflow through CFD–A comprehensive study.Chem. Eng. Process. 49, 1222–1228.

Ghosh, S., Mandal. T. K., Das, G., Das, P. K., 2009. Review of oil water core annular flow. Renew. Sust. Energ. Rev. 13, 1957-1965.

Govindarajan, R., Sahu, K. C., 2014. Instabilities in viscosity-stratified flow. Annu. Rev. Fluid Mech. 46, 331-353.

Grassi, B.,Strazza, D.,Poesio, P., 2008.Experimental validation of theoretical models in two-phase high-viscosity ratio liquid-liquid flows in horizontal and slightly inclined pipes. Int. J. Multiphase Flow 34, 950–965.

Hasan, A. R., Kabir, C. S., 1992. Two-phase flow in vertical and inclined annuli. Int. J. Multiphase Flow 18, 279–293.

Hasson, D., Mann, U., Nir, A., 1970. Annular flow of two immiscible liquids: I mechanisms, Can. J. Chem. Eng. 48, 514–520.

Henau, V., Raithby, G., 1995. A study of terrain induced slugging in two-phase flow pipelines. Int. J. Multiphase Flow 21, 365–379.

Huang, A., Christodoulou, C. and Joseph, D. D., 1994. Friction factor and hold up studies for lubricated pipelining part -2: Laminar and k-ε models of eccentric core flow. Int. J. Multiphase flow 20, 481 – 491.

Issa, R. I. 1986. Solution of the implicitly discretized fluid flow equations by operator splitting. J. Comput. Phys. 62, 40 – 65.

Jana, A. K., Das, G., Das, P. K., 2006. Flow regime identification of two-phase liquid–liquid up flow through vertical pipe. Chem. Eng. Sci. 61, 1500–1515.

Kaushik, V. V. R., Ghosh, S., Das. G., Das, P. K., 2012. CFD simulation of core annular flow through sudden contraction and expansion. J. Pet. Sci. Eng. 86-87, 153–164.

Ko, T., Choi, H. G.,Bai, R., Joseph, D. D., 2002. Finite element method simulation of turbulent wavy core-annular flows using a k-ω turbulence model method. Int. J. Multiphase Flow 28, 1205–1222.

Lum, J. Y. –L., Al-Wahaibi, T. and Angeli, P., 2006. Upward and downward inclination oil-water flows. Int. J. Multiphase Flow 32, 413 – 435.

Lum, J. Y. L., Lovick, J. Angeli, P., 2004. Low inclination oil–water flows. Can. J. Chem. Eng. 82, 303–315.

Mandal, T. K., 2007. Some studies on Liquid–liquid slug flow. Ph.D. Thesis, IIT Kharagpur, India.

Mandal, T. K., Bhuyan, M. K., Das, G., Das, P. K., 2008. Effect of undulation on gas-liquid two-phase flow through a horizontal pipeline. Chem. Eng. Res. Des. 86, 269–278.

Mandal, T. K., Chakrabarti, D. P., Das, G., 2007. Oil Water flow through different diameter pipes: similarities and differences. Chem. Eng. Res. Des. 85, 1123–1128.

Moalem Maron, D., Yacoub, N., Brauner, N., Naot, D., 1991. Hydrodynamic mechanisms in the horizontal slug pattern. Int. J. Multiphase Flow 17, 227–245.

Nadler, M. Mewes, D., 1997. Flow induced emulsification in the flow of two immiscible liquids in horizontal pipes. Int. J. Multiphase Flow 23, 55−68.

Oddie, G., Shi, H., Durlofsky, L. J., Aziz, K., Pfeffer, B., Holmes, J. A., 2003. Experimental study of two and three phase flows in large diameter inclined pipes. Int. J. Multiphase Flow 29, 527–558.

Ooms, G., Vuik, C. and Poesio, P., 2007. Core-annular flow through a horizontal pipe: Hydrodynamic counterbalancing of buoyancy force on core. Phys. Fluids 19, 1 – 17.

Parda, V. J. W., Bannwart, A. C., 2001. Modeling of vertical core-annular flows and application to heavy oil production. J. Energy Resour. Technol. ASME 123, 194–199.

Parvareh, A., Rahimi, M., Alizadehdakhel, A. and Alsairafi, A. A., 2010. CFD and ERT investigations on two-phase flow regimes in vertical and horizontal tubes. Int. Commun. Heat Mass 37, 304 – 311.

Patankar, S. V., 1980. Numerical heat transfer and fluid flow. Hemisphere, Washington, D.C.

Piela, K., Delfos, R., Ooms, G., Westerweel, J., Oliemans, R. V. A., 2008. Phase inversion in the mixing zone between a water flow and an oil flow through a pipe. Int. J. Multiphase Flow 35(1), 91-95.

Poesio, P., Strazza, D. and Sotgia, G., 2012. Two and three-phase mixtures of highly-viscous-oil/water/air in a 50 mm i.d. pipe. Appl. Therm. Eng. 49, 41 – 47.

Poesio, P., Strazza, D., Sotgia, G., 2009. Very-viscous-oil/water/air flow through horizontal pipes: Pressure drop measurement and prediction. Chem. Eng. Sci. 64, 1136-1142.

Raj, T. S., Chakrabarti, D. P., Das, G., 2005. Liquid-liquid stratified flow through horizontal conduits. Chem. Eng. Technol. 28, 899−907.

Redapangu, P. R., Sahu, K. C., Vanka, S. P., 2012a. Study of pressure-driven displacement flow of two immiscible liquids using a multiphase lattice Boltzmann approach. Phys. Fluids 24, 102110.

Redapangu, P. R., Sahu, K. C., Vanka, S. P., 2013. A Lattice Boltzmann Simulation of Three-Dimensional Displacement Flow of Two Immiscible Liquids in a Square Duct. J. Fluids Eng. 135(12), 121202.

Redapangu, P. R., Vanka, S. P., Sahu, K. C., 2012b. Multiphase Lattice Boltzmann Simulations of Buoyancy-Induced Flow of Two Immiscible Fluids With Different Viscosities. Eur. J. Mech. B/Fluids 34, 105–114.

Rodriguez, O. M. H. and Oliemans, R. V. A., 2006. Experimental study on oil-water flow in horizontal and slightly inclined pipes. Int. J. Multiphase Flow 32, 323 – 343.

Rodriguez, O. M. H., and Baldani, L. S., 2012. Prediction of pressure gradient and holdup in wavy stratified liquid–liquid inclined pipe flow. J. Petroleum Sci. Eng., 96-97, 140–151.

Rodriguez, O. M. H., Bannwart, A. C., 2006. Analytical model for interfacial waves in vertical core flow. J. Pet. Sci. Eng. 54, 173–182.

Rodriguez, O. M. H., Bannwart, A. C., 2008. Stability analysis of core-annular flow and neutral stability Wave number. AIChE J. 54 (1), 20−31.

Rodriguez, O. M. H., Castro, M. S., 2014. Interfacial-tension-force model for the wavy-stratified liquid–liquid flow pattern transition. Int. J. Multiphase Flow 58, 114–126.

Russell, T. W. F. and Charles, M. E., 1959. The effect of less viscous liquid in the laminar flow of two immiscible liquids. Can. J. Chem. Eng. 37, 18 – 24.

Russell, T. W. F., Hodgson, G. W., Govier, G. W., 1959. Horizontal pipeline flow of mixtures of oil and water. Can. J. Chem. Eng. 37, 9–17.

Santos, R. G., Rahoma, S. M., Bannwart, A. C., Loh, W., 2006. Contact angle measurements and wetting behavior of inner surfaces of pipelines exposed to heavy crude oil and water. J. Pet. Sci. Eng. 51, 9–16.

Shi, H., Holmes, J. A., Durlofsky, L. J., Aziz, K., Diaz, L. R., Alkaya, B., Oddie, G., 2005. Drift-Flux modeling of multiphase flow in wellbores. SPE J. 84228-PA, 10, 24–33.

Sidi-Ali, K. and Gatignol, R., 2010. Interfacial friction factor determination using CFD simulations in a horizontal stratified two-phase flow. Chem. Eng. Sci. 65, 5160 – 5169.

Silva, R. C. R., Mohamed, R. S., Bannwart, A. C., 2006. Wettability alteration of internal surfaces of pipelines for use in the transportation of heavy oil via core-flow. J. Pet. Sci. Eng. 51, 17-25.

Sotgia, G., Tartarini, P. and Stalio, E., 2008. Experimental analysis of flow regimes and pressure drop reduction in oil-water mixtures. Int. J. Multiphase Flow 34, 1161 – 1174.

Strazza, D., Grassi, B., Demori, M., and Poesio, P., 2011. Core-annular flow in horizontal and slightly inclined pipes: Existence, pressure drops, and hold-up. Chem. Eng. Sci. 66, 2853-2863.

Sun, L., and Mishima, K., 2009. Evaluation Analysis of Prediction Methods for Two-Phase Flow Pressure Drop in Mini-Channels. Int. J. Multiphase Flow, 35, 47–54.

Trallero, J. L., Sarica, C., Brill, J. P., 1997. A study of oil/water flow patterns in pipes. SPE Prod. Fac., SPE 36609, 165−172.

Wallis, G. B., 1969. One dimensional two-phase flow, Mc-Graw-Hill, New York.

WANG, L. Y., WU, Y. X., ZHENG, Z. C., GUO, J., ZHANG, J., TANG, C., 2008. Oil-water two-phase flow inside T-junction. J. Hydrodyn. Ser. B *20*(2), 147-153.

Xu, J.-y., Li, D.-h., Guo, J., Wu, Y.-x., 2010. Investigations of phase inversion and frictional pressure gradients in upward and downward oil–water flow in vertical pipes. Int. J. Multiphase Flow 36, 930–939.

Yipping, L., Hua, Z., Shuhua, W., and Jing, W., 2008. Prediction of pressure gradient and holdup in small Eötvös number liquid-liquid segregated flow. Chin. J. Chem. Eng. 16, 184-191.

Yusuf, N., Al-Wahaibi, Y., Al-Wahaibi, T., Al-Ajmi, A., Olawale, S., Mohammed, I. A., 2012. Effect of oil viscosity on the flow structure and pressure gradient in horizontal oil-water flow. Chem. Eng. Res. Des. 90, 1019–1030.

Zavareh, F., Hil, A.D., Podio, A.L., 1988. Flow Regimes in Vertical and Inclined Oil/Water Flow in Pipes.SPE 18215.

Zhao, Y., Bi, Q., Hu, R., 2013.Recognition and measurement in the flow pattern and void fraction of gas-liquid two-phase flow in vertical upward pipes using the gamma densitometer. Appl. Therm. Eng. 60, 398–410.

Zheng, G., Brill, J.,Shoham, O., 1995. An experimental study of two-phase slug flow in hilly-terrain pipelines, SPE J. Prod.Fac.

Zheng, G., Brill, J.,Taitel, Y., 1994. Slug flow behavior in a hilly-terrain pipeline, Int. J. Multiphas. Flow 20, 63–79.

Zong, Y.-B., Jin, N.-D., Wang, Z.-Y.,Gao, Z.-K., Wang, C., 2010. Nonlinear dynamic analysis of large diameter inclined oil-water two phase flow pattern. Int. J. Multiphase Flow 36, 166–183.

Chapter 2

Experimentation and CFD methodology

2.1 Introduction

The experiments have been reported were performed in both horizontal and undulated pipeline in peak configuration (5° magnitude) and valley configuration (-5° magnitude). A schematic representation of experimental setup is shown in Fig. 2.1. It consists of a fluid handling system (storage tanks, pumps, rotameters) and three test sections (horizontal, peak configuration, valley configuration) as shown in Fig. 2.1. Test section is made up of Perspex for visualization and photographic studies. Test fluids are lube oil (SAE 40 grade) and water. The properties of the test fluids are shown in Table 2.1.

Table 2.1 Physical properties of test fluids measured at 25°C and atmospheric pressure.

Fluid	**Density (Kg/m^3)**	**Viscosity (mPa s)**
Water	1000	1
Lubricating oil	889	107
Interfacial tension	24×10^{-3}N/m	

2.2 Fluid handling systems

It consists of a PVC water tank of capacity 0.5 m^3. Water is circulated through centrifugal pump (CP) of 5 hp into the entire test section. Flow rate of water is adjusted with the help of bypass valve G2 and by the control valves C1 and C2. Oil circulation takes place through gear pump (GP) into the test section from the oil storage tank. The flow rate of oil can be controlled by the simultaneous adjustment of bypass valve (G1).

2.3 Flow rate measuring devices

For measuring the water flow rate, a couple of rotameters (RM1 & RM2) is used. The rotameters for water ranges from 0 to 1.67×10^{-4} m^3/s (0 to 10 LPM) for RM1 and '0' to '9.166×10^{-4}' m^3/s (0 to 55 LPM) for RM2. Two different ranges of rotameters are installed to measure water flow rate over a wider range.

2.4 Oil flow measurement

Oil flow rate (7.4×10^{-6} - 6.1×10^{-4} m^3/s.) is measured by volumetric method where volumetric flow rate of oil which is obtained by subtracting volumetric flow rate of water (obtained from pre calibrated rotameter) from total volumetric flow rate of oil-water mixture. Mixture volumetric flow rate (total volumetric flow rate) is measured from total liquid height of the mixture present in the calibrated decanter at the exit and time required to reach a particular liquid level.

2.5 Test section

It consists of 0.025 m internal diameter Perspex transparent pipe with 7.5 m length. It consists of an entry section (EN), test section (TS) and an exit section (EX). Two fluids enter into the test region with two different pipes. A sufficient length between entry section and test section is provided to get the fully developed flow. Three different pipe orientations are fabricated for this study. The detailed description of three pipelines is shown below.

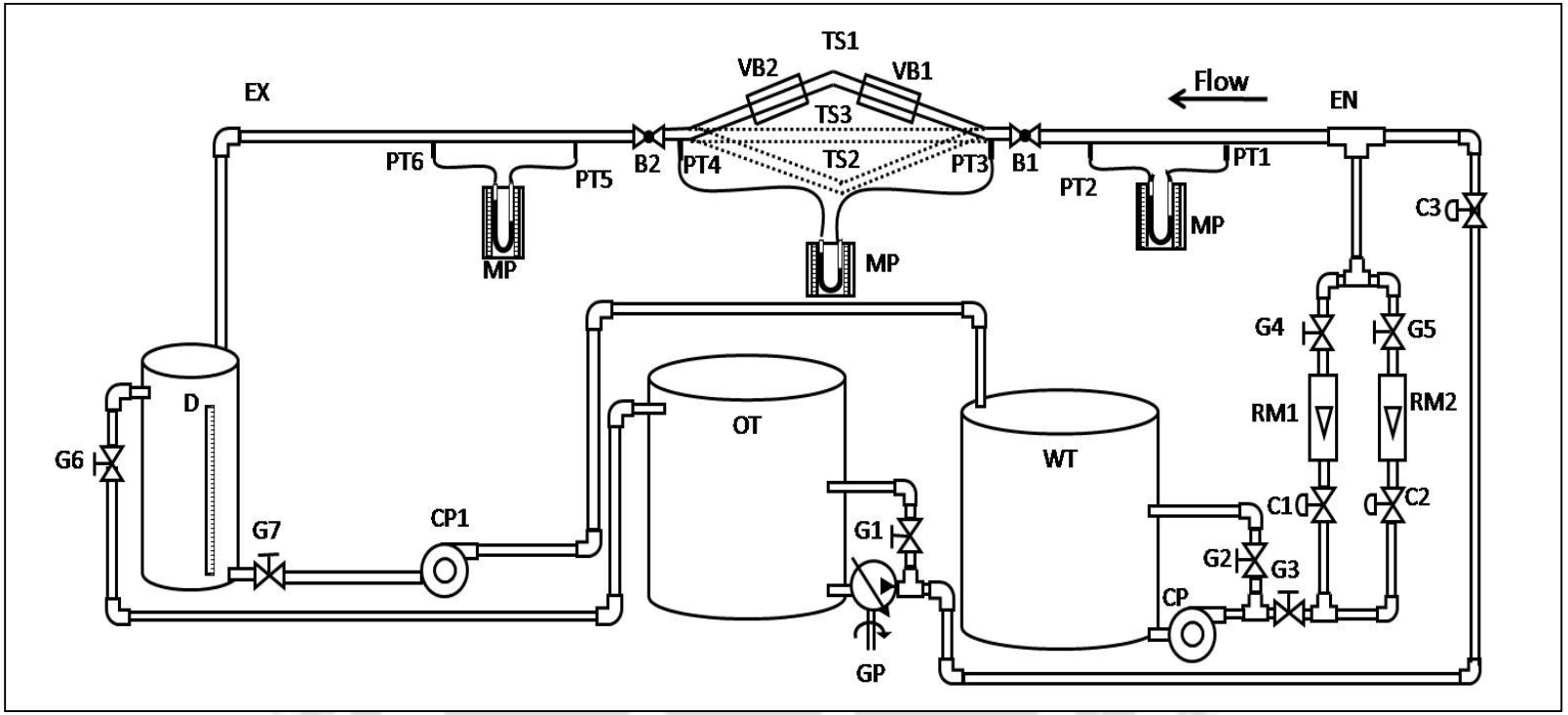

Fig. 2.1. Schematic representation of experimental setup.

CP Centrifugal Pump **D** Decanter **G1 to G7** Gate valves **EX** Exit section

C1 to C3 Control valves **B1 to B2** Ball valves **RM1, RM2** Rotameter **EN** Entry section

GP Gear pump **WT** Water tank **VB1 to VB2** View boxes **OT** Oil tank

PT1 to PT6 Pressure taps **MP** Manometer Panel **TS1** Peak section **TS3** Horizontal section

TS2 Valley section

2.5.1 Peak test section

The test section comprises of an uphill and a downhill section between two horizontal portions in order in the direction of flow. The horizontal sections referred to as upstream and downstream sections according to the direction of fluid flow. The junction of the upstream and uphill region is termed as the uphill elbow and that between the downhill and downstream section is the downhill elbow. The angle of inclination is the same for uphill and downhill which is 5^{o} in magnitude with respect to horizontal. View boxes (VB1 & VB2) are used to minimize the lens effect on pipe during the photography. The view box having length of 0.24m, 0.11m height and width of 0.11m is placed in the upstream, uphill, downhill and downstream sections.

2.5.2 Valley test section

The test section (TS2 shown in dotted line; Fig. 2.1) comprises of a downhill and an uphill section between two horizontal portions in order in the direction of flow. The horizontal sections referred to as upstream and downstream sections according to the direction of fluid flow. The junction of the upstream and downhill regions is termed as the downhill elbow and that between the uphill and downstream sections is the uphill elbow. The angle of inclination is same for uphill and downhill which is -5^{o} in magnitude with respect to horizontal.

2.5.3 Horizontal test section

Test section (TS3 shown in dotted line; Fig. 2.1) is made up with 0.025 m internal diameter Perspex pipe of 1 m length. In between EN and TS2, an L/D ratio of 120 is provided for obtaining fully developed flow and same ratio is maintained from test to exit section to minimize the end effect of the fluids.

2.6 Experimental procedure

The experiments have been carried out in a wide range of superficial velocities for both fluids to cover the entire flow pattern range. Water and lube oil is pumped into the test section with the help of pumps CP & GP respectively. The flow rate of water is measured through rotameters RM1 & RM2. During the experiment water has been pumped first and keeping water flow rate constant oil is pumped into the setup. The fluid mixture is falling into the decanters (D1 and D2) after crossing the exit section where the separation process takes place due to density difference of the fluids. Separated oil and water were recycled into the respective storage tanks. In steady state, a snap shot has been taken using a digital camera (DSC-HX100V, Sony) at the test section to identify the flow pattern. This experiment has been repeated thrice to check the reproducibility of the experimental results. After completion of a set of experiment, the water velocity is changed to the next higher value and the readings are repeated as earlier.

The different ranges of the flow rate are given below.

a) **Horizontal test section**

Water and oil superficial velocity ranges from 0.1 m/s to 1.1 m/s and from 0.015 m/s to 1.25 m/s respectively.

b) **Peak configuration section**

Water and oil superficial velocity ranges from 0.1 m/s to 1.2 m/s and from 0.015 m/s to 1.3 m/s respectively.

c) **Valley configuration section**

Water and oil superficial velocity ranges from 0.1 m/s to 1.12 m/s and from 0.013 m/s to 1.12 m/s respectively.

2.7 Estimation of flow pattern

Desired flow rates of oil and water were adjusted and allowed for steady state for few minutes. When visual observation indicated steady state, flow pattern was noted and photo graphs were taken using a digital camera (DSC-HX100V, Sony) for every flow pattern. These observed flow patterns are represented in flow pattern map.

2.8 Conductance probe technique

The most common way to identify the interfacial configuration is visual/video observations and probe (intrusive and non-intrusive) techniques (Al-wahaibi and Angeli, 2011). In the present work, a conductance probe (intrusive) is used to identify the annular flow (A) (other flow patterns have been identified by photographic technique). During

annular flow, oil flows at the center of the tube as continuous core and water in contact with the pipe wall. A very thin layer of water flows as annulus in annular flow, which is difficult to identify visually, and by photography. Therefore, in the present work, a conductance probe has been used to identify the annular flow. The schematic representation of this probe (Fig. 2.2a) and cross sectional view of flow configuration (Fig. 2.2b) is shown in Fig. 2.2. It consists of two different circuits: circuit - I and circuit –II (Fig. 2.2a). Each circuit is composed of two wires (1 and 2 in circuit -I; 3 and 4 in circuit -II) which acts as electrodes connected to an electrical circuit. The wires used for the probe are 0.35 mm thick. Electrodes 1 and 2 of circuit -I are placed diametrically opposite position on the pipe cross section and 3 and 4 of circuit -II are placed 30 mm apart along the length on top of pipe wall. The electrical circuit consists of LED, Resistor and 9V battery. In each circuit, one wire is connected directly to the cathode of the battery and other wire is connected to the short lead of the LED. Other lead of the LED is connected to one end of the Resistor (250 Ohms) and other end is connected to anode of the battery (Fig. 3). The circuit will be completed through 1 - 2 in circuit – I and 3 - 4 in circuit – II, if water present in between. This circuit is tested by running water and oil separately. LED in this circuit glows when only water is running in the pipe because water is a good conductor of electricity. When only oil is flowing, LED does not glow because oil is a very poor conductor of electricity. Glowing of LED's in both circuits confirms the existence of water layer in annulus position and it confirms the existence of annular flow.

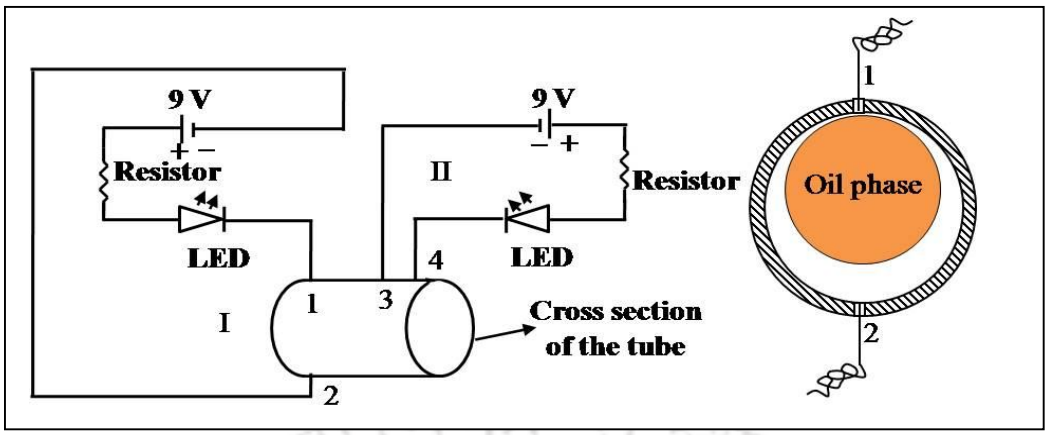

(a) **(b)**

Fig. 2.2. Arrangement of conductance probe and phase configuration; (**a)** Conductance probe; (**b)** Cross sectional view

2.9 Estimation of holdup

Measurement of holdup at different flow rates is by quick closing valve (QCV) technique in horizontal, peak and valley configuration sections. The quick closing valves B1 to B6 (B1 to B2 for peak section, B3 to B4 for horizontal section and B5 to B6 for valley section) in the setup are placed at the two ends of the respective test sections. There is a mechanical adjustment for simultaneous closing of the two valves to trap the flowing mixture instantaneously. Once the system reaches steady state at particular flow rate of two fluids, the flowing mixture is arrested by closing these two valves in the test section instantaneously. The oil-water mixture is collected completely in a measuring flask. The collected mixture is allowed to settle for some time and the volumes of two liquids are measured. These experiments are repeated only at few points. The points are at two ends and middle of the entire range of oil velocity for a particular flow pattern. Based on this a 0.4% average absolute error has been obtained.

By knowing the volume of liquids holdup is calculated from the following formula

$$H_0 = \frac{v_o}{v_w + v_o} \quad (2.1)$$

Where v_w is volume of water (i.e. heavier phase)

v_o is volume of oil (i.e. lighter phase)

2.10 Estimation of pressure drop

Pressure drop is measured in horizontal and different sections of pipe network. An L/D ratio of 30 is maintained between the two pressure taps in respective test section. The taps which are used for the holdup studies are used to find the pressure drop in the pipes. The tubes are always filled with water before the experiment and maintain that no air or oil present in the pressure line. A U-tube manometer is used to determine the pressure difference between the two fluids, which is filled with carbon tetra chloride solution. At different flow patterns, pressure drop is measured in wide range of phase velocities.

2.11 Contact angle measurement

The contact angle between lube oil and solid Perspex wall has been measured in water environment because it is needed in simulation. Phase arrangement in contact angle measurement is shown in Fig. 2.3. The contact angle is measured experimentally and the value of the contact angle is incorporated in the simulation. The pipe material used in the

present study is made up of Perspex. So Perspex surface is used for contact angle measurement. Prior to measurement the perspex surface is equilibrated with water. Then an oil droplet is carefully placed on to the surface, which is already immersed in the water medium (Santos et al. 2006). An image of the oil droplet in this arrangement is taken with aid of digital camera [DSC-HX100V, Sony]. These images are analyzed using the software Adobe Acrobat 9.0. After analyzing the image the contact angle is found to be $8.5^{o}\pm2^{o}$. The average value (8.5^{o}) of this contact angle is used in the present simulation.

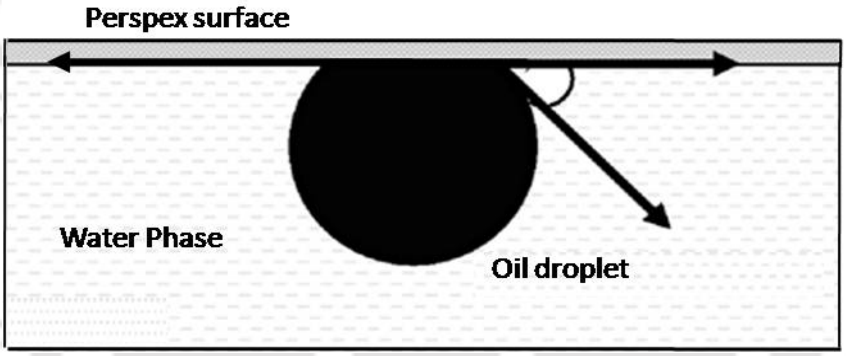

Fig. 2.3. Illustration of the phase arrangement for the contact angle measurement

2.12 Computational Fluid Dynamics (CFD) Methodology

In general, CFD is a means to accurately predict phenomena in applications such as fluid flow, heat transfer, mass transfer, and chemical reactions. CFD is computer-based and requires users to follow a general protocol in order to obtain simulation results. The first step is to define geometry, followed by creating a series of finite volumes that, altogether, make up the whole of the desired geometry. This pattern of finite volumes (or

"elements") is referred to as a "mesh" and is typically formed using triangular / quadrilateral elements for 2-D applications and hexahedral / tetrahedral / pyramidal / prismatic elements for 3-D applications. The purpose of the mesh is to allow for the discretization of the Navier - Stokes partial differential equations so that the computer is capable of the computations required. After creating a mesh, boundary conditions and transport properties must be specified as well as any appropriate turbulence models before the user can initialize a solution. CFD is a popular tool for solving transport problems because of its ability to give results for problems where no correlations or experimental data exist and also to produce results not possible in a laboratory situation. CFD is also useful for design since it can be directly translated to a physical setup and is cost-effective.

The other important issue to address when using CFD to model multiphase flow is how to choose a multiphase model that will be used to compute solutions. An appropriate selection must be made for the multiphase model to ensure that the program is able to utilize the correct continuity equations and also apply them to the fluids in a way that most accurately mimics real - life fluid flow. There are several types of multiphase models and each exhibit a different level of complexity (Andersson et al. 2012). The multiphase model types, in order of increasing complexity and with brief descriptions, are as follows:

1) Lagrangian Model: Continuity equations are solved for the primary phase as the whole entity while individual particles from the secondary phase are tracked throughout the flow and are assumed not to interact with one another.

2) Mixture Model: Primary and secondary phases are treated as one composite mixture and one momentum equation is solved for the combined phases.

3) Eulerian-Eulerian Model: Primary and secondary phases are treated individually as being continuous and separate momentum equations are solved for each phase.

4) Volume of Fluid (VOF) Model: An Eulerian-Eulerian variation in which the secondary phase is not dispersed within the primary phase but rather there is an interface between the phases and so the interface must be tracked while also solving a momentum equation for each phase.

5) Discrete Element Method: The most complex multiphase model in which momentum equations are applied to individual particles of the secondary phase as well as to the primary phase as a whole.

Each multiphase flow model has applications for which it is best adapted depending on the typical flow regime present in a particular multiphase flow system. The most commonly used multiphase models are the Mixture model and the Eulerian-Eulerian/VOF models. For separated flows only the VOF model will work (Andersson et al. 2012) as it predicts the location of interface and uses single phase models to predict the flow in each phase.

There are variety of CFD programs available that possess these capabilities for modeling multiphase flow. Some common programs include ANSYS and COMSOL, which are both multiphysics modeling software packages, and FLUENT, which is a fluid-flow-specific software package. ANSYS FLUENT version 6.3.26 has been chosen in the present work for 2D simulation of pipe flow.

The computation has been performed by assuming unsteady flow, immiscible liquid pair, constant liquid properties, co-axial flow in the pipe and a T-junction ('T') as the entry section. In the present model, the two fluids share a well defined interface. Volume of Fluid (VOF) approach for two phase modeling has been selected in Fluent. VOF solves a single set of momentum equations which is shared by both the fluids. Governing equations and the treatment of the interface are discussed in the next section. Details can be obtained from Fluent user's guide (2006).

2.13 Volume of Fluid (VOF) Approach

In the VOF model, both phases share the same control volume and a single set of conservation equations is shared by the both the phases using mixture properties. In addition, if the control volume is occupied by one of the phases, its related properties are utilized. VOF method is beneficially utilized because it is able to simulate the profile deformation of the continuous interface and dispersed phase particles (i.e. droplets, bubbles). Therefore, it is appropriate to use as an application that focuses on simple flow pattern problems as seen in pipelines (slug, stratified wavy, stratified mixed and annular flow).

2.13.1. Governing Equations

In VOF approach, the continuity equation can, therefore be written as:

$$\frac{\partial(\rho)}{\partial t} + \nabla \cdot (\rho U) = \sum_q S_q \tag{2.2}$$

Where, ρ, *U*, *t*, *S* are density, velocity, time and mass source respectively. In the present case '*S*' is zero.

The equation of momentum conservation can be expressed as follows:

$$\frac{\partial(\rho\vec{U})}{\partial t} + \nabla.\left(\rho\vec{U}\,\vec{U}\right) = -\nabla P + \nabla.\left[\mu\left(\nabla\vec{U} + \nabla\vec{U}^{T}\right)\right] + \rho\vec{g} + \vec{F} \tag{2.3}$$

$$\frac{\partial(\rho U)}{\partial t} + \nabla \cdot (\rho U \cdot U) = -\nabla P + \nabla \cdot [\mu(\nabla U + \nabla U^{T})] + (\rho g) + F$$

The left hand side corresponds to convection and the first term on the right hand side corresponds to pressure, while the other terms represent diffusion, gravitational body force (acting downwards) and external body force (in the present case, *F* is considered as surface force) respectively.

Generally, the Volume of Fluid solves the problem by updating the phase volume fraction field, provided the fixed grid, the phase volume fraction, and the velocity field are available in a given time step. If the volume fraction of q^{th} fluid in a cell is denoted as 'α_q', the following three possibilities would arise:

- α_q = 0: the cell does not contain fluid *q*.
- α_q= 1: the cell is occupied solely by fluid *q*.
- 0<α_q< 1: the cell contains the interface

Depending on the local value of α_q, the density and viscosity in each cell are given by:

$$\rho = \sum_{1}^{p} \rho_q \alpha_q \tag{2.4}$$

$$\mu = \sum_{1}^{p} \alpha_q \mu_q \tag{2.5}$$

A separate continuity equation for 'α_q' is considered as follows:

$$\frac{\partial \alpha_q}{\partial t} + \nabla.(\alpha_q \vec{U}_q) = S_{\alpha_q} \tag{2.6}$$

U_q *and* $S_{\alpha q}$ are velocity and source term of volume fraction of q^{th} component respectively. **Here source term '$S_{\alpha q}$' is zero.**

For each of the cells the following relationship is also valid:

$$\sum_{1}^{p} \alpha_q = 1 \tag{2.7}$$

Where "*p*" is the number of phases. For the present two phase flow, $p = 2$.

The surface tension can be written in terms of the pressure drop across the surface. The force at the surface can be expressed as a volume force using the divergence theorem. This volume force is the source term added to the momentum balance (equation 2.3) and has the following form:

$$F = \sum_{ij} \sigma_{ij} \frac{\sigma_i \rho_i \kappa_j \nabla \sigma_j + \sigma_j \rho_j \kappa_i \nabla \sigma_i}{(1/2)(\rho_i + \rho_j)} \tag{2.8}$$

Where κ is the curvature.

$\kappa_1 = -\kappa_2$ and $\nabla \sigma_1 = -\nabla \sigma_2$ (2.9)

This implies eq. (2.8) as

$$F = \sigma_{12} \frac{\rho \kappa_1 \nabla \sigma_1}{(1/2)(\rho_1 + \rho_2)} \tag{2.10}$$

Where ρ is the volume averaged density computed using Eq. (2.4). The above equation shows that the surface tension source term for a cell is proportional to the average density in the cell.

2.13.2 Turbulence model

In the present study of oil–water flow through horizontal and pipe network, the flow of oil is always in laminar (Re = 3.2 to 153) owing to its very high viscosity (107 mPa s) while the flow of water is in turbulent (Re = 2510 to 17555) region. However, mixture Reynolds number is in laminar region (Re_m = 90 to 1115). Mixture Reynolds number (Re_m) is calculated by the following formula:

$$Re_m = \frac{DU_m\rho_m}{\mu_m}$$

Where, D = Diameter of the pipe (m)

U_m = Mixture velocity (m/s) = $U_{SW} + U_{SO}$

U_{SW} = Water superficial velocity (m/s)

U_{SO} = Oil superficial velocity (m/s)

ρ_m = Mixture density (Kg/m^3) = $\rho_W H_W + \rho_O H_O$

ρ_W = Density of water (Kg/m^3)

ρ_o = Density of oil (Kg/m^3)

H_W = Water holdup

H_O = Oil holdup

μ_m = Mixture Viscosity (Kg/m-s) = $\mu_W X_W + \mu_O X_O$

X_W = Mass fraction of water = $(U_W \times \rho_W) / [(U_W \times \rho_W) + (U_O \times \rho_O)]$

X_O = Mass fraction of oil = $(U_O \times \rho_O) / [(U_W \times \rho_W) + (U_O \times \rho_O)]$

μ_W = Viscosity of water (Kg/m-s)

μ_O = Viscosity of oil (Kg/m-s)

In the present work, *k-ε* model has been used to simulate the flow patterns. In this model the turbulent kinetic energy and viscous dissipation rates have been calculated and used to obtain the turbulent viscosity in the flow field.

$$\frac{\partial(\rho k)}{\partial t} + \nabla.(\rho k U) = \nabla.\left(\frac{\mu_t}{\sigma_k}\nabla k\right) + 2\mu_t E_{ij}E_{ij} - \rho\varepsilon \quad (2.11)$$

$$\frac{\partial(\rho \varepsilon)}{\partial t} + \nabla.(\rho \varepsilon U) = \nabla.\left(\frac{\mu_t}{\sigma_\varepsilon}\nabla \varepsilon\right) + C_{1\varepsilon}\frac{\varepsilon}{k}2\mu_t E_{ij}E_{ij} - C_{2\varepsilon}\rho\frac{\varepsilon^2}{k} \quad (2.12)$$

$$\mu_t = C_\mu \rho \frac{k^2}{\varepsilon} \quad (2.13)$$

Where, *k*, ε, μ_t and *U* are the turbulent kinetic energy, dissipation rate, eddy viscosity and velocity respectively. E_{ij} is defined as

$$E_{ij} = \frac{1}{2}\left(\frac{\partial U_i}{\partial x_j} + \frac{\partial U_j}{\partial x_i}\right) \quad (2.14)$$

The equations also consists of some adjustable constants C_μ, σ_k, σ_ε, $C_{1\varepsilon}$ and $C_{2\varepsilon}$.

The values are $C_\mu = 0.09$, $\sigma_k = 1$, $\sigma_\varepsilon = 1.3$, $C_{1\varepsilon} = 1.44$, $C_{2\varepsilon} = 1.92$.

These default values of the model constants are the standard ones and most widely accepted. Details are obtained from ANSYS FLUENT user's guide 2006.

2.14 Initial and boundary condition

In all cases, the flow has been initialized by filling up the pipe with water from the water inlet with a specified inlet superficial velocity. Oil is then introduced in the pipe. The main steps followed during the simulation are:

- 2-D pressure based segregated grid solver with implicit formulation is selected as solver under unsteady state condition.

- Volume of Fluid (VOF) model is selected with number of phases q = 2. Explicit VOF scheme is selected so that the discretization scheme for VOF changes to Geo-Reconstruct (to get the surface tension effect).
- Test fluids are defined using material data base of Fluent and the properties are changed according to the present work.
- The operating pressure is set as atmospheric pressure (default setting), and gravity is considered in Y-direction as -9.81 m/s^2.
- The inlet velocities of both the fluids are assumed to be uniform and specified as follows:
  - At x = 0, y = 0; $U_x = U_{water}$ and $U_y = 0$ (m/s)
  - At x = 0.15 m and y = -0.0595 m; $U_y = U_{oil}$ and $U_x = 0$ (m/s)

These inlet velocity boundary conditions are obtained based on the fluids velocity inlets defined in the model. A schematic of fluid entry in to the pipeline is shown in Fig. 2.4.

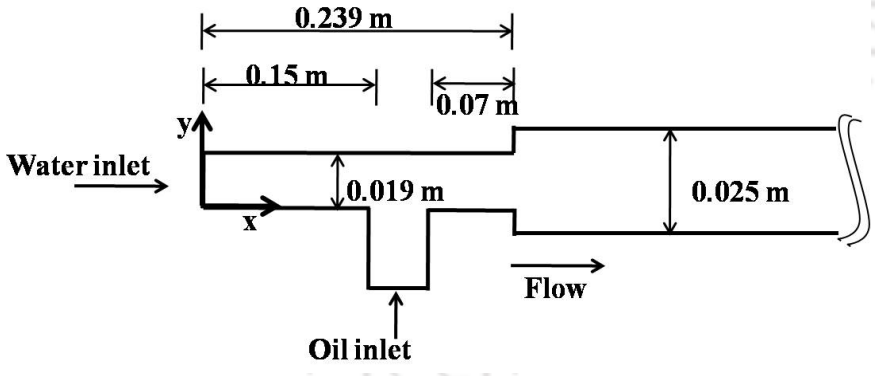

Fig. 2.4 Schematic of the fluid inlet section

- The wall is assumed to be stationary and no slip condition is imposed. A contact angle of 8.5^o is taken to account for the wetting behavior of the wall with the fluids.
- Pressure outlet boundary is selected and the diffusion flux variables at the exit are taken as zero.

2.15 Discretization method

To capture the dynamic nature of two-phase flow, variation of flow patterns with time and space has been considered. A transient simulation has been carried out with a time step of 0.001 s. In this simulation, the continuity equations are discretized by PRESTO algorithm while momentum equations are discretized by QUICK scheme. This scheme is more accurate on structured meshes aligned with the flow direction. SIMPLE (semi–implicit pressure linked equation) algorithm is used for pressure velocity coupling during the numerical analysis of the equations. It employs the relationship between velocity and pressure corrections to impose the mass conservation in consequence to get the pressure. The velocities are typically calculated by a segregated solver and it is coupled with the phases (volume fraction) to maintain the volume continuity.

2.16 Convergence criterion

The convergence is decided based on the residual values of calculated variables, namely velocity components, mass and volume fraction. In the present study, the numerical computation is considered converged when the residuals of the different variables are lowered by three orders of magnitude. After reaching to the desired residual value, the flow of the both the phases are tracked to get the flow pattern.

References

Al-Wahaibi, T., Angeli, P., 2011. Experimental study on interfacial waves in stratified horizontal oil-water flow. Int. J. Multiphase Flow 77, 930–940.

Andersson B, Andersson R, Hakansson L, Mortensen M, Sudiyo R, van Wachem B. Computational Fluid Dynamics for Engineers; 2012: Cambridge University Press: New York.

Fluent 6.3 User's Guide. Fluent Inc., Lebanon, USA, 2005.

Henk Kaarle Versteeg, Weeratunge Malalasekera (2007). ***An Introduction to Computational Fluid Dynamics: The Finite Volume Method*****. Pearson Education Limited.**

Santos, R.G., Rahoma, S.M., Bannwart, A.C., Loh, W., 2006. Contact angle measurements and wetting behavior of inner surfaces of pipelines exposed to heavy crude oil and water. J. Petroleum Sci. Eng. 51, 9–16.

Chapter 3

CFD simulation and experimental validation of flow pattern transition during viscous oil-water flow through a horizontal pipeline

3.1. Introduction

The flow of two immiscible liquids occurs commonly in petroleum industry, where crude oil and water simultaneously produced from wells, are transported over long distances for subsequent separation and processing. In such cases, undulation of pipelines comprising of interconnected horizontal, upward and downward inclined sections are inevitable due to different elevation of the earth surface. So, it is necessary to understand the hydrodynamics of oil-water flow in such pipe networks (undulated pipeline in the present work) for proper designing and sizing of a downstream separation and other unit of processing facilities. It seems that hydrodynamics in such complex system will be more complicated than that in a straight horizontal pipe. Therefore, hydrodynamics of oil-water flow in horizontal pipeline has been studied prior to the investigation of viscous oil-water flow through the undulated pipes. This chapter represents different flow patterns investigation during oil-water flow in horizontal pipeline especially wispy annular flow using conductance probe. Further, flow patterns and its transitional boundaries are predicted using CFD simulation. Simulation results are also validated with the experimental data obtained from experiments on equivalent systems with a wide range of superficial velocities of both oil and water, covering all the flow patterns. Subsequntly efforts have been made to understand the profile of volume fraction, pressure drop and velocity of a separated flow (stratified wavy, stratified mixed and annular flow) using VOF method.

3.2 Experimentation

The schematic representation of the experimental setup is shown in Fig. 3.1. It consists of an entry section (EN), a test section (TS) and an exit section (EX) in the direction of the flow. Exit section is connected with a separator (S) where oil separates from water due to density difference between oil and water. A centrifugal pump (CP) and a Gear pump (GP) respectively pump water and oil to the test section. The detailed dimensions of test section and specification of test fluids are discussed in chapter 2.

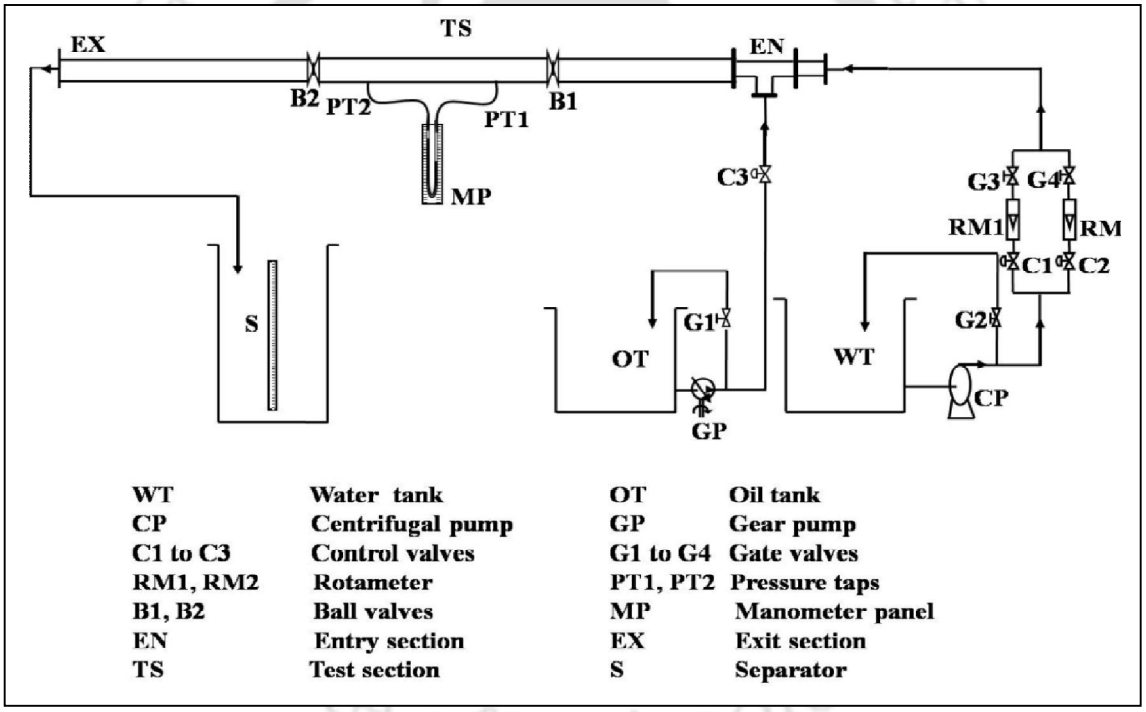

Fig. 3.1. Schematic representation of experimental setup

Experiments of oil-water flow have been conducted for wide range of superficial velocities to get all the probable flow patterns. All the flow patterns except annular flow are identified by visual observation and imaging while a conductance probe is used to

identify the wispy annular flow. Details of conductance probe are not discussed here to avoid repeatability. Detailed analysis of probe is discussed in chapter 2.

Experiments are carried out by gradual increasing the oil velocity at constant water velocity. After attaining the steady state, image of flow pattern is captured using a digital camera (DSC-HX100V, Sony) at the test section and glowing of LED is noted down. To check the reproducibility, experiments are repeated thrice and 99% accuracy is observed. After completion of a set of experiment, water velocity is changed to next higher value and repeated the same procedure as mentioned above.

3.3 Model development

The geometry of the concerned conduit considered for the present computational modeling is shown in Fig. 3.2a. The geometry consists of a horizontal pipeline with an internal diameter 0.025 m and length 7.16 m. The working fluids considered in the present work are moderately viscous oil and water (viscosity ratio: 107 and density ratio: 0.89). Fluids enter into the pipeline through a T- junction at the entry section, where water and oil enter into the pipeline from horizontal and vertical directions, respectively. The geometry of the system consists of four sections - water inlet, oil inlet, test section and outlet of the pipe. Geometry of the pipe is modeled in GAMBIT and exported to FLUENT. Fig. 3.2b represents the meshed model of pipeline. The mesh consists of 44330 and 2707 quadrilateral mesh elements for pipeline and entry section respectively. Quadrilateral mesh geometry is selected to account for the surface tension effect more accurately.

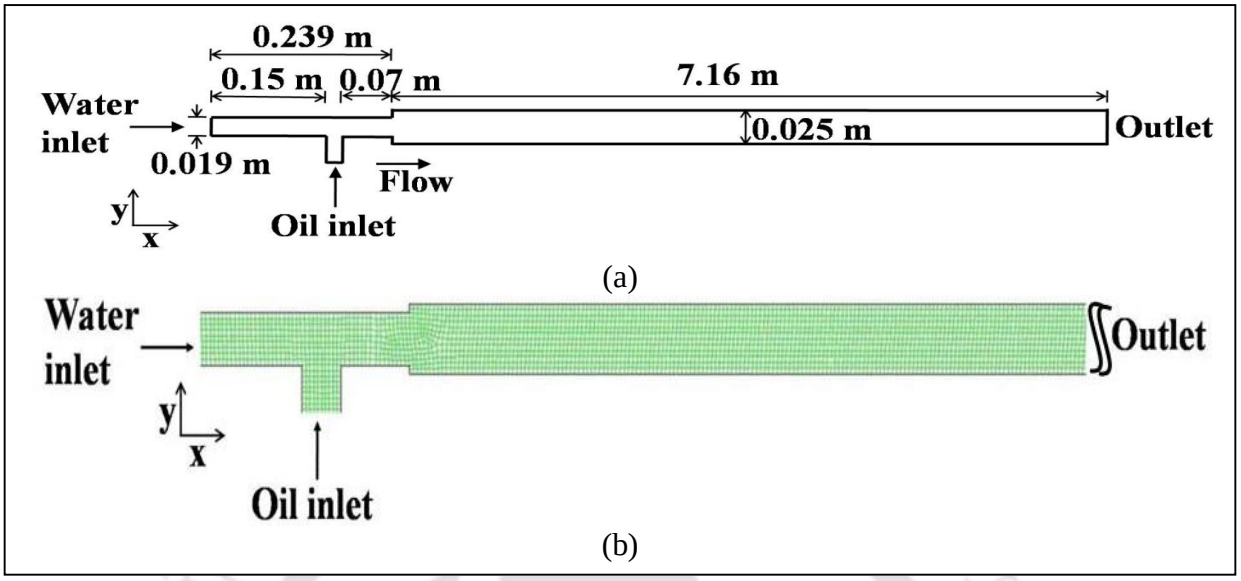

Fig. 3.2. Modeling of horizontal pipe **(a)** Detailed dimensions, **(b)** Meshing of model

The CFD software package of ANSYS FLUENT^{TM} is used for simulating oil-water two-phase flow under the following assumptions: unsteady flow, immiscible liquid pair, constant liquid properties, and co-axial flow in the pipe and T- junction ('T'). In the present model, it is assumed that the two fluids share a well-defined interface. Volume of Fluid (VOF) model with k-ε turbulence model is used, which solves a single set of momentum equations for both the fluids. The details of the governing equations, treatment of the interface and initial and boundary conditions are discussed in Chapter 2.

3.4 Experimental results

During the experiments, the oil superficial velocity (U_{SO}) has been varied from 0.015 m/s - 1.25 m/s and the water superficial velocity (U_{SW}) has been varied from 0.1 - 1.1 m/s to get transition boundaries of all the flow patterns. Seven different flow patterns have been

observed: plug (P), slug(S), wavy stratified (SW), stratified mixed (SM), Annular (A), oil dispersed in water ($D_{O/W}$) and water dispersed in oil ($D_{W/O}$).

At very low flow rate of oil (U_{SO} = 0.015 m/s), small plugs of oil are swarming in the continuous water phase and are known as plug flow (P, in Fig. 3.3a). Further increasing in oil flow rate (U_{SO} = 0.04 m/s), size of oil plugs are increasing and length of water bridge between two successive discrete oil mass decreases. This configuration is known as slug flow (S) as shown in Fig. 3.3b. Stratification occurs by increasing the oil flow rate marked by a phase separation between two phases with a clear interface. The interface between the two phases is observed as wavy at this oil flow rate (U_{SO} = 0.075 m/s). Amplitude of wave increases with increasing the phase flow rates. This type of flow is known as wavy stratified flow (SW, in Fig. 3.3c.).

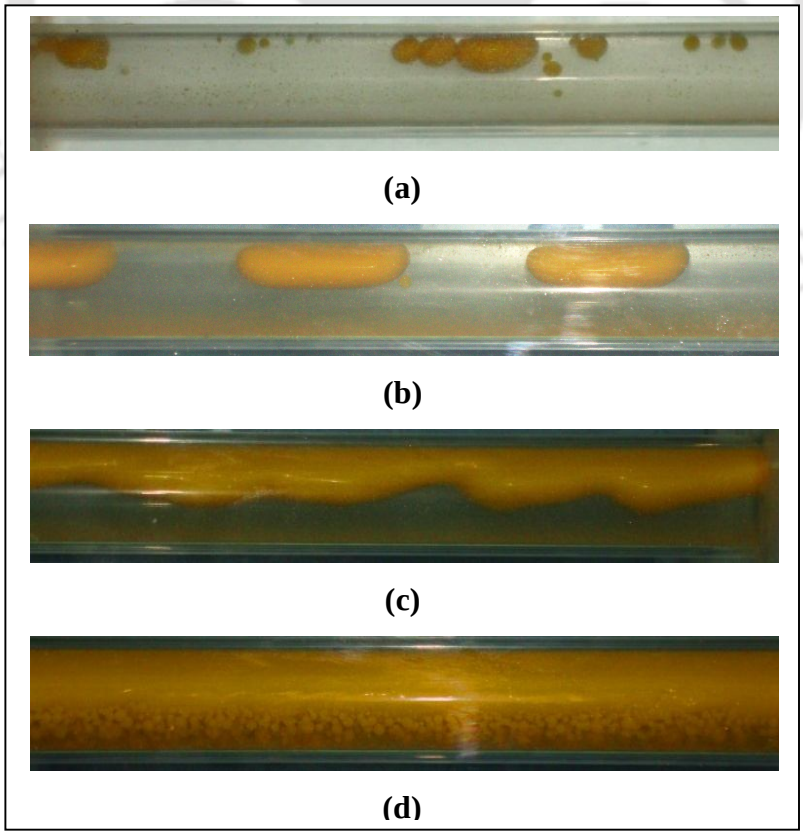

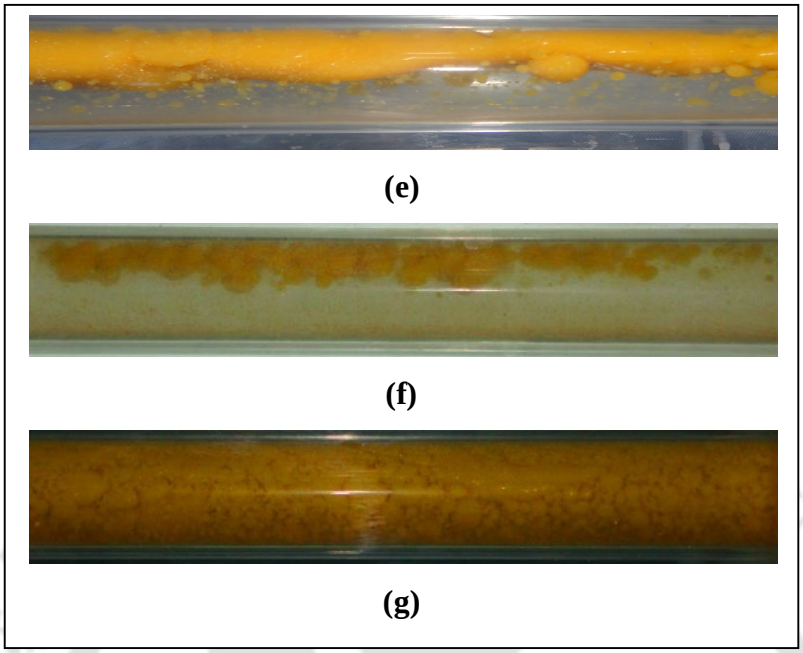

Fig. 3.3 Experimental images of flow patterns; **(a)** Plug flow at U_{SO} = 0.015 m/s, U_{SW} = 0.197 m/s; **(b)** Slug flow at U_{SO} = 0.04 m/s, U_{SW} = 0.197 m/s; **(c)** Stratified wavy flow at U_{SO} = 0.075 m/s, U_{SW} = 0.197 m/s; **(d)** Stratified mixed flow at U_{SO} = 0.22 m/s, U_{SW} = 0.197 m/s; **(e)** Wispy annular flow at U_{SO} = 0.4 m/s, U_{SW} = 0.45 m/s; **(f)** Dispersion of oil in water at U_{SO} = 0.12 m/s, U_{SW} = 0.53 m/s; **(g)** Dispersion of water in oil at U_{SO} = 0.68 m/s, U_{SW} = 0.2 m/s.

Further increasing the oil flow rate (U_{SO} = 0.22 m/s), the wave amplitude increases and bubble entrainment is observed at critical wave amplitude. This flow pattern is called stratified mixed (SM) flow as shown in Fig. 3.3d. At moderate phase velocities, annular (A) flow is observed in a small velocity range (U_{SO} = 0.27 – 0.6 m/s and U_{SW} = 0.4 – 0.63 m/s). In this configuration, oil flows at the centre of the tube as continuous core and water in contact with the pipe wall, forming annular geometry as shown in Fig. 3.3e. The dispersion forms when the motions of two phases are sufficiently intense. Two types of dispersions are possible: dispersion of oil in water (Do/w) and dispersion of water in oil

(Dw/o). Fine dispersion of oil is observed at the top, and most of the cross-section of the pipe is occupied by water during dispersion of oil in water flow as shown in Fig. 3.3f. The velocity range of this flow pattern is (U_{SO} = 0.08 – 0.53 m/s and USW = 0.43 – 1.06 m/s). At higher oil flow rate, very fine dispersion of water is observed, and oil occupies most of the pipe cross section as shown in Fig. 3.3g. This flow pattern is known as dispersion of water in oil (U_{SO} = 0.6 – 1.25 m/s and U_{SW} = 0.13 – 1.06 m/s). All the flow patterns are plotted in the form of a flow pattern map in Fig. 3.4 to represent the experimental results in a concise form.

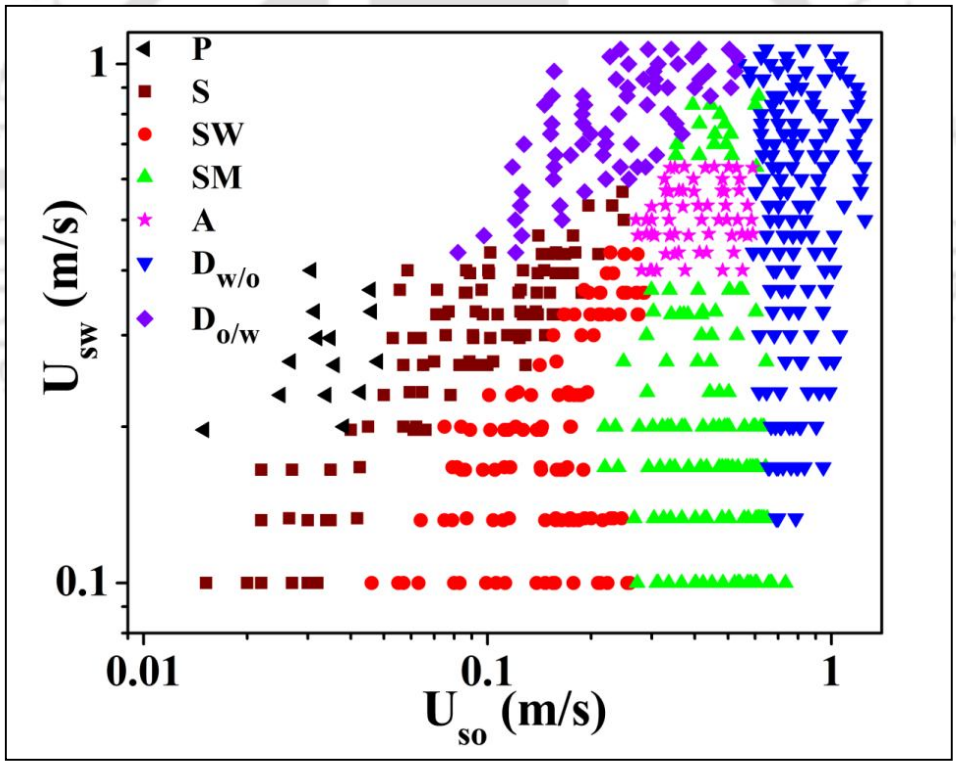

Fig. 3.4 Experimental flow pattern map (P - Plug flow; S - Slug flow; SW - Stratified wavy flow; SM – Stratified mixed flow; A- Annular flow; $D_{o/w}$ - Dispersion of oil in water; $D_{w/o}$ - Dispersion of water in oil)

3.5. Simulated results

The computational grids of 14732, 47037 and 63191 cells have been tested for the grid independent study to find out the optimum size of the mesh to be used for simulation. From the study, the system with 47037 and 63191 cells closely predicts the oil volume fraction with clear interface. Therefore, based on the contour results of oil volume fraction, 47037 cells are selected as the optimum number of cells for simulation. Simulations have been performed by taking different data points along the transition boundaries observed from the experimental flow pattern map. Using VOF model, successfully predicted plug, slug, stratified wavy, stratified mixed flow, annular flow patterns, and transitions boundary of (1) plug flow to slug flow, (2) slug flow to stratified wavy flow, (3) stratified wavy flow to stratified mixed flow, and (4) a region of annular flow instead of its transition boundaries. The other transitions (viz., SM to $D_{W/O}$ and SM to $D_{O/W}$) observed at higher phase velocities are difficult to predict by using VOF. The reason can be attributed to the method of interface reconstruction scheme of VOF model (Ghosh et al., 2010), which fails to capture the waviness of oil-water interface properly. Therefore, the transition boundaries observed at higher phase velocities are not simulated in this study. Below, prediction of different transition boundaries are discussed as mentioned above.

3.5.1 Plug to Slug transition boundary (P-S)

To show the transition between plug and slug flow patterns, simulation is run at U_{SW} = 0.23 m/s, U_{SO} = 0.04 m/s for plug flow and U_{SW} = 0.23 m/s, U_{SO} = 0.05 m/s for slug flow. The simulated result at these boundary conditions is validated with the experimental images captured at the same flow conditions as shown in Fig. 3.5. Here the length of the section in both CFD and experimental image is 0.24m.

The volume fraction contours of oil and water are plotted in all the cases to mimic the interfacial morphology of flow patterns. In these figures, blue and red color represents the presence of water and oil. Fig. 3.5a shows the contours of oil fraction for plug flow at U_{SW} = 0.233 m/s, U_{SO} = 0.04 m/s and Fig. 3.5b shows the experimental image taken at the same velocity. Similarly, the simulated result of slug flow at U_{SW} = 0.23 m/s, U_{SO} = 0.05 m/s is shown in Fig. 3.5c and the experimental image taken at the same velocity is shown in Fig. 3.5d. Fig. 3.5 (a and c) portrays the prediction of transition from plug to slug flow using CFD simulation. A good match between the simulated result and experimental result is observed. Present simulation results based on the VOF method, is well matched with the experimental results reported by Chakrabarti et al. (2007).

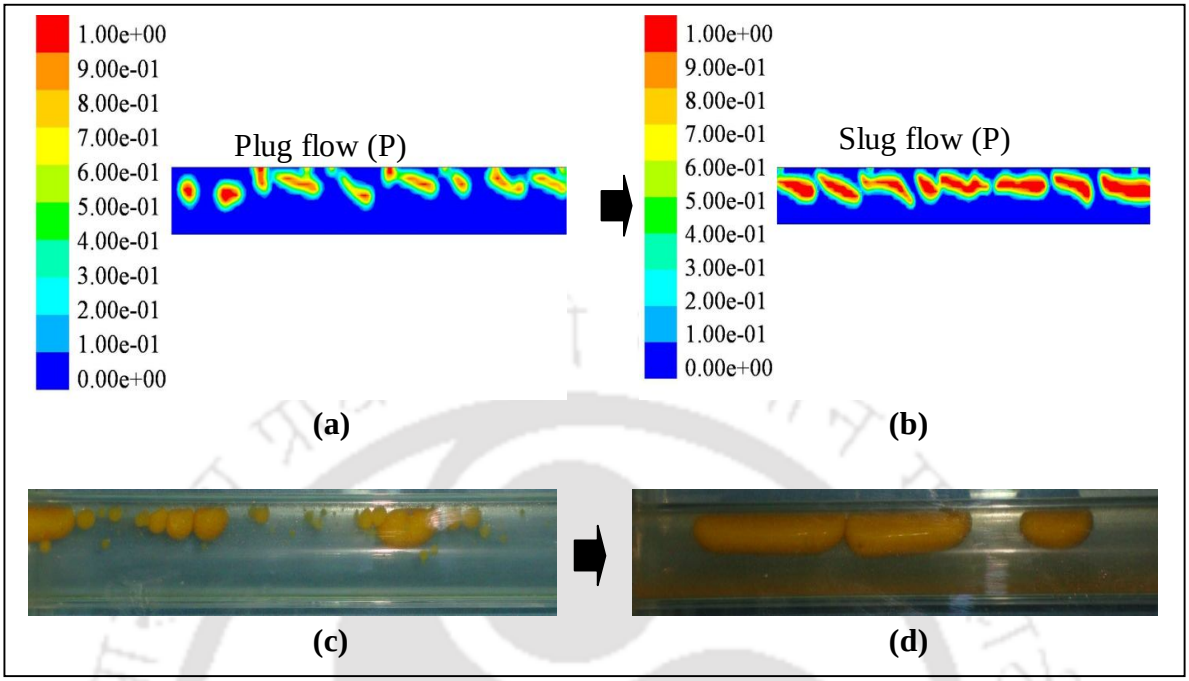

Fig. 3.5. Transition of Plug to Slug flow (P-S); (a) Simulated result at U_{SW} = 0.23 m/s, U_{SO} = 0.04 m/s; (b) Experimental image at U_{SW} = 0.23 m/s, U_{SO} = 0.04 m/s; (c) Simulated result at U_{SW} = 0.23 m/s, U_{SO} = 0.05 m/s; (d) Experimental image at U_{SW} = 0.23 m/s, U_{SO} = 0.05 m/s.

3.5.2 Slug to Stratified wavy flow transition boundary (S-SW)

It is well known that at the slug flow, if oil velocity is increased at a constant water velocity, the individual slugs are coalesced leading to a stratified flow pattern. The waviness at the interface can be accounted for by taking into consideration of the interfacial tension and interfacial shear. To show the transition, simulations have been done at U_{SW} = 0.23 m/s, U_{SO} = 0.078 m/s for slug flow and U_{SW} = 0.23 m/s, U_{SO} = 0.1

m/s for stratified wavy flow. The transition boundary of S-SW from experiment and simulation is shown in Fig. 3.6. The transition from Slug to wavy stratified flow pattern at U_{SW} = 0.23 m/s is clearly visible and good agreement with experimental result is observed.

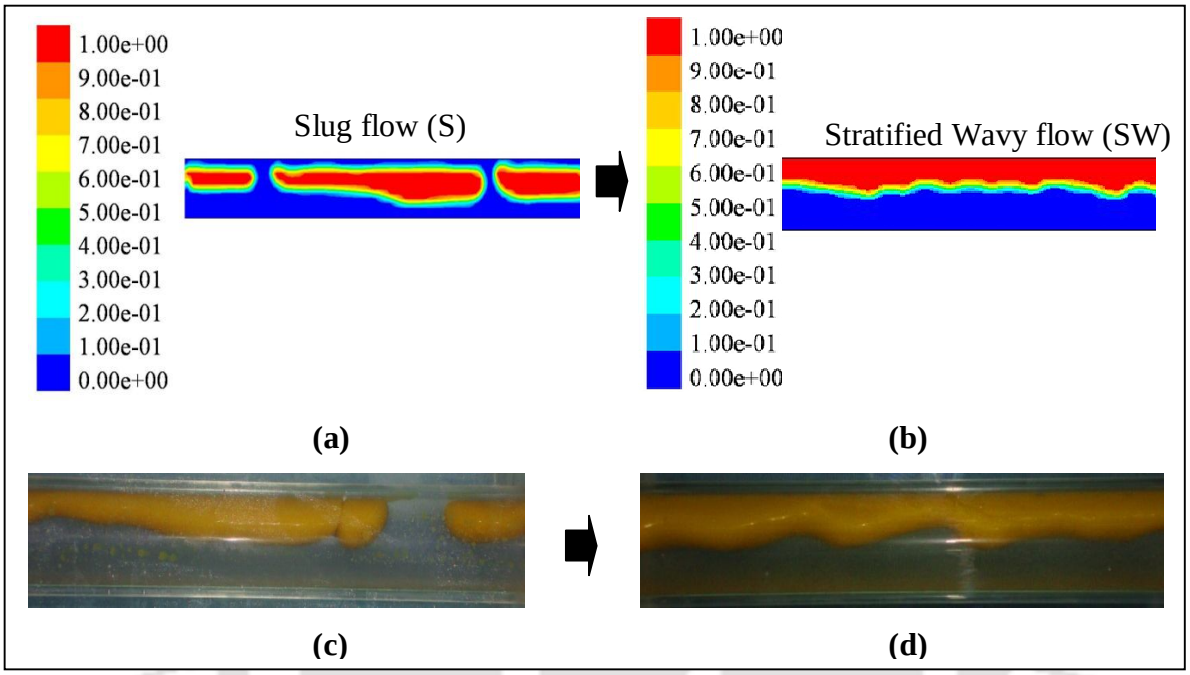

Fig. 3.6 Transition of Slug to Stratified wavy flow (S-SW); (a) Simulated result at U_{SW} = 0.23 m/s, U_{SO} = 0.078 m/s; (b) Experimental image at U_{SW} = 0.23 m/s, U_{SO} = 0.078 m/s; (c) Simulated result at U_{SW} = 0.23 m/s, U_{SO} = 0.1 m/s; (d) Experimental image at U_{SW} = 0.23 m/s, U_{SO} = 0.1 m/s.

3.5.3 Stratified wavy to mixed flow transition boundary (SW-SM)

The transition of SW-SM is obtained from the simulation and experiment at U_{SW} = 0.2 m/s, U_{SO} = 0.17 m/s for stratified wavy flow and U_{SW} = 0.2 m/s, U_{SO} = 0.21 m/s for

stratified mixed flow (Fig. 3.7). The simulated result (Fig. 3.7a) shows stratified flow with clear interface between the two phases with some wavy nature. By increasing the oil flow rate, the wave amplitude increases and bubble entrainment is observed at critical wave amplitude as is shown in Fig. 3.7c. Experimental photograph in Fig. 3.7b and 3.7d clearly shows this phenomenon of bubble entrainment at the interface of oil and water. A good agreement is achieved between experimental and simulated results. Unlike previous literature work (Al-Yaari and Abu-Sharkh, 2011), stratified and stratified mixed flow have successfully predicted with good accuracy.

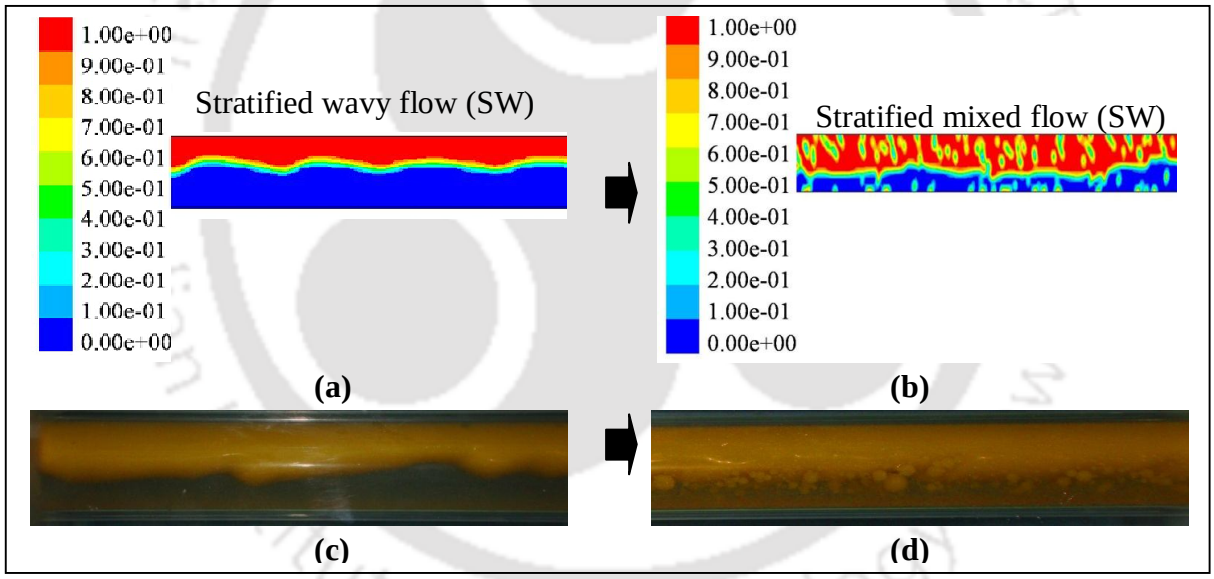

Fig. 3.7. Transition of Stratified wavy to Stratified mixed flow (SW-SM); (a) Simulated result at U_{SW} = 0.2 m/s, U_{SO} = 0.17 m/s; (b) Experimental image at U_{SW} = 0.2 m/s, U_{SO} = 0.17 m/s; (c) Simulated result at U_{SW} = 0.2 m/s, U_{SO} = 0.21 m/s; (d) Experimental image at U_{SW} = 0.2 m/s, U_{SO} = 0.21m/s.

3.5.4. Region of annular flow (A)

During the annular flow, oil flows as core in the center and a thin layer of water flows as annulus in a pipe. Five different transitions are observed around the annular flow (Fig. 3.8): slug, stratified wavy, stratified mixed and dispersion of both oil and water. In the present work, prediction of these transition boundaries is not done due to the limitation of the VOF at higher phase fractions. However, the region of annular flow is simulated successfully. Simulation result of annular flow at flow condition U_{SW} = 0.4 m/s, U_{SO} = 0.45 m/s is shown in Fig. 3.8a. The experimental image of annular flow at the same condition is also shown in Fig. 3.8b. The figures are showing good agreement between experimental and simulated results. Simulations have been done at various combinations of velocities to get the entire region of annular flow. Similar prediction of core-annular flow has been reported for a horizontal flow through sudden change in cross-sectional area (Kaushik et al., 2012) and in a return bend (Ghosh et al., 2011).

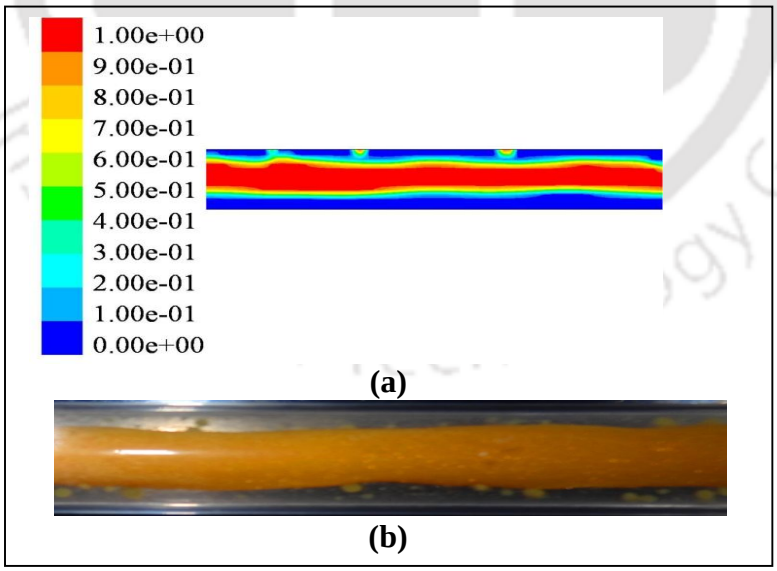

Fig. 3.8 Annular flow; (a) Simulated result at U_{SW} = 0.45 m/s, U_{SO} = 0.4 m/s; (b) Experimental image at U_{SW} = 0.45 m/s, U_{SO} = 0.4 m/s.

3.6. Validation

In order to validate the simulation, the results are compared with the experimental data of the present work. For this, oil volume fraction of separated flow has been simulated and compared with the experimental result as shown in Fig. 3.9. Area average volume fraction is calculated from simulation and considered as equivalent to the experimental volume fraction. The figure shows a good agreement with the experiments. The figure shows that the model predicts volume fraction of oil with an average absolute error of 11.7%.

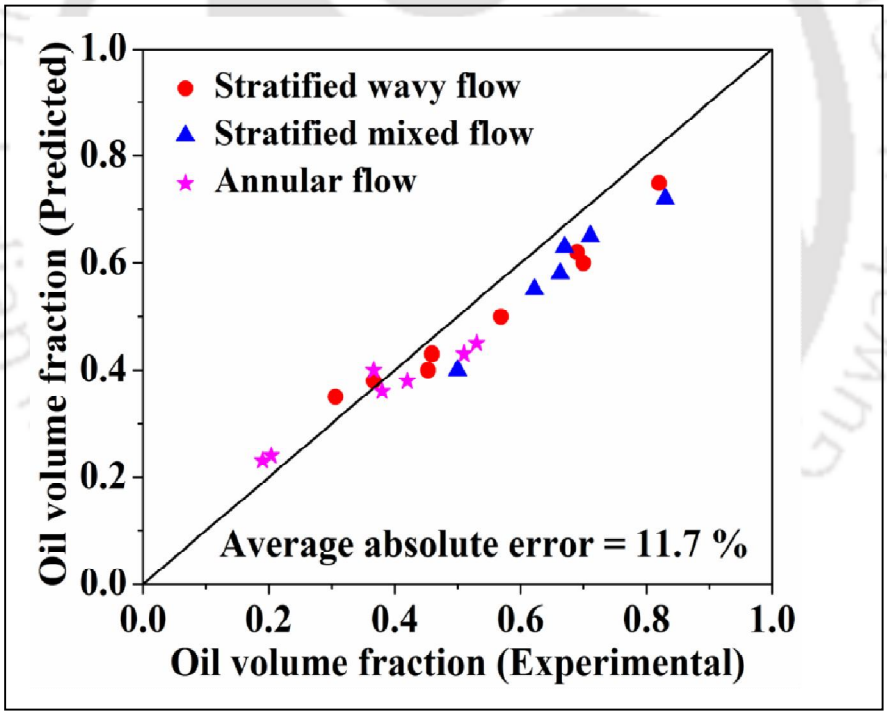

Fig. 3.9. Comparison of experimental and predicted oil volume fraction.

In the present work simulated results are also compared with the experimental flow pattern map. So, the simulated points (of different flow patterns) have been superimposed on the horizontal flow pattern map (Fig. 3.10). Marked (by circle) data points represent

simulated data while solid and broken lines are experimental transition boundaries. Line 1, 2, 3 and 4 represent the transition boundary of plug to slug, slug to stratified wavy, stratified wavy to stratified mixed and boundary around annular flow respectively. The circled data points around the respective boundary are simulated results of respective flow regimes. The figure (Fig. 3.10) depicts a good matching between the simulated and the experimental flow patterns.

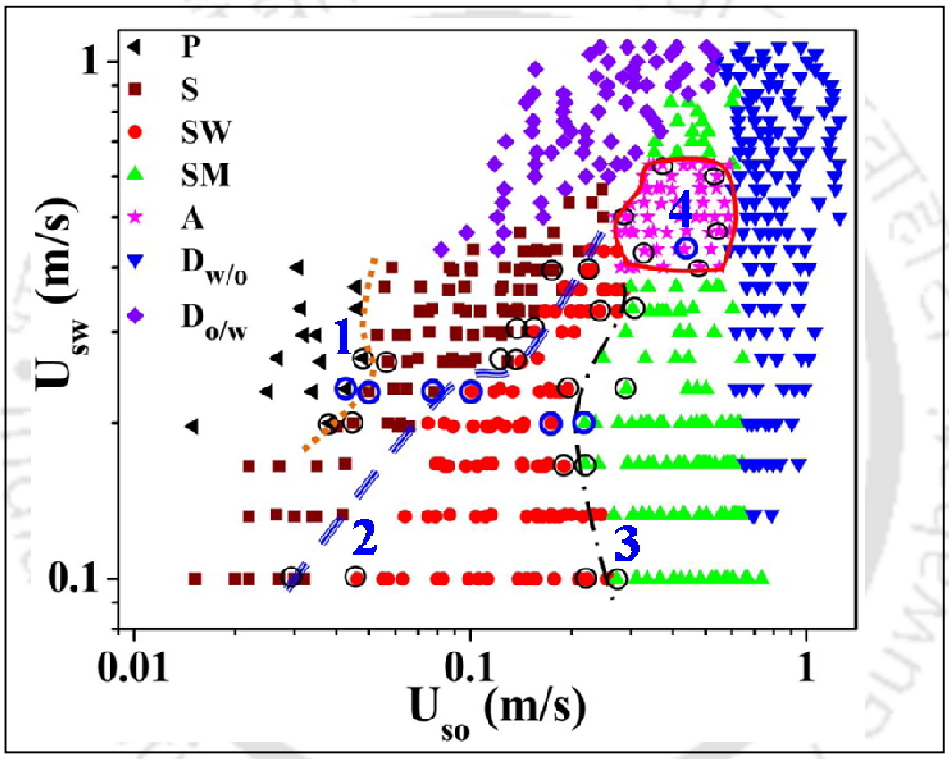

Fig. 3.10. Validation of Simulation results with experimental results (P – Plug flow; S – Slug flow; SW – Stratified wavy flow; SM – Stratified mixed flow; A – Annular flow; $D_{o/w}$ – Dispersion of oil in water; $D_{w/o}$ – Dispersion of water in oil; Dotted line – P/S transition boundary; solid line – SW/SM transition boundary; Triple lined dash – S/SW transition boundary; Black color dashed line- Annular flow transition; Circled data points are simulation data points along the transition boundaries; Blue color circled data points are sample simulation results shown in the current work).

After validation with experiments, the model is used to generate useful information about flow characteristics (volume fraction, pressure and velocity profile) of a separated flow (viz., stratified wavy, stratified mixed and annular flow) which is encountered commonly in chemical and petroleum industries. It may help in understanding the mechanism of flow phenomena and to determine the interfacial parameters such as interfacial velocity, and shear. Using the interfacial velocities one can improve the prediction accuracy of two-phase pressure drop. The detailed analysis of modelling and importance of flow characteristics are discussed in the next section.

3.7. Radial distribution of volume fraction, pressure and velocity of a separated flow

In the following section, the volume fraction profile, local pressure across a cross section and velocity profile along the radius of seperated flow at different phase velocities have been reported. The schematic representation of radial positions of a circular pipe under consideration is shown in Fig. 3.11. All the contours ofseperated flow have been shown by considering a line across the cross section at L/D = 120 (Fig. 3.11).

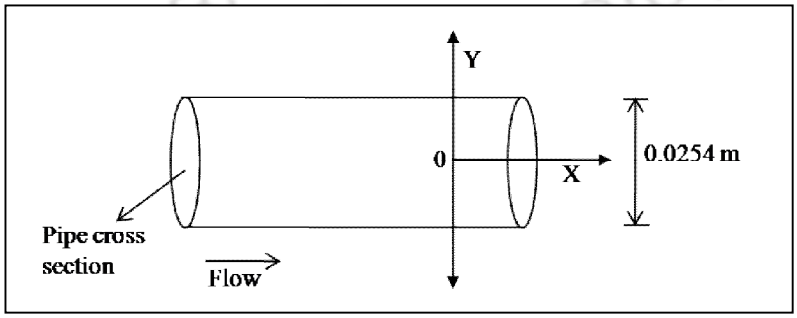

Fig. 3.11 Schematic representation of radial positions of a circular pipe under consideration.

3.7.1. Volume fraction profile

This profile helps to characterize the two-phase flows. It is the key physical value for determining numerous other important parameters, such as the two-phase density and the two-phase viscosity, for obtaining the relative average velocity of the two phases, and is of fundamental importance in models for predicting flow pattern transitions and pressure drop. The radial behavior of oil volume fraction for stratified wavy (Fig. 3.12a), strafied mixed (Fig. 3.12b) and annular (Fig. 3.12c) flow is shown in Fig. 3.12. Fig. 3.12a shows the variation of oil fraction with increasing oil velocity (U_{SO} = 0.1 and 0.2 m/s) at a constant water velocity (U_{SW} = 0.23 m/s). During stratified wavy flow, oil phase thickness increases as oil velocity increases. Similarly oil volume fraction profile of stratified mixed flow pattern is shown in Fig. 3.12b at constant water velocity (U_{SW} = 0.33 m/s) and different oil velocities (U_{SO} = 0.1 and 0.2 m/s). The figure depicts the distinct three layers,- 1) a continuous water layer at bottom, 2) a continuous oil layer at top and 3) a mixed layer of oil droplets in continuous water inbetween continuous layer of oil and water. The profile is bimodal due to the presence of a mixed layer (3rd layer). The small hub of the plot indicates the oil droplets in continuous water.

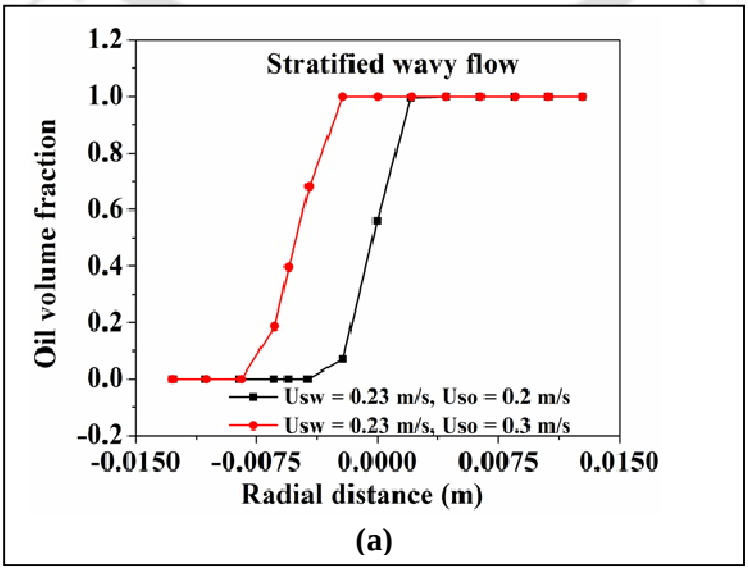

(a)

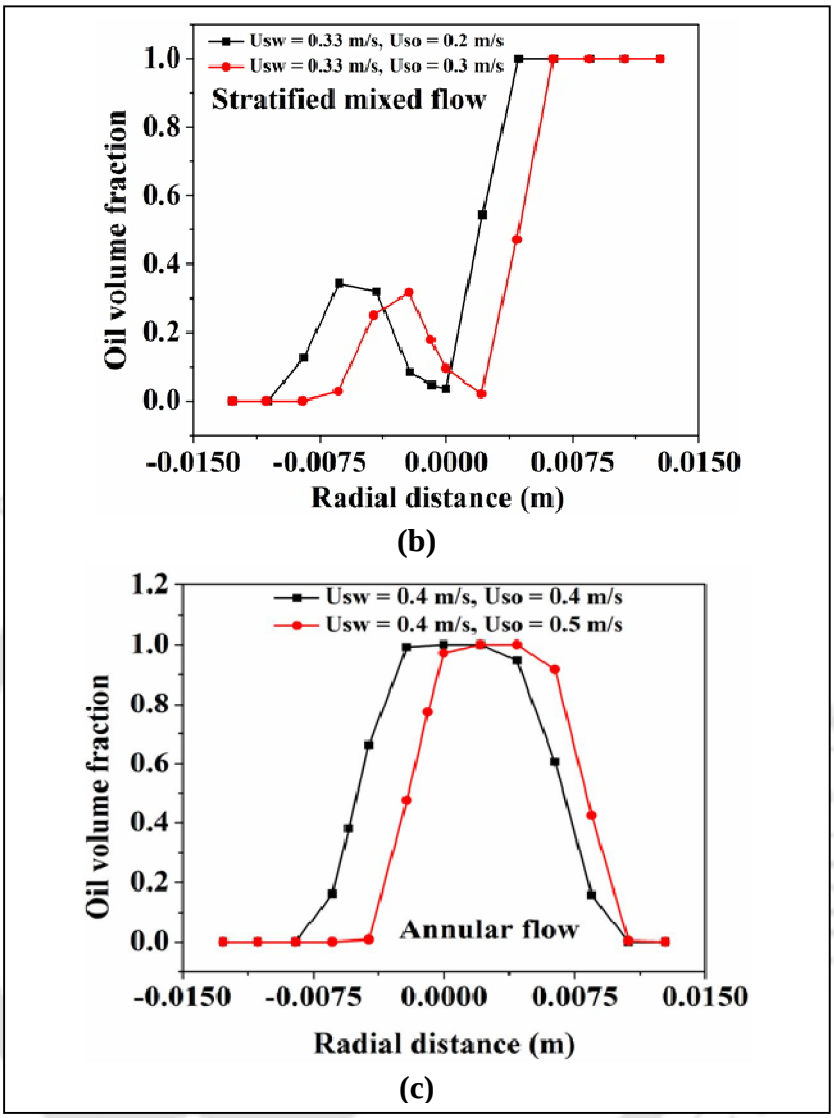

Fig. 3.12. Radial distribution of oil volume fraction. (a) Stratified wavy flow; (b) Stratified mixed flow; (c) Annular flow

During the annular flow, the oil phase flows in the center as core and water phase flows through annulus between pipe wall and oil core (Fig. 3.3). This is confirmed from the radial distribution of oil volume fraction which is shown in Fig. 3.12c. This results show good acceptability with the experimental results with an average error of 11.7 % (Fig. 3.9).

3.7.2. Pressure profile

Pressure drop in two-phase flow is a major design parameter, governing the pumping power required to transport two-phase fluids. Variation of local pressure (mixture) along the radial direction for separated flow is shown in Fig. 3.13. Fig. 3.13a to c depicts numerically predicted pressure variation along axial position at L/D = 120. For stratified wavy flow, the pressure will be maximum at the oil-water interface due to slip between the phases. Fig. 3.13a depicts the same showing maximum pressure at interface. Simillar observation is also noted incase of stratified mixed flow (Fig. 3.13b). During the annular flow, total pressure decreases with increase in oil velocity at constant water velocity as shown in Fig. 3.13c. The figure (Fig. 3.13c) depicts maximum pressure at top interface of annular flow due to higher shear at that interface.

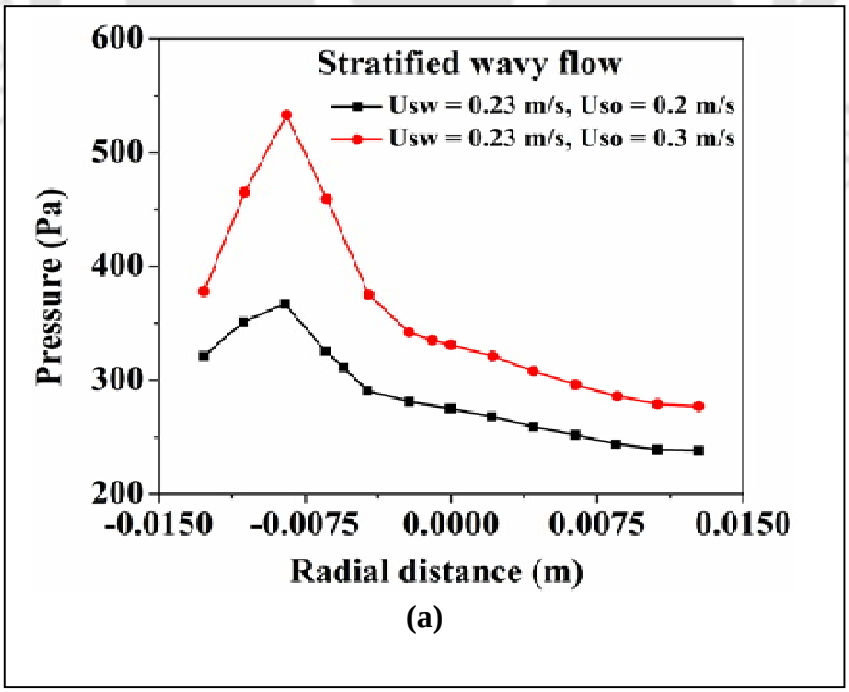

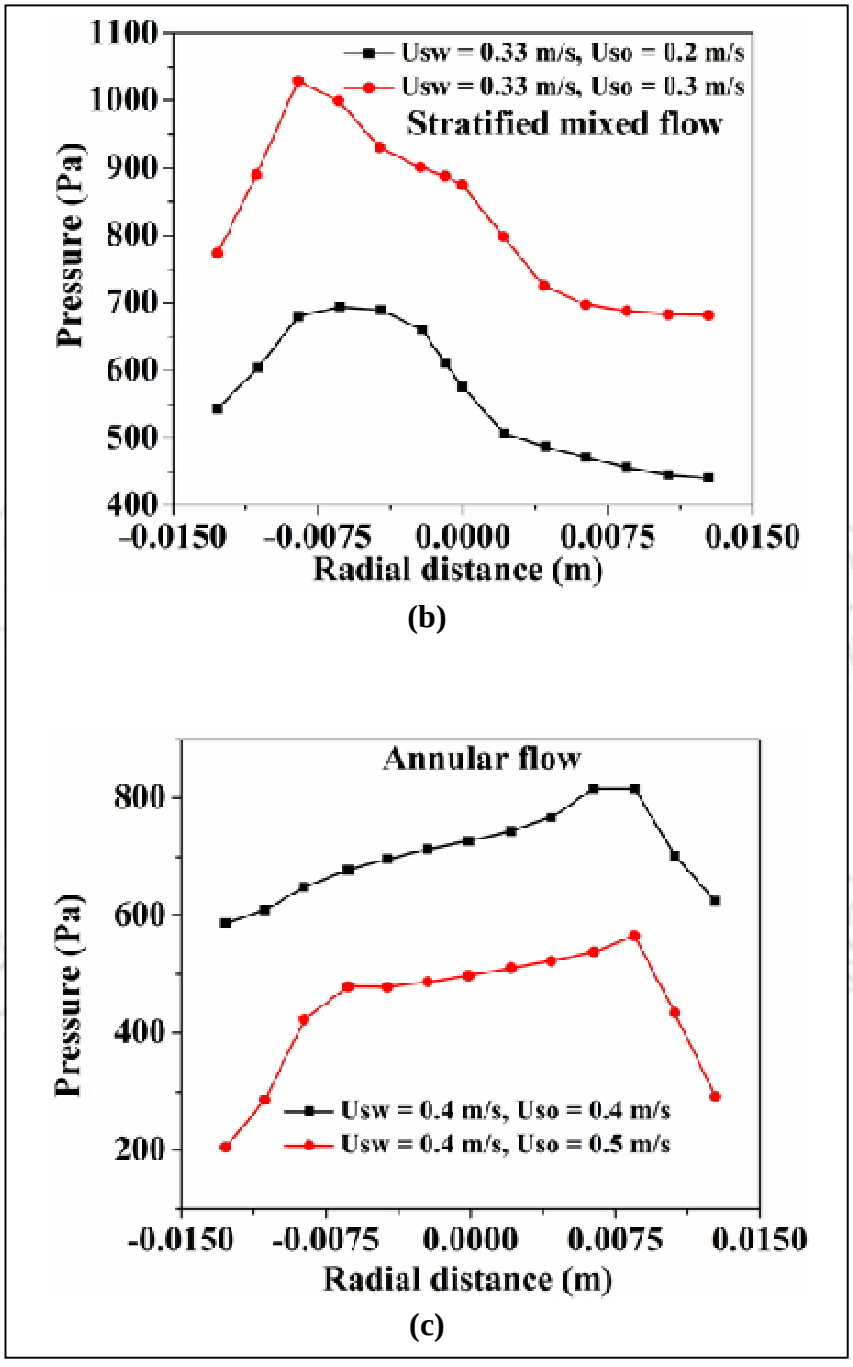

Fig. 3.13. Radial distribution of total pressure. (a) Stratified wavy flow; (b) Stratified mixed flow; (c) Annular flow

3.7. 3. Velocity profile

The velocity profile depends on the type of flow (flow through confined conduite, openchannel flow and flow through paprallel plates, etc.) and conduite geometry. . It may give accurate value of kinetic turbulent energy, turbulent dissipation rate, momentum correction factor, etc. Ghorai et al. (2006) and Sidi-Ali et al.(2010) predicted the velocity profile for gas-liquid two-phase flow. Till now there is no such literature that describes the velocity profile of liquid – liquid flow using CFD. In the present work, efforts have been made to understand the radial distribution of velocity for stratified wavy (Fig. 3.14a), stratified mixed (Fig. 3.14b) and annular flow (Fig. 3.14c). The velocity profiles of stratified wavy flow is drawn for U_{SO} = 0.2 m/s and U_{SO} = 0.3 m/s at constant water velocity of U_{SW} = 0.23 m/s in Fig. 3.14a. Similarly Fig. 3.14b shows the velocity profile of stratified mixed flow at U_{SW} = 0.33 m/s, U_{SO} = 0.2 m/s and U_{SW} = 0.33 m/s, U_{SO} = 0.3 m/s). In stratified wavy and stratified mixed flow, oil phase is in laminar and water phase is in turbulent flow. Hence the velocity is high for water phase and low for oil phase (see Fig. 3.14a,b). In annular flow, the velocity profiles (at U_{SW} = 0.4 m/s, U_{SO} = 0.4 m/s and U_{SW} = 0.4 m/s, U_{SO} = 0.5 m/s) look like an inverted "U" showing maximum velocity at the centre (which is occupied by oil phase) as shown in Fig. 3.14c.

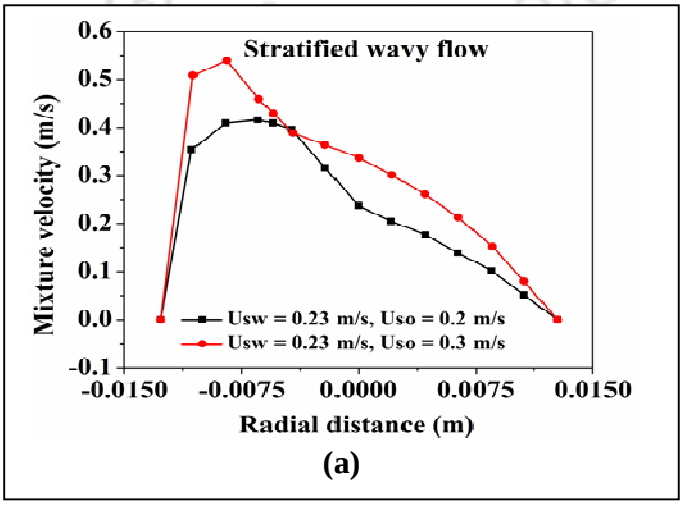

(a)

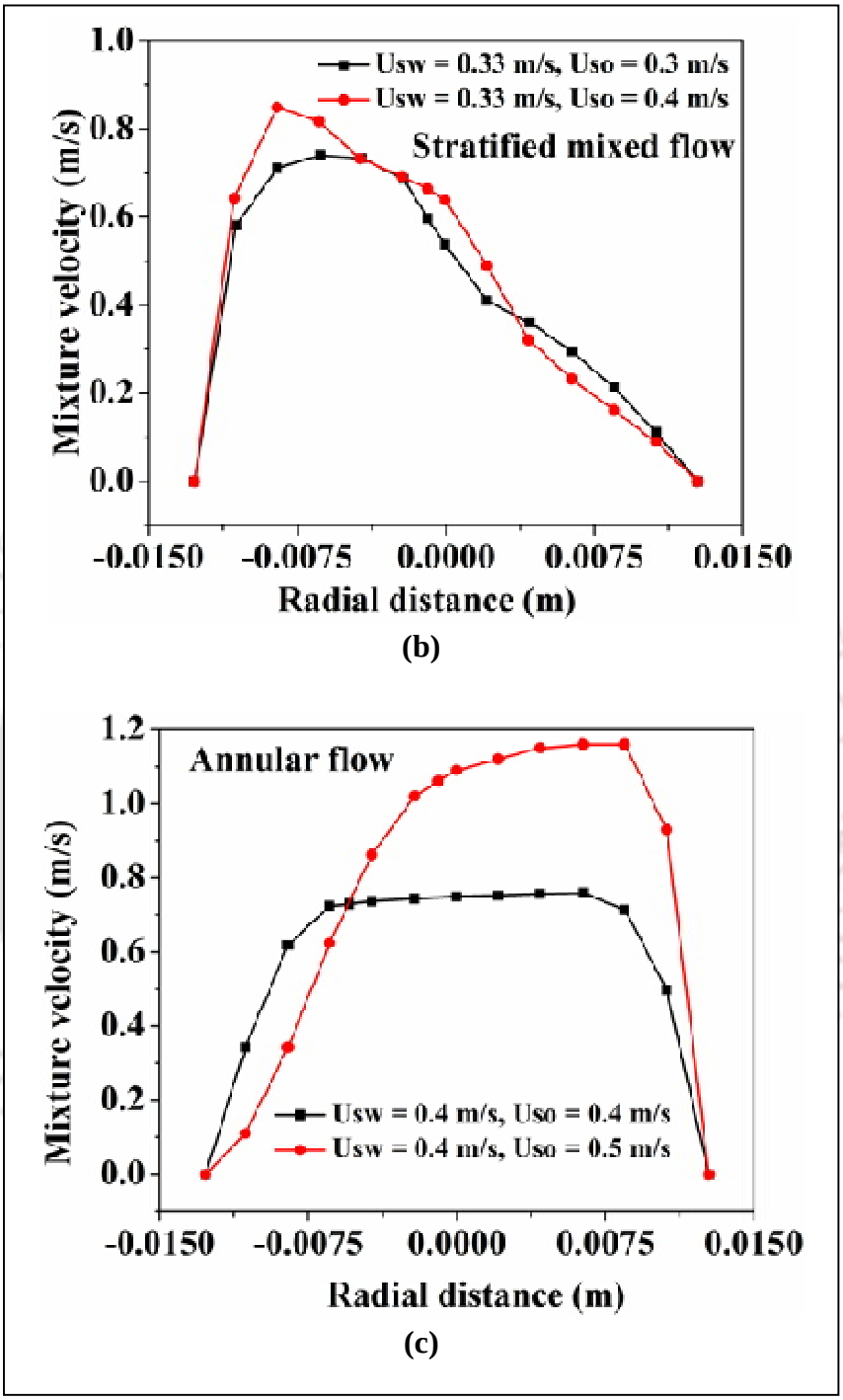

Fig. 3.14. Radial distribution of velocity profile. (a) Stratified wavy flow; (b) Stratified mixed flow; (c) Annular flow

3.8. Conclusion

Computational fluid dynamics study has been conducted to predict the transition boundaries of viscous oil-water two-phase flow through a horizontal pipeline. Based on the grid independent study, 47037 numbers of cells are selected as optimum number of cells for simulation. Successfully simulated plug, slug flow along with other separated flow patterns (viz., stratified wavy, stratified mixed and annular flow), and their transition boundaries. VOF technique successfully predicts transition boundaries of plug to slug, slug to wavy stratified and wavy stratified wavy to stratified mixed flow. Experimentally, seven different flow patterns including annular flow are observed. Simulation results show an excellent agreement with experimental results in predicting of volume fraction, flow patterns and transition boundaries. Annular flow and its region (not all the boundaries related to the annular flow) are simulated with an appreciable accuracy. VOF also predicts the volume fraction, pressure and velocity profile of the separated flow. The present findings reveal the ability of VOF to predict the hydrodynamics of viscous oil-water two-phase flow.

References

Al-Yaari, M. A. and Abu-Sharkh, B. F., 2011. CFD prediction of stratified oil-water flow in a horizontal pipe. Asian Trans. Eng. 01, 68 – 75.

Chakrabarti, D. P., Das, G. and Das, P.K., 2007. Identification of stratified liquid–liquid flow through horizontal pipes by a non-intrusive optical probe. Chem. Eng. Sci. 62, 1861 –1876.

Fluent 6.3 User's Guide, 2005. Fluent Inc., Lebanon, USA.

Ghorai, S. and Nigam, K. D. P., 2006. CFD modeling of flow profiles and interfacial phenomena in two-phase flow in pipes. Chem. Eng. Process. 45, 55 – 65.

Ghosh, S., Das, G. and Das, P. K., 2010. Simulation of core annular downflow through CFD – A comprehensive study. Chem. Eng. Process. 49, 1222 – 1228.

Ghosh, S., Das, G. and Das, P. K., 2011. Simulation of core annular in return bends – comprehensive CFD study. Chem. Eng. Res. Des. 89, 2244 – 2253.

Kaushik, V. V. R., Ghosh, S., Das. G. and Das, P. K., 2012. CFD simulation of core annular flow through sudden contraction and expansion. J. Pet. Sci. Eng. 86-87, 153 – 164.

Sidi-Ali, K. and Gatignol, R., 2010. Interfacial friction factor determination using CFD simulations in a horizontal stratified two-phase flow. Chem. Eng. Sci. 65, 5160 – 5169.

Chapter 4

Experimental study of viscous oil-water two-phase flow through an undulated pipeline in peak configuration

4.1 Introduction

The flow of two immiscible liquids occurs commonly in petroleum industry, where crude oil and water produced from wells, are transported over long distances for subsequent separation and processing. In such cases, undulation of pipelines comprising of interconnected horizontal, upward and downward inclined sections are inevitable due to different elevation of the earth surface. Therefore, it is necessary to understand the different flow patterns and their transition boundaries for proper designing and sizing of a downstream separation and other unit of processing facilities. Although the hydrodynamics of low viscous oil-water flow in hilly terrain and undulated pipeline has been studied, the flow behavior of moderately viscous oil-water flow is poorly understood. Hilly terrain and undulation of pipeline is a more realistic situation for a transportation pipeline. This chapter mainly focused on the effect of undulation (viz., peak configuration with an angle of 5°) on the hydrodynamics of moderately viscous oil-water flow (oil viscosity = 107 mPa s). Crude oil with viscosity ≥ 100 mPa s is quite relevant to oil refineries in coming years (Poesio et al. 2012; Abdurahman et al. 2012 and Balakhrisna et al. 2010).

4.2. Experimentation

The schematic diagram of the experimental setup is shown in Fig. 4.1. It consists of 7.4 m long transparent Perspex (PMMA) pipe with 0.025 m internal diameter. It consists of an entry section (EN), a test section (TS) and an exit section (EX) in order of the direction of

flow. The exit section is connected with the separator (S1). In the test sections, view boxes (VB1 to VB4) are provided to minimize the lens effect of the pipe material during the photography. Water and lube oil are selected as test fluids and the physical properties are presented in Table 2.1. Detailed dimensions of the test section are shown in Figure 4.2. Test section of peak configuration comprises of an uphill (UH) and a downhill section (DH) between two horizontal portions (upstream (US) and downstream (DS) section) in order of the direction of flow. The junction of the upstream and uphill section is termed as the uphill elbow and that between the downhill and downstream section is the downhill elbow. The angle of inclination is equal for both the uphill and downhill sections with $\pm 5^{o}$ with respect to the horizontal.

Experiments have been performed at a particular oil and water velocity. In steady state, a snapshot has been taken using a digital camera (Make-SONY, Model-DSC HX100V) at all test sections to identify the flow pattern. A U-tube manometer (with CCl_4 as manometric fluid) is used to determine the pressure difference across the undulated section. This experiment has been repeated three times to check the reproducibility of the experimental results. More than 99% reproducibility has been obtained in most of the cases. After completion of a set of experiments, oil velocity is increased step-by-step (by gradual opening the control valve C3), keeping the water velocity constant and readings are repeated as earlier. Likewise, the experiments are completed for entire range of velocities.

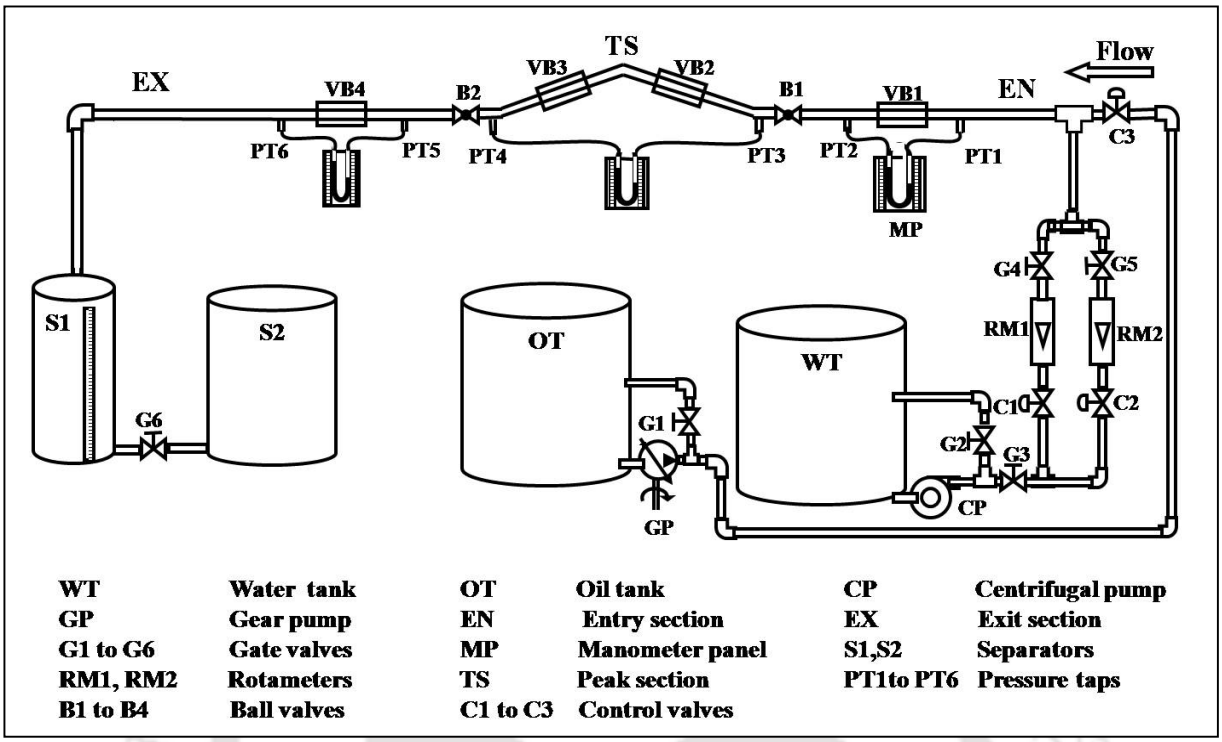

Fig. 4.1. Schematic representation of experimental setup

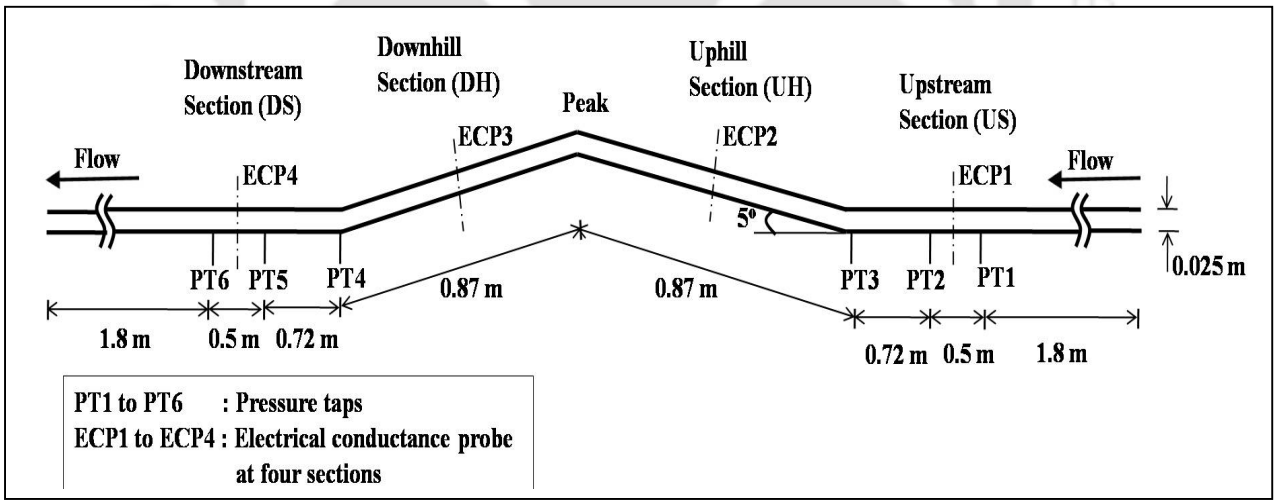

Fig. 4.2. Detailed dimensions of the test section (peak configuration)

4.3 Results and Discussion

The experiments have been conducted for a wide range of superficial velocity of oil and water (U_{SO} = 0.015 m/s to 1.3 m/s) and (U_{SW} = 0.1 m/s to 1.2 m/s) respectively, to cover the entire range of flow patterns. Flow patterns except wispy annular are identified by imaging technique and wispy annular flow is identified using both probe and imaging technique.

4.3.1 Identification of wispy annular flow and comparison with literature

Wispy annular flow is first identified by Bennett et al. (1965). In wispy annular flow, the structures are actually quite difficult to observe visually because the thin water film (especially on top region of oil core in horizontal flow) tends to be highly disturbed with considerable bubble entrainment. Sometimes the wave crest may touch upon the pipe wall. In the present study, wispy annular flow has been identified by probe and photographic technique as discussed in the experimental section. The result of this technique at U_{SW} = 0.4 m/s is summarized in Table 4.1 for upstream section. Top view, front view and a sketch of the cross sectional vies of the flow pattern are shown in 4th, 5th and 6th column of the table respectively. Status of LED at particular flow rate is mentioned in 7th column, and over all remark is given in 8th column. At U_{SW} = 0.4 m/s and U_{SO} = 0.33 m/s, top (4th column) and front view (5th column) shows that water warps the core oil phase. The oil bubble entrainment into the water layer is also clearly noticed (Sl. no. 1 of Table 4.1). All the LEDs in circuit-I and II, are glowing at the same flow

condition. It proves the occurrence of wispy annular flow pattern at this phase flow rate. Similarly, this flow pattern is identified at other velocities as mentioned in Sl. no. 2 and 3 of Table 4.1. By increasing the oil velocity from 0.33 m/s to 0.685 m/s, bubble entrainment in water layer increases as in Sl. No. 2 and 3 of Table 4.1. Further increasing the oil velocity, dispersion of water in oil flow pattern is observed and LED is not glowing further.

Table 4.1. Identification of annular flow

S. No.	U_{SW} (m/s)	U_{SO} (m/s)	Photograph of the flow		Cross sectional view	LED glowing	Flow pattern
			Top view	Front view			
1	0.4	0.33				Yes	Wispy Annular flow
2	0.4	0.50				Yes	Wispy Annular flow
3	0.4	0.68				Yes	Wispy Annular flow

The wispy annular flow region is observed at U_{SO} = 0.28 - 0.73 m/s and U_{SW} = 0.39 - 0.59 m/s for both upstream and uphill sections. For downhill and downstream sections the wispy annular flow is observed at U_{SO} = 0.25 m/s - 0.73 m/s with the same water velocities (viz., U_{SW} = 0.39 - 0.59 m/s) (see section 3.3 for flow pattern map). At lower

velocities of oil and water, the wispy annular flow is not stable because of capillary instability (due to interfacial tension) and it breaks the oil core (Bensakhira et al. 2004). However, at higher velocity, interfacial frictional instability factor reduces the capillary instability and stabilizes the wispy annular flow. For higher velocities, wispy annular flow becomes again unstable due to the domination of the interfacial friction, which breaks the core.

Table 4.2. Comparison of annular flow velocity: Experimental results with literature data

Author	**System**	**Pipe diameter (cm)**	**Core fluid viscosity (kg/m S)**	**Velocity range of core fluid (m/s)**	**Velocity range of water (m/s)**
Charles et al. (1961)	Horizontal	2.5	0.0063, 0.0168, 0.065	0.015-0.9	0.03-1.07
Grassi et al. (2008)	Horizontal, upward downward	2.1	0.799	0.186-0.7	0.15-1.95
Sotgia et al. (2008)	Horizontal	2.6	0.9	0.28-0.97	0.16-1.73
Pietro Poesio et al. (2012)	Horizontal	5.0	0.9	0.25-0.48	0.3-0.55
Present work	Upstream Uphill Downhill Downstream	2.5	0.107	0.28-0.73 0.28-0.73 0.25-0.73 0.25-0.73	0.40 - 0.60

The wispy annular flow observed in present experimental condition has been compared with the literature data of annular flow in Table 4.2. The table shows the viscosity of oil used in the present work is less than the others except Charles et al. (1961). Pipe diameter is also comparable with all the works except Poesio et al. (2012). The velocity range of wispy annular flow observed in the present study lies within the ranges reported in the past literature (Table 4.2) but the magnitude of the range is less in present work. This is due to the destabilizing effect of peak configuration. Poesio et al. (2012) and Sotgia et al. (2008) work shows that larger diameter destabilizes the annular flow. Sotgia et al. (2008) and Grassi et al. (2008) also concluded that the stability of the annular flow depends on the pipe geometry, operating conditions, viscosity and density of the liquids used in the system.

4.3.2 Different flow patterns:

Seven different flow patterns are observed at each section during oil-water flow through peak configuration of the undulated pipeline. Those are plug flow (P), slug flow (S), stratified wavy flow (SW), stratified mixed flow (SM), wispy annular flow (A) (see section 4.3.1 for details), dispersion of oil in water flow ($D_{O/W}$) and dispersion of water in oil flow ($D_{W/O}$). The representative photographs of different observed flow patterns in peak configuration are shown in Fig. 4.3. There is no significant influence of this small undulation (undulation is 5°, see Fig. 4.2 for detail dimension of the set up) on the flow patterns at four different sections. Several forces, such as, inertial, surface, buoyancy, viscous and gravity, govern stability of a particular flow pattern.

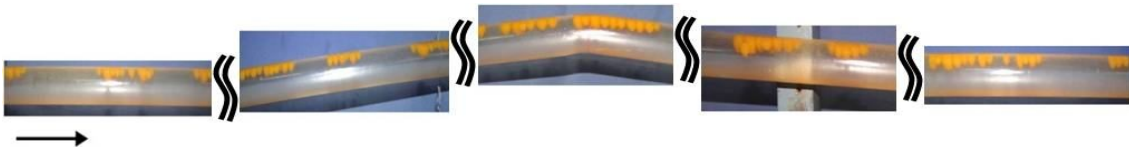

a. Plug flow (P) at U_{SO} = 0.032 m/s, U_{SW} = 0.3 m/s

b. Slug flow (S) at U_{SO} = 0.061 m/s, U_{SW} = 0.23 m/s

c. Stratified Wavy flow (SW) at U_{SO} = 0.165 m/s, U_{SW} = 0.165 m/s

d. Stratified Mixed flow (SM) at U_{SO} = 0.42 m/s, U_{SW} = 0.2 m/s

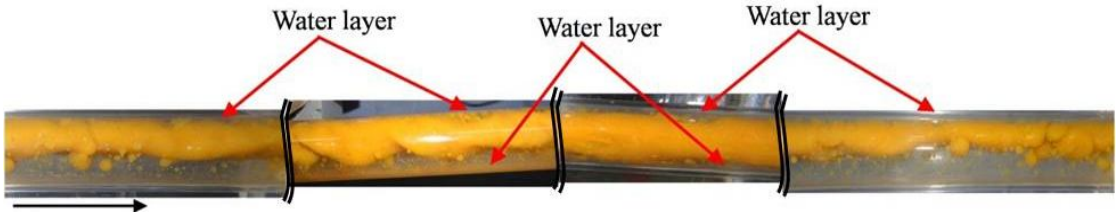

e. Wispy annular flow (A) at U_{SO} = 0.48 m/s, U_{SW} = 0.5 m/s

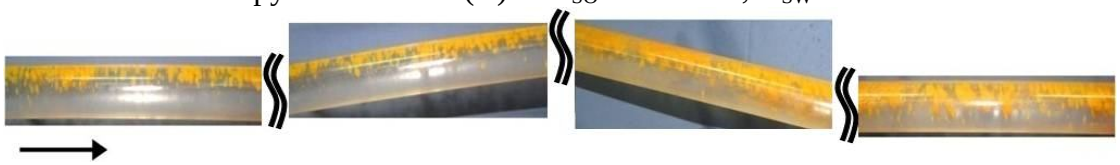

f. Dispersion of oil in water flow ($D_{O/W}$) at U_{SO} = 0.21 m/s, U_{SW} = 0.70 m/s

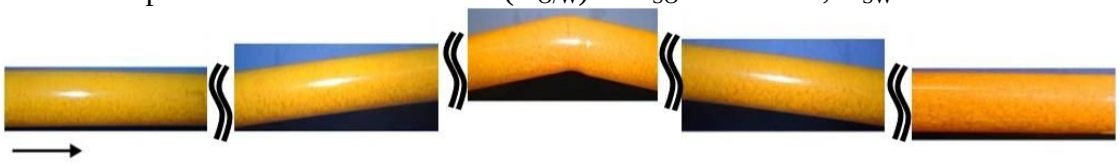

g. Dispersion of water in oil flow ($D_{W/O}$) at U_{SO} = 0.84m/s, U_{SW} = 0.40 m/s

Fig. 4.3. Experimental images of observed flow patterns

At low oil and water velocity (U_{SW} = 0.13 - 0.59 m/s and U_{SO} = 0.017 - 0.28 m/s), surface, buoyancy and gravity forces dominate over inertial and viscous forces. As a result, shape of oil slug nose (Fig. 4.3a and b) and interfacial waves (Fig. 4.3c) vary along the pipeline. Droplet concentration at the interface of stratified mixed flow (Fig. 4.3d) varies across the sections, where viscous, buoyancy and gravity dominate over others. Also observed that, the shape of the lower interfacial wave in wispy annular flow is also changing from section to section (Fig. 4.3e). Concentration of oil droplet in $D_{O/W}$ is more at the downstream section starting from the end of downhill section (Fig. 4.3f). At this section, gravity facilitates the water phase (heavier) to move faster than the oil phase (lighter) and increases the slippage between the phases. As a result, oil droplet concentration increases. Dispersion of water in oil ($D_{W/O}$) flow (Fig. 4.3g) is observed at higher oil velocity (U_{SO} = 0.8 m/s).

4.3.3 Flow pattern maps at four sections and a comparison among them

The observed flow patterns at four different sections (upstream, uphill, downhill and downstream) of the undulated pipeline are presented in the form of flow pattern maps (Fig. 4.4a-d respectively). The superficial velocities of oil (U_{SO}) and water (U_{SW}) are selected as coordinate axes of the plots. Scattered points in Fig. 4.4 represent different flow patterns observed at different phase velocities. Figure 4.4a-d depicts same flow patterns at each section differing in velocity ranges. For a better understanding, four flow pattern maps for four different sections are superimposed on each other in Fig. 4.5 to understand the effect of undulation on flow patterns.

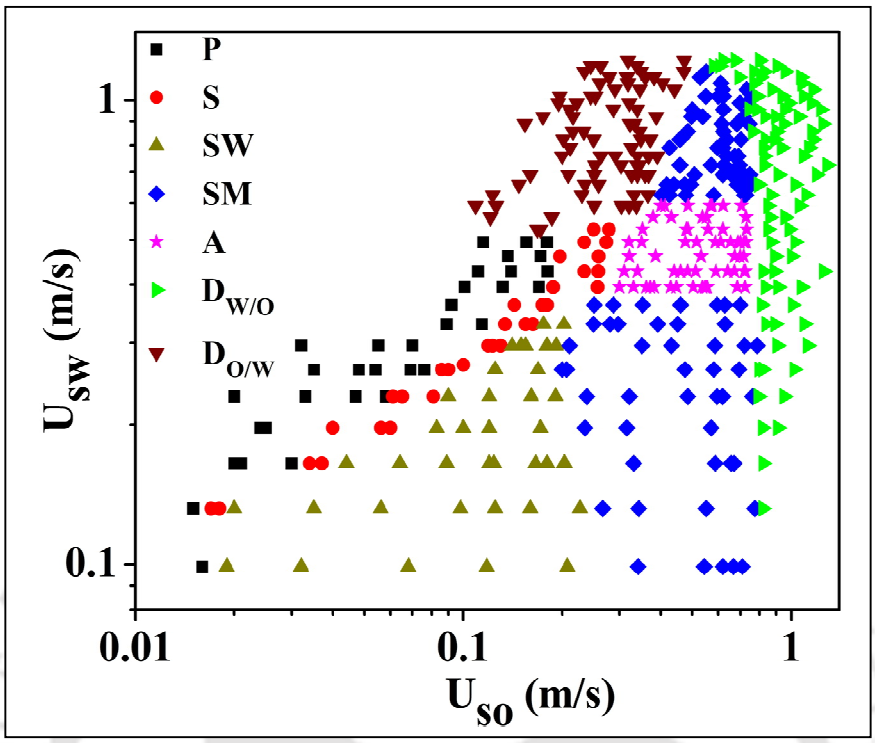

a. Upstream section

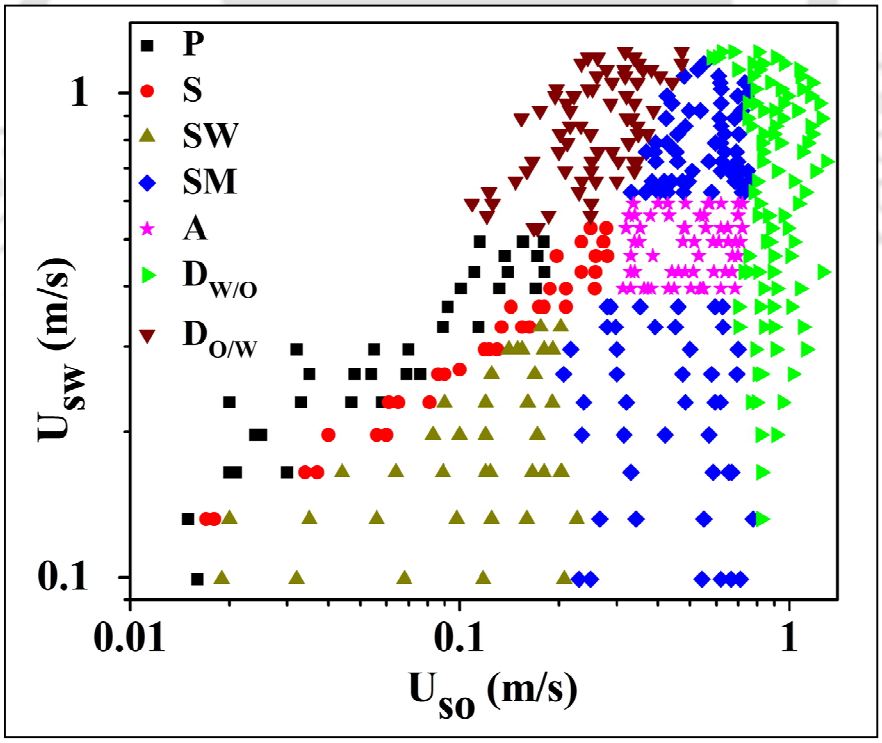

b. Uphill section

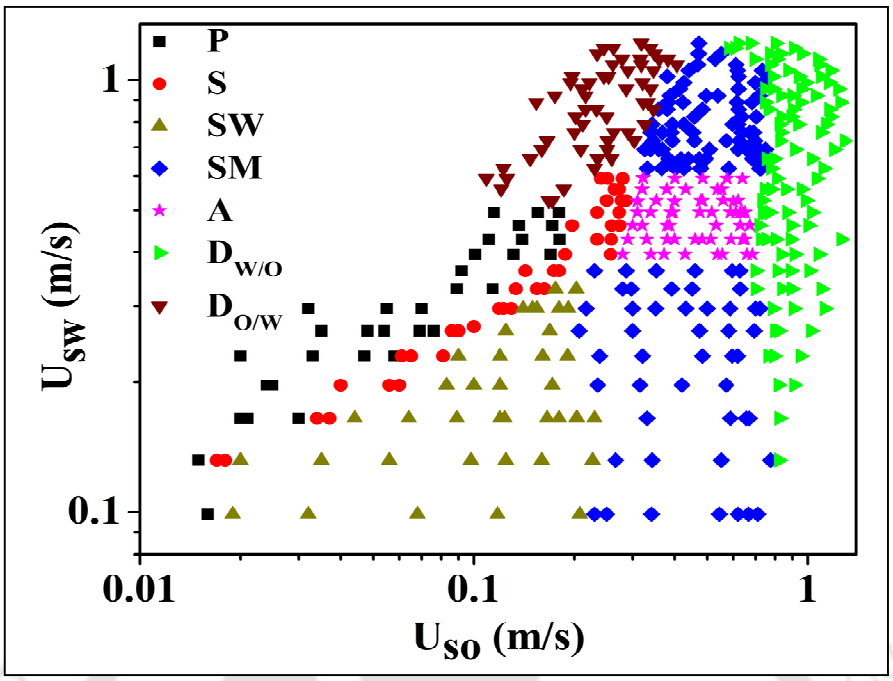

c. Downhill section

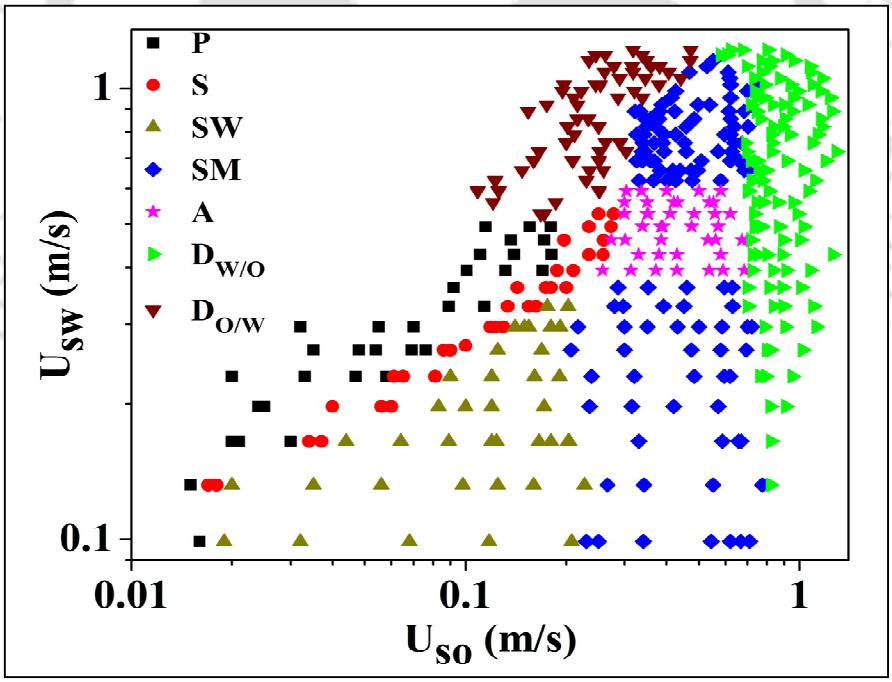

d. Downstream section

Fig. 4.4. Observed flow pattern maps. (P - Plug flow, S - Slug flow, SW - Stratified wavy flow, SM - Stratified mixed flow, A – Wispy annular flow, $D_{W/O}$ - Dispersion of water in oil flow, $D_{O/W}$ - Dispersion of oil in water flow)

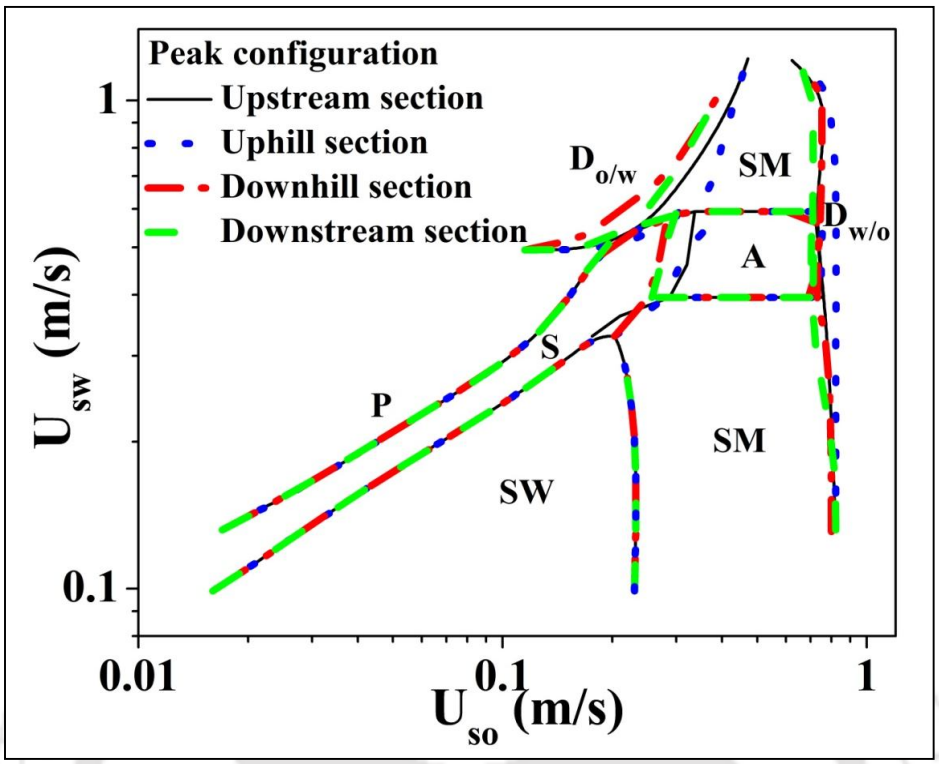

Fig. 4.5. Comparison of flow pattern maps observed at upstream, uphill, downhill and downstream sections (P - Plug flow, S - Slug flow, SW - Stratified wavy flow, SM - Stratified mixed flow, A – Wispy annular flow, $D_{W/O}$ - Dispersion of water in oil flow, $D_{O/W}$ - Dispersion of oil in water flow)

In the Fig. 4.5, solid black color line shows the transitions at upstream section, dotted blue color line shows the transitions at uphill section, red color dash dot line shows the transitions at downhill section and green color dashed line shows the transitions observed at downstream section. The salient features of the observations are described below.

- The transition boundaries of P to S, S to SW, SW to SM and SM to A are almost identical at all the four sections.
- A small variation is observed in the transition of slug to annular flow at upstream and uphill section. Slug flow occupies a larger area in upstream and uphill section as compared to the other sections. Uphill elbow at peak configuration decelerate the

velocity at uphill section (Al-Safran et al. 2005), where, surface force dominates over other forces. As a result, and annular flow breaks up into large slugs giving rise to slug flow.

- Similar deviations are also observed for the transition boundaries of $D_{O/W}$ to SM at upstream and uphill sections. However, $D_{O/W}$ flow is observed at higher oil velocity at these two sections.
- SM to $D_{W/O}$ and A to $D_{W/O}$ flow transition is observed at higher oil velocities at uphill section. Flow direction changes form horizontal to upward inclination at uphill section, where gravity retards the flow and reduces the wave amplitude causing the onset of $D_{W/O}$ at higher velocity.

From the above discussion, it appears that the influence of undulation on flow patterns is reasonably small.

4.3.4 Comparison with horizontal flow pattern map

To find out the effect of peak configuration on hydrodynamics, aforementioned results are compared with horizontal flow pattern map. For this, the upstream flow pattern map of peak configuration has been superimposed on the horizontal flow pattern map as shown in Fig. 4.6. In Fig. 4.6, solid lines indicate the transition boundaries of upstream flow pattern map and the legends represent data of horizontal map. Numerical numbers from 1 to 8 as shown in Fig. 4.6 marks different transition boundaries.

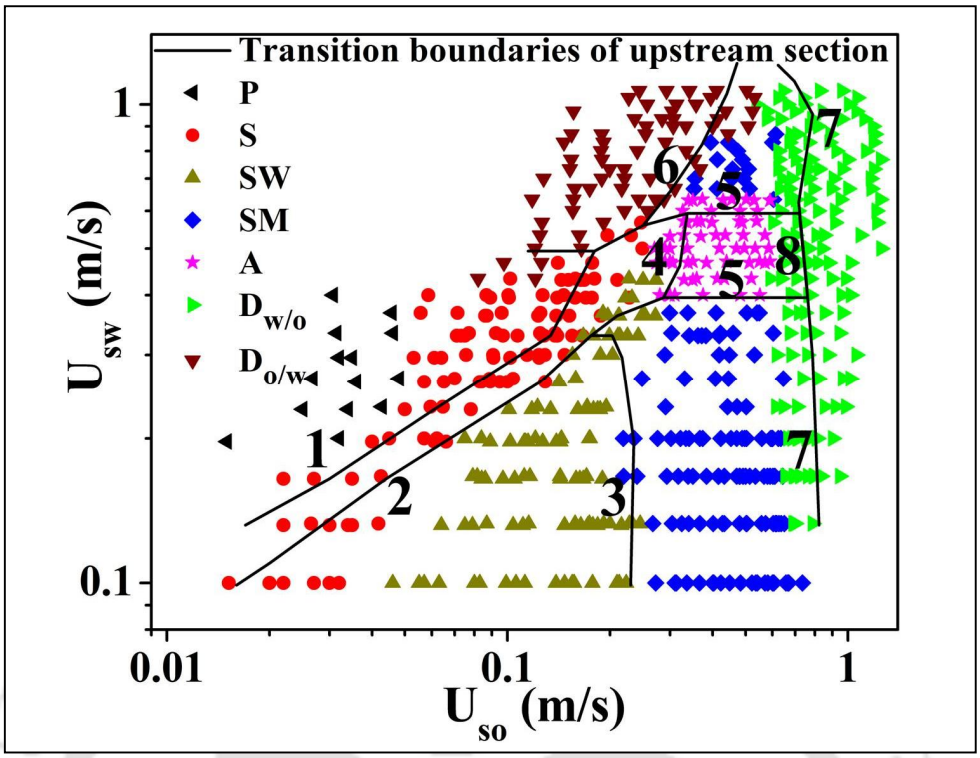

Fig. 4.6. Comparison of upstream section flow pattern map with horizontal map

1. Line 1 represents the transition boundary of plug to slug flow.
2. Line 2 represents the transition boundary of slug to stratified wavy flow.
3. Line 3 represents the transition boundary of stratified wavy to stratified mixed flow.
4. Line 4 represents the transition boundary of slug to wispy annular flow.
5. Line 5 represents the transition boundary of stratified mixed to wispy annular flow.
6. Line 6 represents the transition boundary of oil dispersed in water to stratified mixed flow.
7. Line 7 represents the transition boundary of stratified mixed to water dispersed in oil flow.
8. Line 8 represents the transition boundary of wispy annular to water dispersed in oil flow.

Figure 4.6 shows that transition boundaries of upstream section slightly deviate from the horizontal flow pattern map. The transition of SM to $D_{W/O}$ in undulated pipeline (no. 7) is shifted to higher oil velocities (0.76 m/s) than the horizontal one (0.65 m/s) and the area under stratified mixed flow (SM) is increased in the present work (upstream section). This deviation is due to the presence of undulation in peak configuration, which increases the instability at the interface. Similarly, transition of stratified mixed to dispersion of oil in water flow is shifted towards lower oil velocity (0.47 m/s) as compared to horizontal flow pattern map (0.53 m/s). Small undulation has a negligible effect on the range of wispy annular flow (U_{SW} = 0.63 m/s and 0.6 m/s for horizontal and undulated flow respectively, with same range of oil velocity). This velocity range is in accord with the range reported in literature (Grassi et al. 2008; Poesio et al. 2012).

4.3.5 Effect of viscosity on flow pattern in undulated pipeline

To understand the effect of viscosity on the flow patterns, the present work is compared with the flow pattern maps given by Mandal (2007) for peak configuration. Pipe material, pipe diameter and pipe inclination used in the present study is same as Mandal (2007). The only difference is in the physical properties of oil. Oil viscosity is almost 90 times higher than that of Mandal (2007). Figure 4.7 shows the comparison between these two flow pattern maps at upstream section. In figure, the scattered data points show the experimental results and solid black line shows the flow transitions boundaries observed by Mandal (2007). Dispersion of oil-in-water and water ($D_{O/W\ \&\ W}$) and three layer (TL) flow of Mandal (2007) are considered as dispersion of oil in water ($D_{O/W}$) and stratified mixed flow (SM) respectively in the present work to avoid the complexity in nomenclature of different flow patterns. The salient differences are as follows.

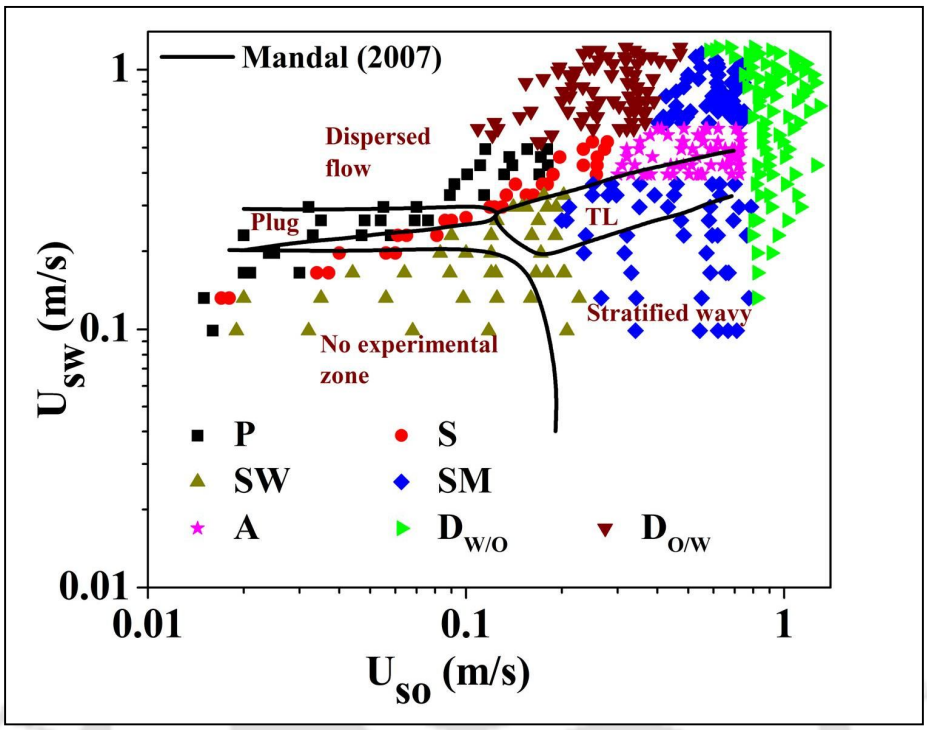

Fig. 4.7. Comparison of upstream flow pattern map with Mandal (2007)

- Slug and Wispy annular flow observed in present work those are not reported by Mandal (2007) because high viscosity favors all these flow. Russell et al. (1959) and Grassi et al. (2008) also observed similar observation in horizontal flow. Plug and stratified mixed flow observed at lower water velocities (0.1 m/s) and occupy larger area of the flow pattern map in the present work (U_{SW} = 0.1 - 1.15 m/s and U_{SO} = 0.2 - 0.76 m/s) as compared to his work (U_{SW} = 0.2 – 0.48 m/s and U_{SO} = 0.12 - 0.7 m/s). Balakhrisna et al. (2010) also reported wide velocity span of such flow at downstream section of a sudden expansion/contraction horizontal pipeline. They used a viscous oil having viscosity of 200 mPa-s. It happens because higher viscosity ratio of the fluids decreases the instability at the interface and favors the stratification in larger domain.

- Velocity range of stratified wavy (U_{SW} = 0.035 - 0.28 m/s and U_{SO} = 0.05 - 0.7 m/s) and dispersion of oil in water flow (U_{SW} = 0.292 - 0.68 m/s and U_{SO} = 0.02 - 0.7 m/s) in his work is larger than the present work (U_{SW} = 0.1 - 0.33 m/s, U_{SO} = 0.02 - 0.23 m/s for SW and U_{SW} = 0.52 - 1.22 m/s, U_{SO} = 0.11-0.47 m/s for $D_{O/W}$). His $D_{O/W}$ flow is shared by plug, slug, stratified mixed and wispy annular flow pattern in the present work. Mandal (2007) and Rodriguez and Oliemans (2006) works show the larger velocity span of stratified wavy flow for low viscous oil, having viscosity = 1.2 mPa s and 7.17 mPa s respectively in horizontal pipeline. Dispersion of oil in water starts at higher phase velocities in the present work. Comparison at other three sections shows quite similar differences as discussed above, except minor deviation in velocity ranges for different flow patterns.

4.3.6 Effect of undulation (peak configuration) on pressure gradient

A comparison of pressure gradient at the upstream (PT1 – PT2), across peak (i.e. combination of uphill and downhill sections, PT3 – PT4) and downstream (PT5 – PT6) sections of peak configuration at different constant water velocities (U_{SW} = 0.2, 0.4, 0.6, 1.0 m/s) have been plotted in Fig. 4.8a to d as a representative results. The distance between the pressure taps of upstream (PT1 – PT2), across peak (PT3 – PT4), downstream (PT5 – PT6) sections are 0.5m, 1.74 m and 0.5 m respectively as shown in Fig. 4.2. This actual distance is used to get pressure gradient from the pressure drop data. Error bars is not shown in Fig. 4.8 (a-d) because experiments are repeated only at few points. The points are at two ends and middle of the entire range of oil velocity. Based on this a 2% average absolute error has been obtained. Figure 4.8a to d depicts that, pressure

gradient at three sections increases with increasing the oil velocity for all the cases. This trend has also been reported by Abduvayt et al. (2006) in their experimental work on hilly terrain pipeline and commonly observed in horizontal (Bensakhria et al. (2004), Grassi et al. (2008)) and inclined (Rodriguez and Oliemans's (2006)) pipeline flow. The pressure gradient in three different section of peak configuration are comparable (Fig. 4.8a and b) at low flow rate (U_{SW} = 0.2 m/s, U_{SW} = 0.4 m/s). At these flow rates pressure gradient decreases from upstream to downstream section. This trend is very similar with the pressure gradient of water only values as shown in Fig. 4.9. Error of single phase pressure drop of water and oil are estimated following the same methodology as done for two-phase flow (mentioned above). The calculation shows 1% and 1.5 % average absolute error for only water and only oil flow respectively. Nevertheless, the pressure gradient at downstream section is lower than that of the upstream and across the peak for all the cases.

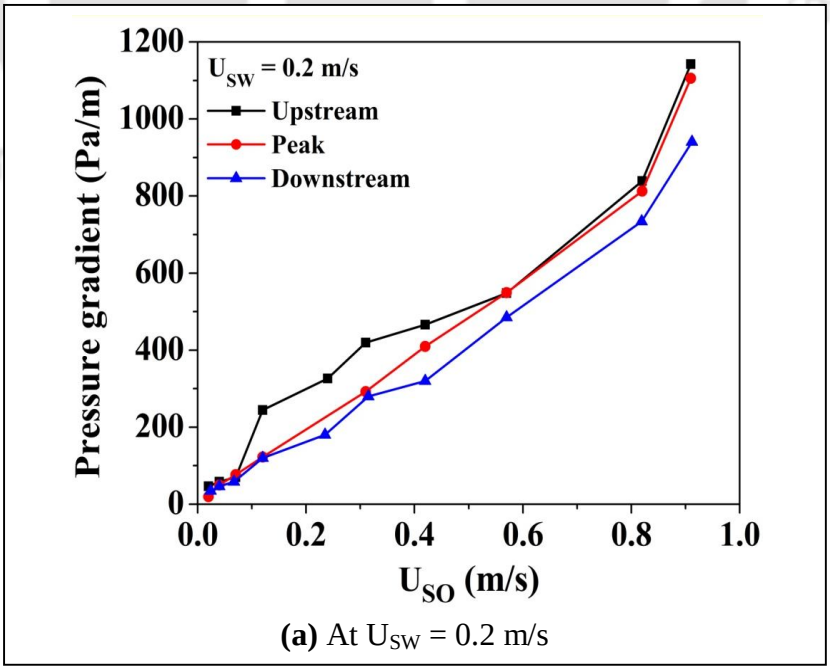

(a) At U_{SW} = 0.2 m/s

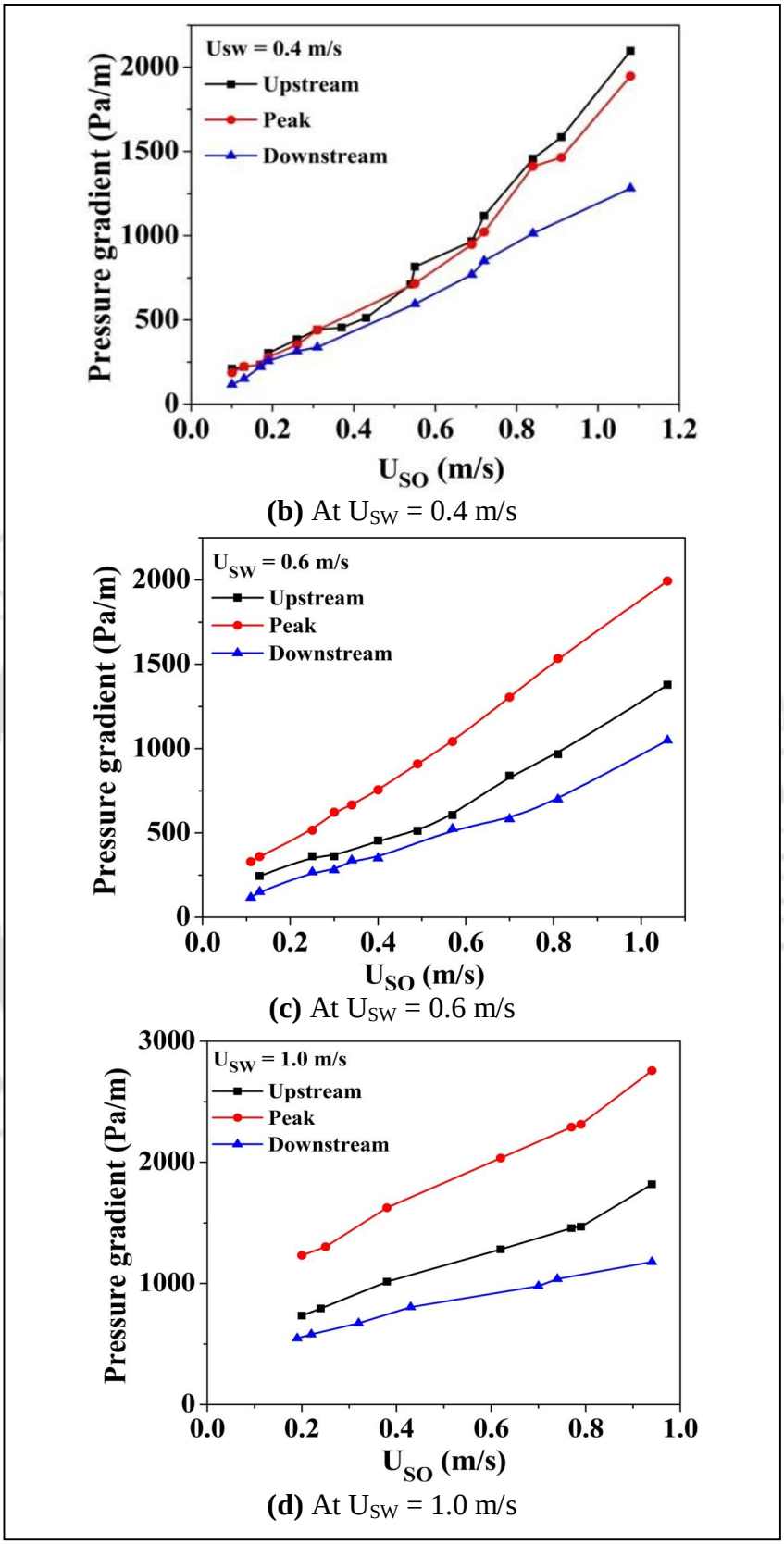

Fig. 4.8. Variation of pressure gradient with increase in oil and water velocities

The pressure gradient of three different section in peak does not remain comparable at intermediate (U_{SW} = 0.6 m/s) and higher water (U_{SW} = 1.0 m/s) flow rate (Fig. 4.8c and d). It is maximum across a peak and minimum at downstream, which is different from water only values (Fig. 4.9). In the peak configuration, the gravity opposes the fluid motion at uphill section. Then fluid losses its energy. On the other hand, the fluid regains its energy at downhill section due to gravity. It accelerates the fluid velocity at downhill section. For these reason, slip is more around the peak and net pressure gradient across the peak increases as shown in Fig. 4.8 a - d.

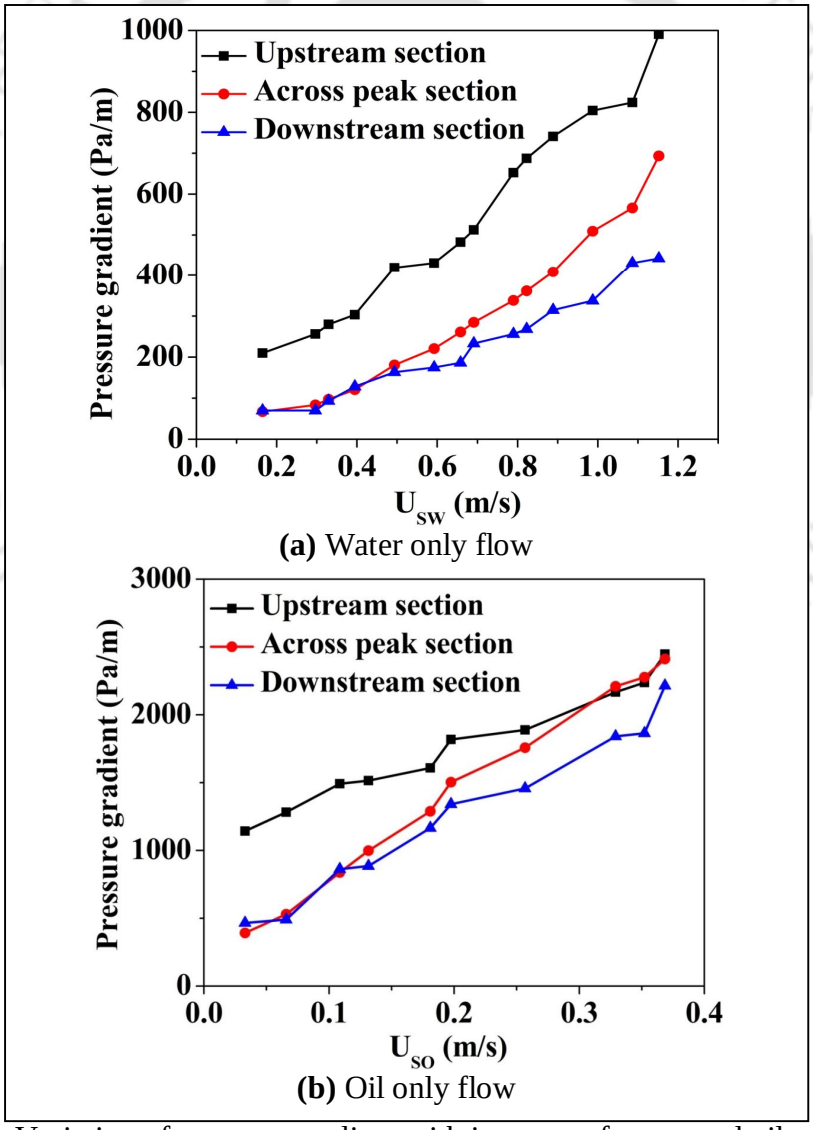

Fig. 4.9. Variation of pressure gradient with increase of water and oil velocities

4.4. Conclusion

In the present work, experiments of oil-water flow have been conducted in undulated pipeline to understand the effect of undulation on the hydrodynamics. For this, a peak configuration (with 5° inclination) is selected to represent undulation along the pipeline. Seven different flow patterns (viz., plug flow, slug flow, stratified wavy flow, stratified mixed flow, wispy annular flow, dispersion of oil in water flow and dispersion of water in oil flow) have been observed at all the four sections. These flow patterns of all four sections are presented in the form of flow pattern maps, and compared with each other. Comparison across the sections shows that small undulation (5°) has a marginal effect on the flow behavior of viscous oil-water mixture. All the flow patterns have been observed in all the cases; however, the range of fluid velocity differs for a particular flow pattern. The velocity span of wispy annular flow obtained in the present study is comparable with the reported literature data. Present work deals with moderately viscous oil. Comparison of experimental results with the work by Mandal (2007) shows that, higher viscosity favors annular, slug and dispersion of water in oil flow pattern as compared to low viscous oils. The pressure drop data indicates that it decreases at downstream section of peak configuration due to the effect of undulation along the flow path. The understanding on the effect of undulation on the hydrodynamics of moderately viscous oil-water two–phase flow would be helpful in industrial design such as, pipe network for oil transportation.

References:

Abdurahman, N. H., Rosli, Y. M., Azhari, N. H. and Hayder, B. A., 2012. Pipeline transportation of viscous crudes as concentrated oil-in-water emulsions. J. Petrol. Sci. Eng. 90–91, 139 – 144.

Abduvayt, P., Manabe, R., Watanabe, T. and Arihara, N., 2006. Analysis of oil/water-flow tests in horizontal, hilly terrain, and vertical pipes. SPE Prod. Oper. 90096, 123 – 133.

Balakhrisna, T., Ghosh, S., Das, G. and Das, P.K., 2010. Oil-water flows through sudden contraction and expansion in a horizontal pipe– Phase distribution and pressure drop. Int. J. Multiphase Flow 36, 13 – 24.

Bennett, A.W., Hewitt, G. F., Kearsey, H. A., Keeys, R. K. F. and Lacey, P. N. C., 1965. Flow visualization studies of boiling at high pressure. Proc. Inst. Mech. Eng. 180 (Part 3), 1 – 11.

Bensakhria, A., Peysson, Y. and Antonini, G., 2004. Experimental study of the pipeline lubrication for heavy oil transport. Oil Gas Sci. Technol. -Rev. IFP 59, 523 – 533.

Charles, M. E., Govier, G. W. and Hodgson, G. W., 1961. The horizontal flow of equal density oil-water mixtures. Can. J. Chem. Eng. 39, 27 – 36.

Grassi, B., Strazza, D. and Poesio, P., 2008. Experimental validation of theoretical models in two-phase high-viscosity ratio liquid-liquid flows in horizontal and slightly inclined pipes. Int. J. Multiphase Flow 34, 950 – 965.

Mandal, T. K. 2007. Some studies on Liquid–liquid slug flow. Ph.D. Thesis, IIT Kharagpur, India.

Poesio, P., Strazza, D. and Sotgia, G., 2012. Two and three-phase mixtures of highly-viscous-oil/water/air in a 50 mm i.d. pipe. Appl. Therm. Eng. 49, 41 – 47.

Rodriguez, O. M. H. and Oliemans, R. V. A., 2006. Experimental study on oil-water flow in horizontal and slightly inclined pipes. Int. J. Multiphase Flow 32, 323 – 343.

Sotgia, G., Tartarini, P. and Stalio, E., 2008. Experimental analysis of flow regimes and pressure drop reduction in oil-water mixtures. Int. J. Multiphase Flow 34, 1161 – 1174.

Chapter 5

CFD simulation of hydrodynamics of viscous oil-water flow through an undulated pipeline in peak configuration

5.1 Introduction

In petroleum industry, the oil-water two-phase flows are widely encountered in production processes such as exploration and transportation. In these applications, two-phase flow can attribute different interfacial configurations called flow regimes or patterns such as plug, slug, wavy, mixed, dispersed, and annular flow. The understanding of flow behavior is important in control, safety operation and design of the downstream separator. The design parameters such as pressure drop, holdup and flow regimes in a single phase flow in conduits can be modeled easily. However the existence of secondary phase such as water can lead to increase the complexity in hydrodynamics, and creates different challenges in modeling the system. In order to predict the pressure drop and holdup precisely, it is necessary to know the flow pattern under specific flow conditions. Computational Fluid Dynamics (CFD) has proven to be an efficient tool for an engineering system investigation that includes fluid flow, design and performance analysis.

There are several types of multiphase models in use, and each exhibits a different level of complexity (Andersson et al. 2012). To carry out simulation in two-phase flow using CFD, one has to select an appropriate model to address the problem accurately. An appropriate selection must be made to ensure that the program is able to utilize the correct continuity equations, and also apply them to the fluids in a way that most accurately mimics real life fluid flow. Each multiphase flow model has applications for which it is best adapted depending on the typical flow regime present in a particular multiphase flow system. The most commonly used multiphase models are the Mixture

model and the Eulerian-Eulerian/VOF models. For separated flows VOF model is most suitable as it predicts the location of the interface while using single phase models to predict flow in each phase.

VOF has been applied successfully in multiphase flow with different pipe orientations such as horizontal, vertical and inclined as discussed above. However, the applicability of VOF in an undulated system (viz., combination of horizontal, upward and downward inclined) has not been investigated. In this chapter, detail analysis on oil-water two-phase flow by applying VOF in an undulated pipeline is presented. Subsequently, VOF method is used to simulate all the flow patterns (except dispersion of oil in water and water in oil), which are experimentally realizable in an equivalent system.

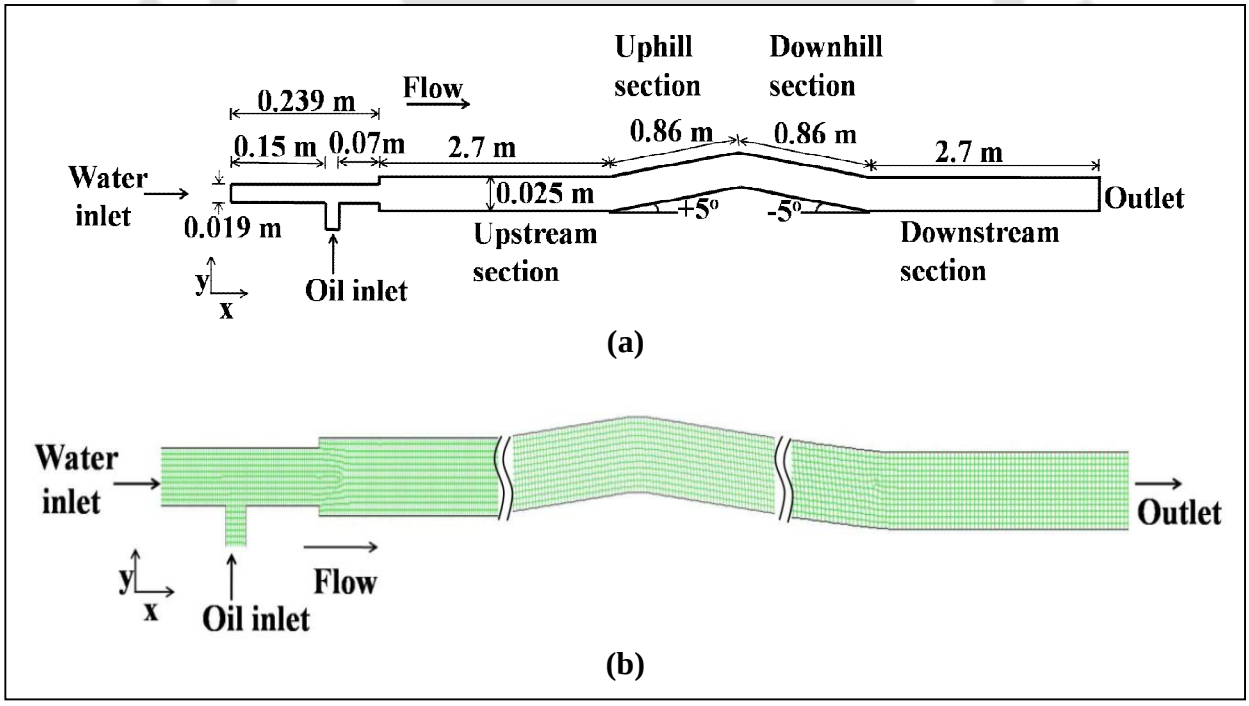

Fig. 5.1. Modeling of the undulated pipeline in peak configuration. **(a)** Detailed dimensions of the model. **(b)** Meshing of the model

5. 2 Model Development

The geometry and detailed dimensions of the concerned conduit considered for the present computational modeling is shown in Fig. 5.1a. The geometry of the system consists of four sections -water inlet, oil inlet, outlet of the pipe and the test section. The test section consists of upstream (US), uphill (UH, inclination: $+5^{o}$), downhill (DH, inclination: -5^{o}) and downstream sections (DS) in the direction of the flow. The fluids were introduced into the pipe through a T-junction (entry section) where water and oil enter into the pipe from the horizontal and vertical directions, respectively. The length and internal diameter of the pipe are 7.36 m and 0.025 m respectively. Water and lubricating oil (Viscosity = 107 mPa s, Density = 890 Kg/m^3) are used as test fluids which has an interfacial tension of 0.024 N/m. The grid was generated using Gambit 2.2, which is compatible with Fluent 6.3.26. Based upon the maximum time step used in the VOF method, initial mesh size is chosen. From the mesh independent study, system with 45682 cells is selected as optimum mesh elements and this number is used throughout the simulation. The meshed geometry is shown in Fig. 5.1b. Quadrilateral mesh geometry is selected to account for the surface tension effect more accurately.

The CFD software package of ANSYS FLUENT^{TM} has been used for simulating the flow. The computation has been performed by assuming unsteady flow, immiscible liquid pair, constant liquid properties, co-axial flow in the pipe and a T- junction ('T') as the entry section. In the present model, the two fluids share a well defined interface. Volume of Fluid (VOF) approach for two phase modeling has been selected in Fluent. VOF solves a single set of momentum equations which is shared by both the fluids.

5.2.1 Volume of Fluid (VOF) Approach

In the VOF model, both phases share the same control volume and a single set of conservation equations is shared by the both the phases using mixture properties. In addition, if the control volume is occupied by one of the phases, its related properties are utilized. VOF method is beneficially utilized because it is able to simulate the profile deformation of the continuous interface and dispersed phase particles (i.e. droplets, bubbles) (Delnoij et al. 1999). Therefore, it is appropriate to use as an application that focuses on simple flow pattern problems as seen in pipelines (slug, stratified wavy, stratified mixed and annular). Brief discussion on governing equations, treatment of the interface and boundary conditions is discussed in Chapter 2 and details can be obtained from Fluent user's guide (2006).

5.3. Results and Discussion

In the present study, using VOF model, successfully predicted plug (Fig. 5.2a), slug (Fig. 5.2b), stratified wavy (Fig. 5.2c), stratified mixed (Fig. 5.2d) and annular (Fig. 5.2e) flow patterns as shown in Fig. 5.2. The other flow patterns, dispersion of oil in water and water in oil observed at higher phase velocities are difficult to predict by using VOF. This is due to the method of interface reconstruction scheme of VOF model, which fails to capture the waviness of oil-water interface properly (Ghosh et al. 2011). Therefore, the dispersed flow patterns observed at higher phase velocities are not simulated in this study. Below, different flow patterns investigated using simulations at different velocities are discussed. Subsequently, annular flow characteristics observed in the present system is also discussed.

5.3.1. Different flow patterns

- **Plug flow (P):** This flow pattern is observed at lower velocities of both the phases. Fig. 5.2a shows a snapshot from our simulation at oil (U_{SO}) and water (U_{SW}) velocities of 0.025 m/s and 0.197 m/s respectively. The oil plugs appears in the continuous water phase. These plugs float up in water due to the effect of buoyancy.

- **Slug flow (S):** Simulation at higher oil velocity (U_{SO} = 0.04 m/s) keeping water velocity constant (at U_{SW} = 0.197 m/s as mentioned above for plug flow) shows that oil plugs become larger (Fig. 5.2b). A distinct water bridge between two consecutive large oil droplets is observed and it is known as slug flow. The length of the slugs is comparable with the internal diameter of the pipe.

- **Stratified wavy flow (SW):** In this flow pattern oil and water are separated with a wavy oil/water interface. These waves formed at the interface and are affected by the angle of inclination (See Fig. 5.2c). This flow pattern is simulated at same water velocity (U_{SW} = 0.197 m/s) as mentioned for plug and slug flow and at higher oil velocity (U_{SO} = 0.085 m/s).

- **Stratified mixed flow (SM):** When the oil velocity (U_{SO} = 0.235 m/s) is above SW flow, the wave ruptures to form droplets at the interface. This results in the formation of three layers or mixed flow pattern with oil at the top, water at the bottom, and mixed layer comprising of oil and water droplets present in the middle. The simulated result at this velocity is shown in Fig. 5.2d (keeping water velocity constant at U_{SW} = 0.197 m/s).

- **Annular flow (A):** This flow pattern is noticed at moderate velocities of oil (U_{SO} = 0.3-0.73 m/s) and water (U_{SW} = 0.4-0.6 m/s). In this flow pattern, oil flows at the center of the pipe as a continuous core and the water flows as an annulus and in contact with the pipe wall. A simulated result of this pattern at U_{SO} = 0.46 m/s and U_{SW} = 0.46 m/s is shown in Fig. 5.2e.

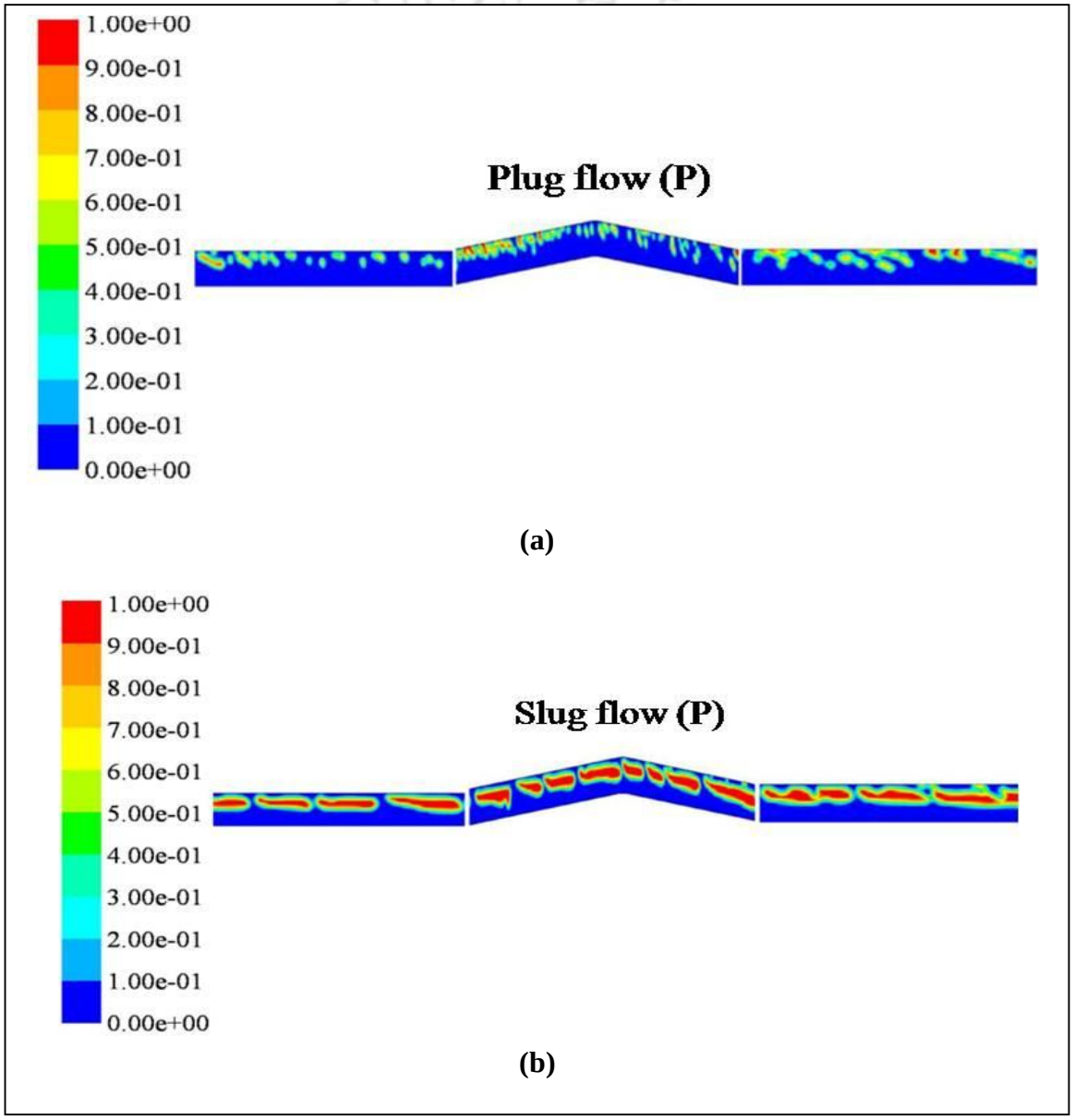

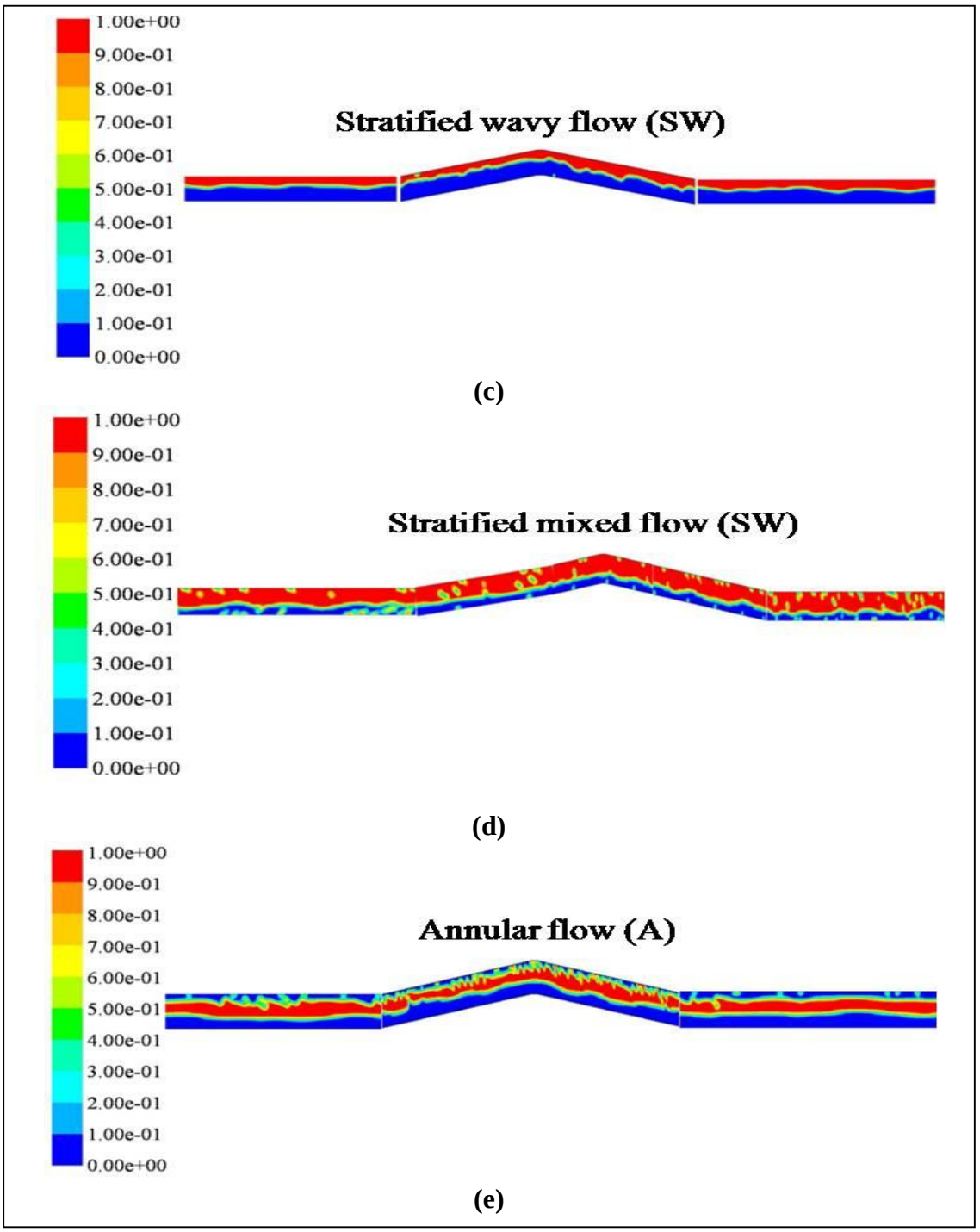

Fig. 5.2. Simulation results of flow patterns. **(a)** Plug flow at U_{SO} = 0.025 m/s and U_{SW} = 0.197 m/s. **(b)** Slug flow at U_{SO} = 0.04 m/s and U_{SW} = 0.197 m/s. **(c)** Stratified wavy flow at U_{SO} = 0.085 m/s and U_{SW} = 0.197 m/s. **(d)** Stratified mixed flow at U_{SO} = 0.235 m/s and U_{SW} = 0.197 m/s. **(e)** Annular flow at U_{SO} = 0.32 m/s and U_{SW} = 0.46 m/s.

Simulated results of all the flow patterns investigated at different water and oil velocities are compared with experimental results shown in Fig. 4.4. Simulation results are superimposed on the experimental flow pattern map of undulated pipeline in peak configuration as shown in Fig. 5.3.

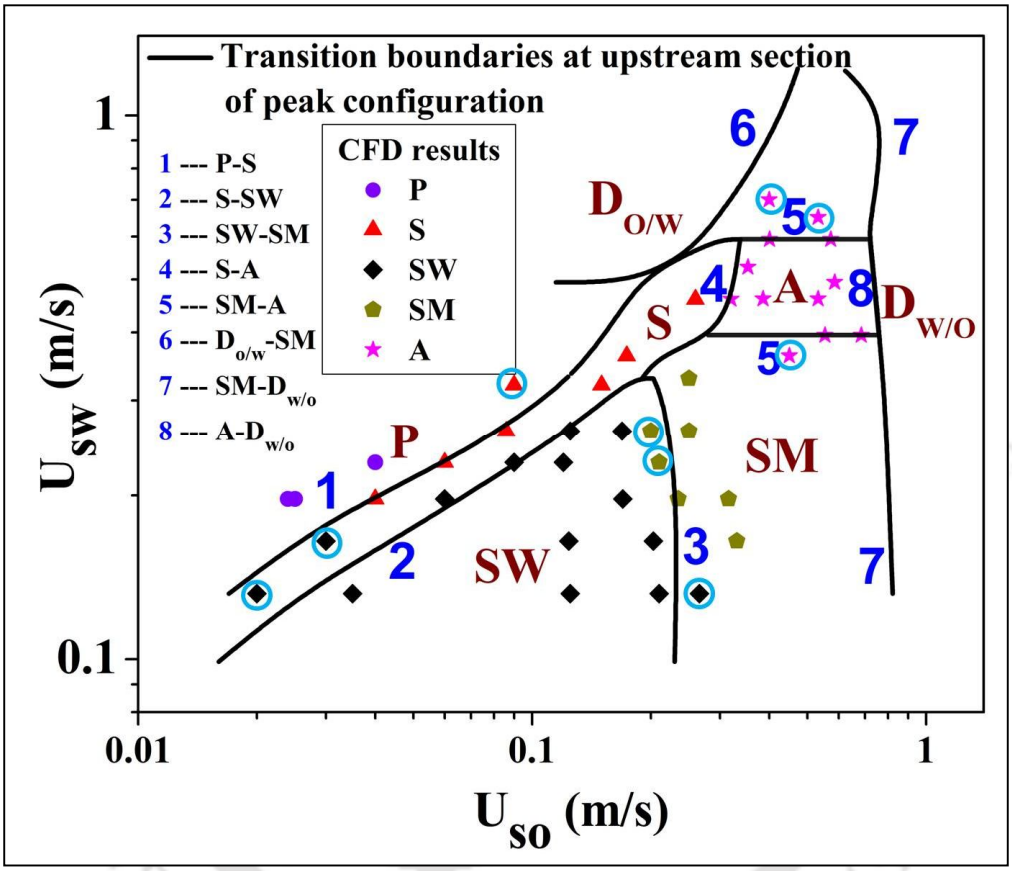

Fig. 5.3. Comparison with upstream transition boundaries of peak configuration

In Fig. 5.3, the solid lines depict the transition boundaries of different flow patterns and these are numbered from 1 to 8.

Line 1 represents the transition boundary of plug to slug flow.

Line 2 represents the transition boundary of slug to stratified wavy flow.

Line 3 represents the transition boundary of stratified wavy to stratified mixed flow.

Line 4 represents the transition boundary of slug to annular flow.

Line 5 represents the transition boundary of stratified mixed to annular flow.

Line 6 represents the transition boundary of oil dispersed in water to mixed flow.

Line 7 represents the transition boundary of stratified mixed to water dispersed in oil flow.

Line 8 represents the transition boundary of annular to water dispersed in oil flow.

The scattered points in Fig. 5.3 represent different flow patterns observed in CFD simulation. Almost all the flow patterns are predicted with good accuracy, and mismatching points are marked by circles in Fig. 5.3. It shows only one mismatching point in plug flow region and two mismatching points in slug flow region. These points are lying close to the respective transition boundaries. Similarly, marginal deviation is observed at transition boundary of stratified wavy to stratified mixed flow (Fig. 5.3). The region of annular flow shows good conformity with the experimental region of present work.

5.3.2 Comparison with horizontal flow pattern map

To elucidate the effect of undulation on flow patterns, simulation results are compared with the horizontal flow pattern map as shown in Fig. 5.4. Solid lines and different legends in Fig. 5.4 indicate the experimental transition boundaries and simulation data points of present work. Numerical numbers from 1 to 3 as shown in Fig. 5.4 marks different transition boundaries of horizontal flow pattern map, as follows:

1. Line 1 represents the transition boundary of plug to slug flow.
2. Line 2 represents the transition boundary of slug to stratified wavy flow.

3. Line 3 represents the transition boundary of stratified wavy to stratified mixed flow.
4. Line 4 represents the transition boundary of annular to stratified mixed flow

In the present work only five flow patterns (viz., plug, slug, stratified wavy, stratified mixed and annular flow) are observed. Fig. 5.4 shows that almost all the flow patterns obtained from the simulation (present work) are well matched with the corresponding flow region reported in horizontal flow map. Few simulated data points of SW pattern at lower water velocities (U_{SW} = 0.132 m/s to 0.197 m/s) deviate slightly from the horizontal flow pattern map. Those are appearing in slug flow region of horizontal flow pattern map. Simulated results of SW pattern are also in the range of horizontal map reported by Nadler and Mewes (1997), Trallero et al. (1997). The simulation results also show the annular flow within the velocity range of U_{SW} = 0.4 - 0.6 m/s and U_{SO} = 0.3 - 0.6 m/s. This velocity range is in almost accord with the range reported in literature (Grassi et al. 2008; Sotgia et al. 2008 and Poesio et al. 2012).

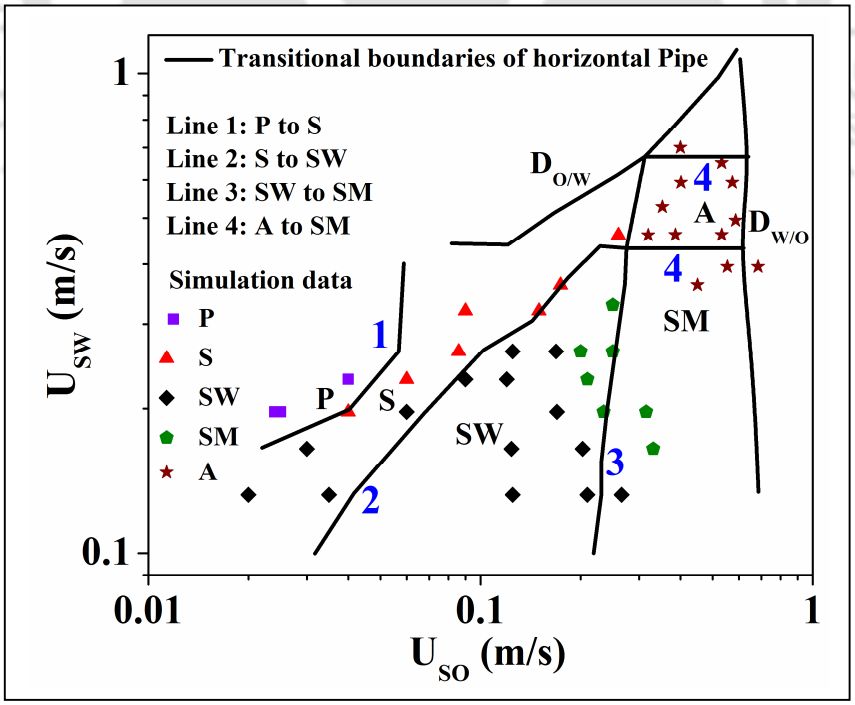

Fig. 5.4. Comparison with transition boundaries of horizontal pipeline

5.4 Annular flow characteristics

Annular flow is a frequently occurring flow regime in many industrial applications. It occurs in the transportation of oil and natural gas (Manabe et al. 2001), petrochemical processes, and refrigeration systems (Mac Gillivray et al. 2002). Annular flow is mainly inertia driven flow with little effect of buoyancy. During this flow regime, oil phase flows continuously as core and water phase as annulus making complete contact with pipe wall (Joseph et al. 1997; Grassi et al. 2008). In the present study, annular flow is observed at different water velocities (U_{SW} = 0.4 m/s, 0.5 m/s and 0.6 m/s) keeping oil velocity (U_{SO}) constant at 0.35 m/s. The snapshots from simulation at these three velocities are shown in Fig. 5.5. From the figure, a thin layer of water is seen at upper inner wall of the pipe with a wavy interface. The same type of annular flow has been observed in various experimental systems and the flow range investigated from simulation is in accord with the literature (Grassi et al. 2008; Sotgia et al. 2008; Yusuf et al. 2012 and Poesio et al. 2012).

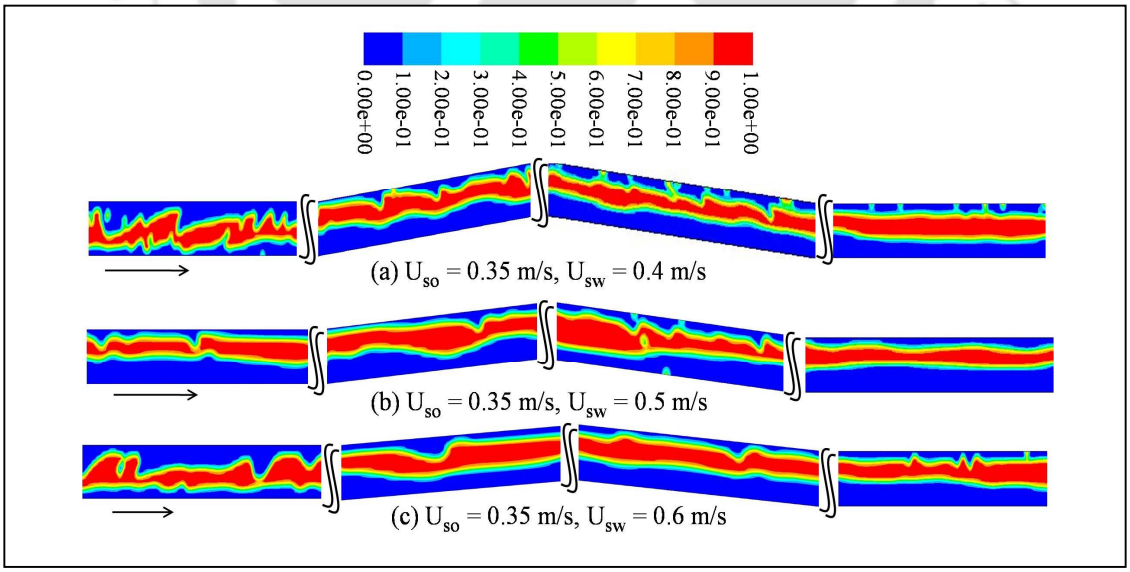

Fig. 5.5. Simulation result of annular flow (A) at different water velocities

Pressure, velocity and volume fraction of annular flow have been measured numerically at a cross section which is a vertical line (Positive Y-direction) shown in Fig. 5.6.

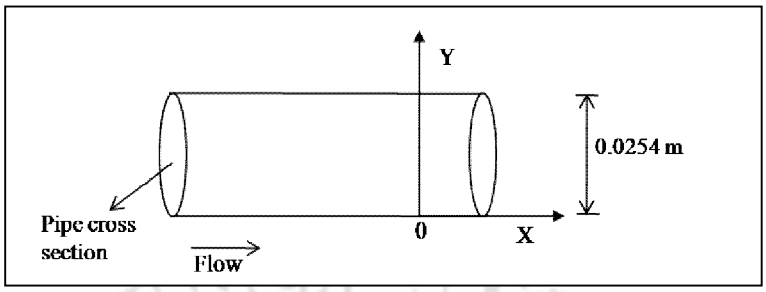

Fig. 5.6. Schematic of measurement of flow characteristics across the pipe cross section

Fig. 5.7 represents the flow characteristics of annular flow, namely pressure (Fig. 5.7a), velocity profile (Fig. 5.7b) and volume fraction (Fig. 5.7c) along the pipe cross section. In Fig. 5.7a, Variation of total pressure at constant oil velocity (U_{SO} = 0.35 m/s) and at different water velocities (U_{SW} = 0.4 m/s, 0.5 m/s and 0.6 m/s) in upstream section of the pipe is shown. From Fig. 5.7a, by increasing the water velocity from U_{SW} = 0.4 m/s to 0.5 m/s (for a constant oil velocity, U_{SO} = 0.35 m/s), clearly observed the decrease of pressure, which is a characteristics of annular flow (Rovinsky et al. 1997; Panda et al. 2001 and Bensakhira et al. 2004). However, pressure moderately increases on increasing U_{SW} from 0.5 m/s to 0.6 m/s. Therefore, the annular flow is most stable around U_{SW} = 0.5 m/s (with U_{SO} = 0.35 m/s) and unstable beyond U_{SW} = 0.6 m/s. The trend of pressure from our simulation are in excellent agreement with the experimental observations reported by Poesio et al. (2012) and Sotgia et al. (2008) in two-phase flow through a horizontal pipe. Similarly, variation of velocity and oil volume fraction along the positive Y-axis is shown in Fig 5.7b and 5.7c. Variation of mixture velocity (Fig. 5.7b) near the wall is more than the center of the pipe, which are the typical characteristics of annular flow (Ghosh et al. 2011 and Kaushik et al. 2012). Even velocity at centre is almost

constant (negligible velocity gradient) for U_{SW} = 0.5 m/s and 0.6 m/s. Magnitude of velocity is highest at this region. Variation of oil volume fraction along the cross section (Fig. 5.7c) helps in finding the thickness of water layer during the annular flow. Simulation shows maximum oil volume fraction at the oil core and minimum in annular region as expected. The volume fraction data obtained from the simulation across the peak section shows 10.8% over prediction when compared with the experimental data as shown in Fig. 5.8.

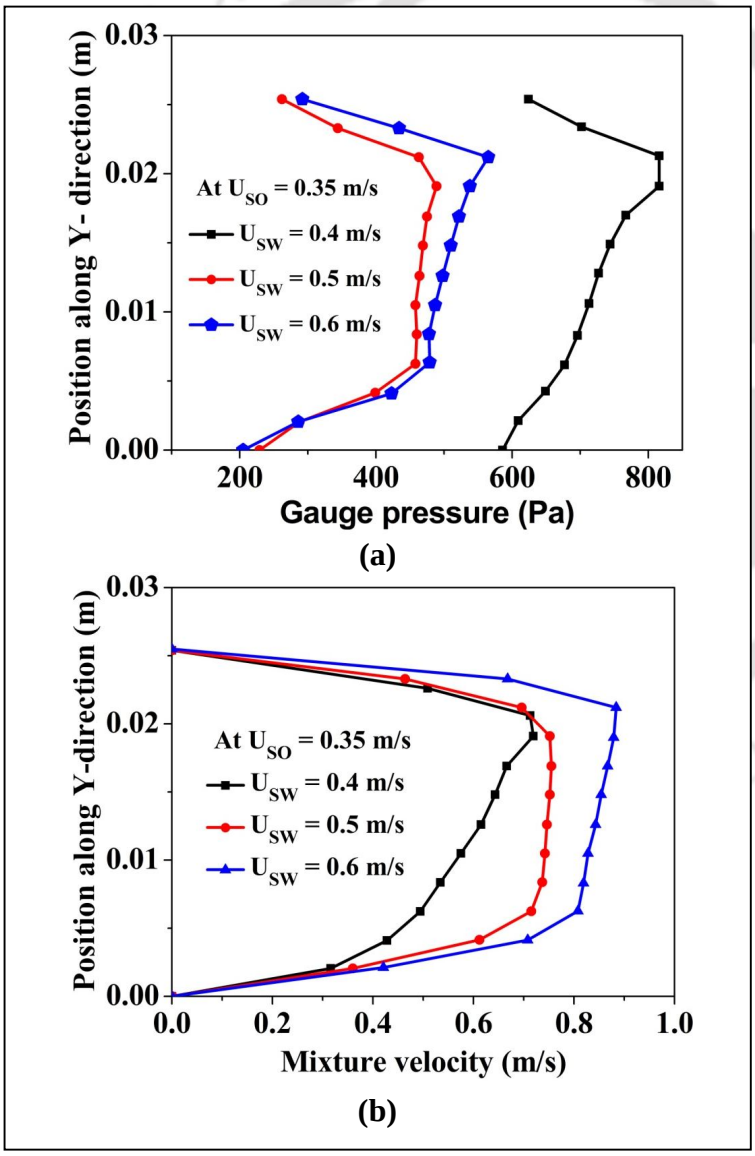

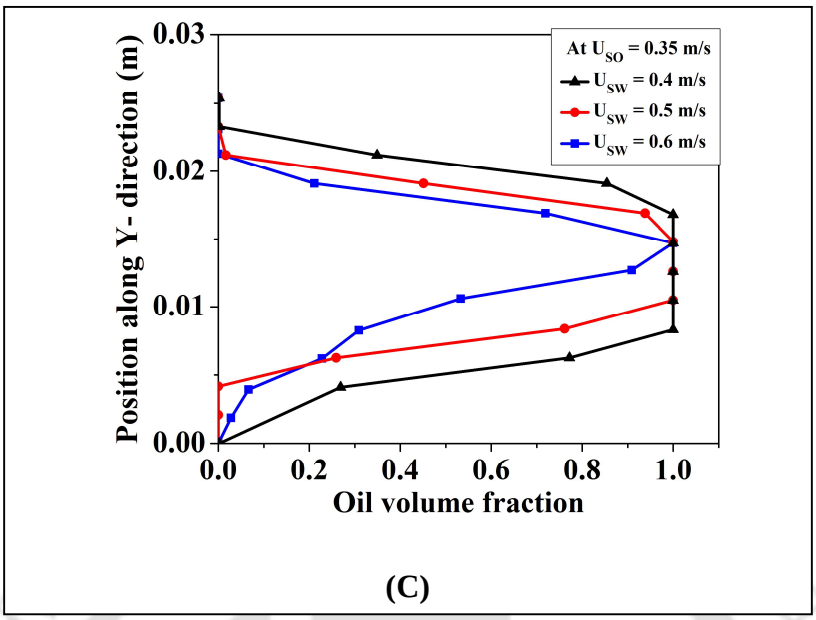

Fig. 5.7. Annular flow characteristics. **(a)** Pressure profile **(b)** Velocity profile **(c)** Oil volume fraction profile.

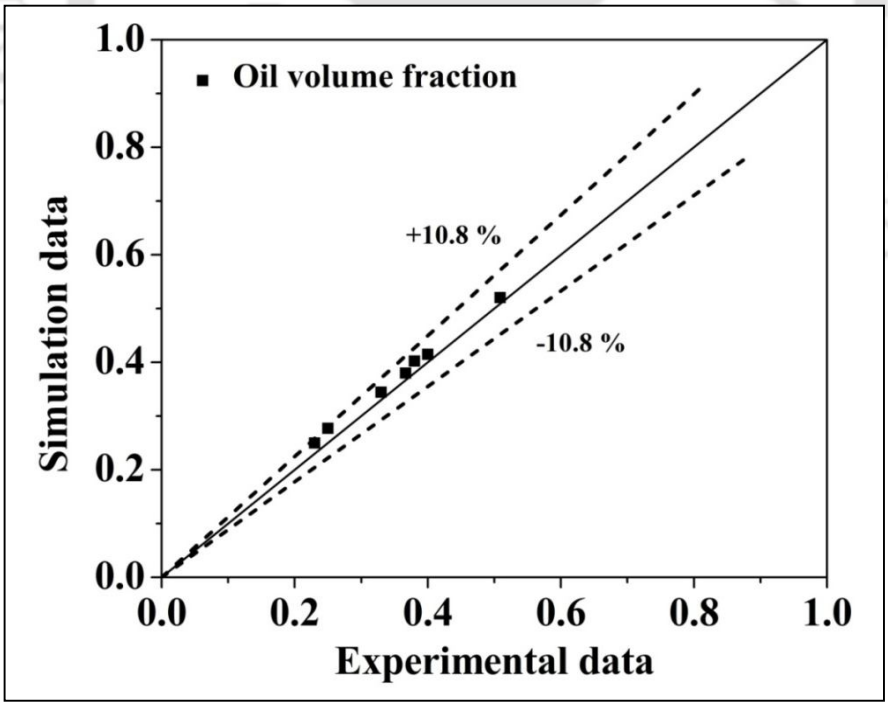

Fig. 5.8 Validation of oil volume fraction across the peak section of the annular flow

5.5 Conclusion

Flow patterns of viscous oil-water two-phase flow through an undulated pipeline are predicted using computational fluid dynamics. Based on the grid independent study, 45682 numbers of cells are selected as optimum number of cells for simulation. Using VOF method successfully simulated plug and slug flow along with other separated flow patterns (viz., stratified wavy, stratified mixed and annular flow). Simulated results of flow patterns are compared with the experimental results and noticed good conformity between the results except at lower water velocities. Simulation results are compared with literature data to show the effect of viscosity. Comparison shows that, higher viscous oil favors the formation of slug and annular flows and earlier transition of plug and stratified wavy flow pattern. There is no effect of undulation on flow patterns when results compared the results with horizontal experimental and simulation flow pattern maps. The flow conditions and fluid properties are same in both the studies. Annular flow characteristics have been discussed and noticed decrease in pressure when increasing the water velocity during the annular flow. Annular flow region is successfully simulated and noticed good conformity when compared with the literature data. The present findings reveal the inherent ability of VOF to predict almost entire flow pattern map with excellent accuracy except two dispersed regions.

Reference

Andersson, B., Andersson, R., Hakansson, L., Mortensen, M., Sudiyo, R. and van Wachem, B., "Computational Fluid Dynamics for Engineers," Cambridge University Press: New York (2012).

Bensakhria, A., Peysson, Y. and Antonini, G., "Experimental study of the pipeline lubrication of heavy oil transport," Oil Gas Sci. Technol. –Rev. IFP, **59**, 523 – 533 (2004).

Delnoij, E., Kuipers, J. A. M. and van Swaaij, W. P. M., "A three - dimensional CFD model for gas-liquid bubble columns," Chem. Eng. Sci., **54**, 2217 – 2226 (1999).

Fluent 6.3 User's Guide, Fluent Inc., Lebanon, USA (2006).

Ghosh, S., Das, G. and Das, P. K., "Simulation of core annular downflow through CFD–A comprehensive study," Chem. Eng. Process., **49**, 1222 – 1228 (2010).

Ghosh, S., Das, G. and Das, P. K., "Simulation of core annular in return bends – A comprehensive CFD study," Chem. Eng. Res. Des. **89**, 2244 – 2253 (2011).

Grassi, B., Strazza, D. and Poesio, P., "Experimental validation of theoretical models in two-phase high-viscosity ratio liquid-liquid flows in horizontal and slightly inclined pipes," Int. J. Multiphase Flow, **34**, 950 – 965 (2008).

Joseph, D. D., Bai, R., Chen, K. P., Renardy, Y. Y., "Core-annular flows," Ann. Rev. Fluid Mech., **29**, 65 (1997).

Kaushik, V. V. R., Ghosh, S., Das, G. and Das, P. K., "CFD simulation of core annular flow through sudden contraction and expansion," J. Pet. Sci. Eng., **86-87,** 153 – 164 (2012).

Mac Gillivray, R. M. and Gabriel, K. S., "Annular flow film characteristics in variable gravity," Annals of the New York Academy of Sciences, **974**, 306 – 315 (2002).

Manabe, R., Zhang, H. Q., Delle-Case E. and Brill, J. P., "Crude oil-natural gas two-phase flow pattern transition boundaries at high pressure conditions," SPE Annual Technical Conference and Exhibition, Paper no. **71563**, Louisiana (2001).

Nadler, M. and Mewes, D., "Flow induced emulsification in the flow of two immiscible liquids in horizontal pipes," Int. J. Multiphase Flow, 23, 55 – 68 (1997).

Parda, V. J. W. and Bannwart, A. C., "Modeling of vertical core-annular flows and application to heavy oil production," J. Energy Resour. Technol. ASME, **123**, 194 – 199 (2001).

Poesio, P., Strazza, D. and Sotgia, G., "Two and three-phase mixtures of highly-viscous-oil/water/air in a 50 mm i.d. pipe," Appl. Therm. Eng. **49**, 41 – 47 (2012).

Rovinsky, J., Brauner, N. and Moalem, M. D., "Analytical solution for laminar two-phase flow in a fully eccentric core annular configuration," Int. J. Multiphase Flow, **23**, 523 – 543 (1997).

Sotgia, G., Tartarini, P. and Stalio, E., "Experimental analysis of flow regimes and pressure drop reduction in oil-water mixtures," Int. J. Multiphase Flow, **34**, 1161 – 1174 (2008).

Yusuf, N., Al-Wahaibi, Y., Al-Wahaibi, T., Al-Ajmi, A., Olawale, S. and Mohammed, I. A., "Effect of oil viscosity on the flow structure and pressure gradient in horizontal oil-water flow," Chem. Eng. Res. Des. **90**, 1019 – 1030 (2012).

Chapter 6

Flow pattern investigation of viscous oil-water flow through an undulated pipeline in valley configuration by experiment and CFD simulation

6.1 Introduction

Pipeline transportation is a common and most efficient process to supply crude oil from its sources (viz., oil well) to refineries for further processing. The transportation line is basically a pipe network consists of a number of interconnected horizontal and inclined sections, resulting undulation or hilly terrain along the pipe line. The hydrodynamics of multiphase flow through undulated or hilly terrain pipeline is distinct from horizontal or inclined flow. Parametric information of such hydrodynamics is essential for designing of a realistic pipe network. A vast majority of research work is devoted to the flow in horizontal and inclined (including vertical) pipelines. A combination of horizontal and inclined (viz., valley configuration) would behave differently than that of horizontal or inclined alone.

Although the hydrodynamics of low viscous oil-water flow through hilly terrain and undulated pipeline has been studied, the flow behavior of moderately viscous oil- water flow is poorly understood. In this chapter, experimental and CFD simulated results on an undulated pipeline with valley configuration (viz., it consists of two interconnected horizontal, one upward and one downward inclined (±5°) section) are reported. Further experimental findings of various flow patterns of moderately viscous oil-water flow (oil viscosity = 107 mPa s) are described and subsequently, CFD simulation results based on VOF (Fluent 6.3) model for two-phase flow are also discussed. Finally, results of present findings are compared with the literature.

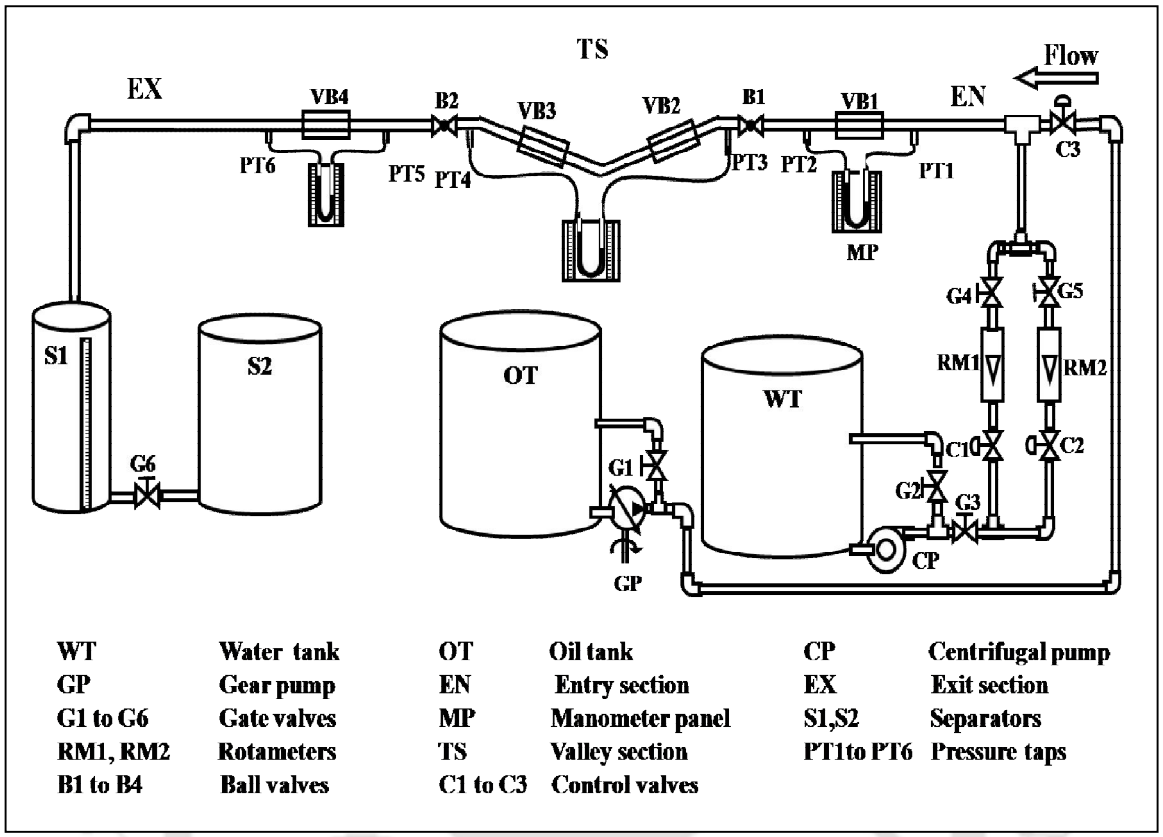

Fig. 6.1. Schematic representation of experimental setup

6.2 Experimentation

The schematic representation of the experimental setup used for the identification of flow patterns during viscous oil-water flow through undulated pipeline (valley configuration) is shown in Fig. 6.1. It consists of an entry section (EN), a test section (TS) and an exit section (EX) in the direction of flow of liquids. Exit section is connected with separator (S). Test section is made up with 0.025 m internal diameter transparent perspex pipe (for better visualization and imaging studies) and consists of four sections: upstream, downhill, uphill and downstream sections in the direction of flow. In the test section, four

view boxes (VB1-VB4) are provided to minimize the lens effect of pipe material during the photography. Detailed experimentation and flow pattern measuring techniques are discussed in chapter 2.

6.3 Model development

Figure 6.2a shows detailed dimensions of the conduit geometry considered in the present computational work to mimic the actual experimental test loop. The geometry consists of an interconnected downhill and uphill section in between two horizontal pipes with an internal diameter and a length of 0.025 m and 7.36 m respectively. Oil and water were introduced into the pipe through a T-junction at the entry section where water and oil enter into the pipe from the horizontal and vertical directions, respectively. The CFD software package of ANSYS FLUENT^{TM} has been used for simulation. Meshing of the model has been done using GAMBIT. Fig. 6.2b shows the 2D-mesh of the pipe used in simulation.

The mesh consists of 50117 quadrilateral mesh elements for entire pipe geometry. Quadrilateral mesh geometry is selected for accounting surface tension effect more accurately (Fluent user's guide 6.3, 2006). Volume of Fluid (VOF) approach for two phase modeling has been selected in Fluent in which two fluids share a well defined interface. VOF solves a single set of momentum equations, which is shared by both the fluids. The details of the governing equations, boundary conditions and the treatment of the interface is shown in chapter2.

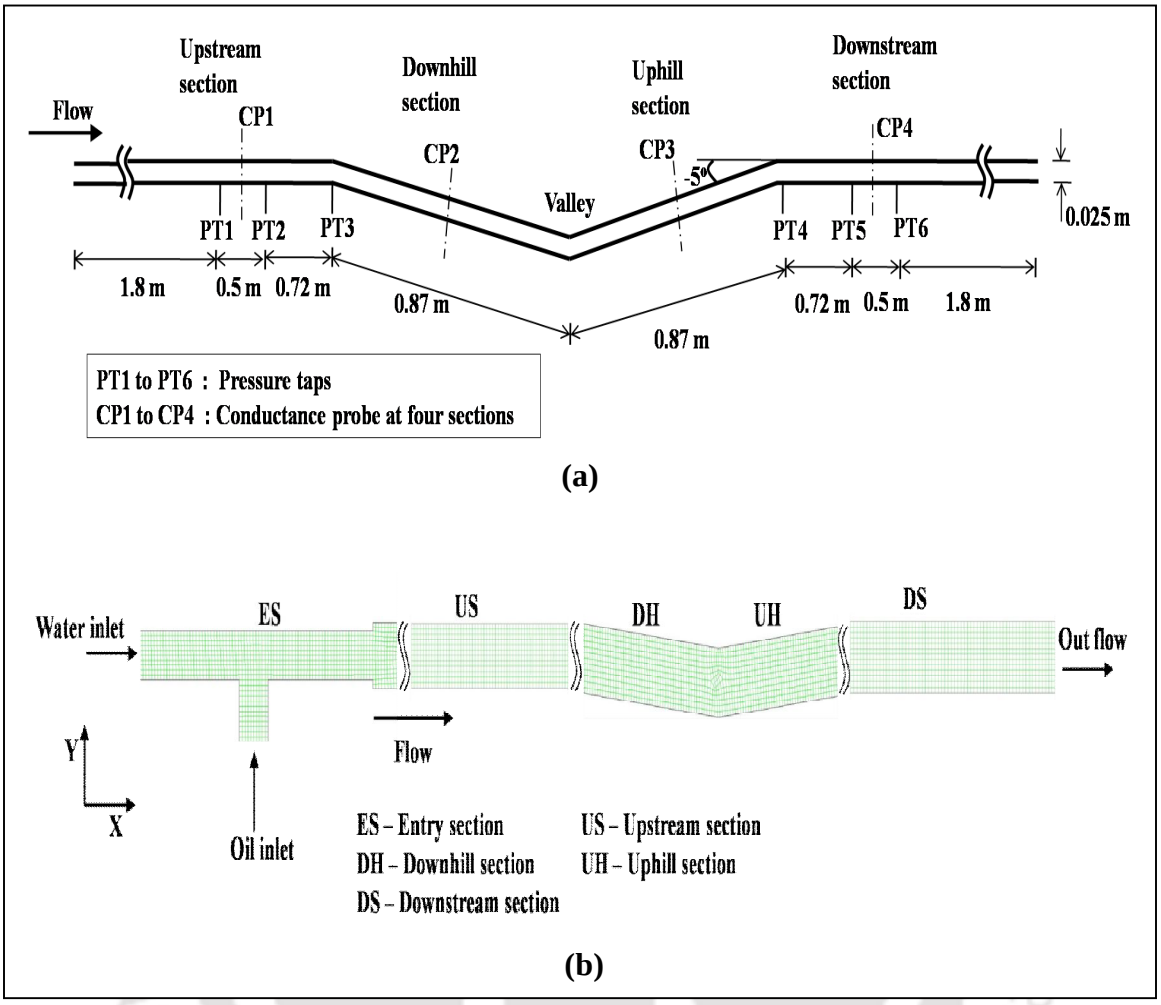

Fig. 6.2. Undulated pipeline in valley configuration; (**a)** Detailed dimensions of model; **(b)** Meshing of the model

6.4 Results and Discussion

In this work, flow patterns from experiment and CFD simulation (using VOF) are discussed. Subsequently, flow pattern maps at four test sections highlighting effect of undulation on flow patterns are also discussed. The simulated results are validated by comparing predicted volume fraction value with those obtained from experiment. The

experimental flow pattern maps are compared with the literature data to understand the effect of viscosity and undulation on flow behaviour.

6.4.1 Observed flow patterns

Seven different flow patterns are observed during oil-water flow through an undulated pipeline in valley configuration as shown in Figs. 6.3 to 6.8. Those are plug flow (P; Fig. 6.3a), slug flow (S; Fig. 6.4a), stratified wavy flow (SW; Fig. 6.5a), stratified mixed flow (SM; Fig. 6.6a), annular flow (A; Fig. 6.7a), dispersion of oil in water ($D_{O/W}$; Fig. 6.8a) and dispersion of water in oil ($D_{W/O}$; Fig. 6.8b). The results do not show a significant influence of this small undulation (undulation is ±5°, see Fig. 6.2a for detail dimension of the set up) on the flow patterns at different sections. The same flow patterns are also observed in our simulation using VOF method at the same flow conditions except two dispersions (oil in water and water in oil). In this study plug (Fig. 6.3b), slug (Fig. 6.4b), stratified wavy (Fig. 6.5b), stratified mixed (Fig. 6.6b) and annular (Fig. 6.7b) flow patterns have been successfully simulated. The other flow patterns (viz., dispersion of oil in water and water in oil) observed at higher phase velocities are difficult to predict by using VOF method. This is due to the limitation of VOF method. The interface reconstruction scheme of VOF model fails to capture the oil-water interface properly at higher velocities (Ghosh et al. 2010). Therefore, the dispersed flow patterns observed at higher phase velocities are not simulated in this study. Axial development of the flow patterns at four different sections (upstream, uphill, downhill, and downstream) are briefly described below.

- ***Plug flow (P):*** This flow pattern is observed at lower velocities of both oil (U_{SO} = 0.013 m/s) and water velocities (U_{SW} = 0.197m/s). The small discrete oil droplets are observed in continuous water phase. Due to the bouncy effect, they are floating up and flowing through the upper side of the pipe. These are known as plug flow (P) and appear at all four sections of the undulated pipe. Experimental and simulated images of this flow pattern captured at U_{SW} = 0.197 m/s and U_{SO} = 0.013 m/s are shown in Fig. 6.3(a) and (b) respectively as a representative results. The figure shows the variation in plug concentration (number of plug) along the length. It is slightly more at valley and less at up and down stream due to the effect gravity. Water moves faster than the oil at downhill section. Hence, oil plugs are accumulated and its population is increased at this section.

- ***Slug flow (S):*** On increasing the oil velocity (U_{SO} = 0.02 m/s) keeping water velocity (U_{SW} = 0.197 m/s) constant, oil plugs become larger in size and flow pattern termed as slug flow. A representative experimental and simulated result is shown in Fig. 6.4a and Fig. 6.4b respectively. Nose of the slug changes section to section of the undulated pipeline due to the effect of gravity. The diameter and length of an oil slug grows continuously by gradual increase in oil velocity and slug flow is transformed into a stratified flow.

- ***Stratified wavy flow (SW):*** In this flow pattern, oil and water are flowing as two separate layers with a clear wavy oil/water interface. Oil flows on top of the water layer as shown in Fig. 6.5a and b. The figure shows a good agreement of simulation (Fig. 6.5b) with experiment (Fig. 6.5a). Nature of the waves formed at the interface is affected by the velocity of both the phases, fluid properties, pipe geometry and orientation

(inclination). Wave amplitude increases at downhill section after crossing the upstream section and diminishes at uphill section. This is because of change in angle of inclination from horizontal to valley section. Amplitude of the waves increase at all section with increasing the oil velocity.

- ***Stratified mixed flow (SM):*** Further increasing of oil velocity, wave becomes unstable as drag force overcomes the interfacial tension and results a number of droplets at the at the oil/water interface. The phenomena leads to form a "three layers" at interface which comprises of a continuous oil layer (on the top), a continuous water layer (at the bottom) and a layer of oil droplets in continuous water medium (in between continuous oil and water layer). This flow pattern is termed as three layer or stratified mixed flow pattern as shown in Fig. 6.6a (an experimental image at U_{SO} = 0.132 m/s and U_{SW} = 0.3 m/s). Simulated result of this flow pattern at the same velocity is reported in Fig. 6.6b. The droplet concentration at the interface is less at upstream section and is more at other three sections. Downhill section enhances the instability at the interface and creates more number of droplets there and effect of downhill persists till upstream section as short length of uphill section in the present work.

- ***Annular flow (A):*** This flow pattern is identified using conductance probe and is noticed at moderate velocities of both the phases. The detailed description of the conductance probe is discussed in chapter 2. In this configuration, oil flows at the center of the tube as a continuous core and the water flows as an annulus between oil core and pipe inner wall. Here, a thin water layer wets inside upper wall of the pipe as observed in its actual image (at U_{SW} = 0.4 m/s and U_{SO} = 0.4 m/s) shown in Fig. 6.7a. Same

observation is also noticed by simulation as shown in Fig. 6.7b. Sometimes, wave crest at oil-water interface may touch inner pipe wall at top periodically. In this situation the flow is not perfect annular and it is known as wispy annular flow**.** Identification of such thin water layer by imaging technique is difficult. So probe technique is used to identify the annular flow and its transition boundary accurately. This flow pattern is very much important from the energy saving point of view because it gives minimum fractional pressure drop as pipe wall completely wetted by water only. Interfacial tension and buoyancy opposes this flow while inertia and viscous force stabilize the flow. So it is least stable in case of horizontal flow and observed at moderate velocities.

- ***Dispersion of oil in water flow ($D_{O/W}$):*** This flow pattern is observed at high water velocities (U_{SW} = 0.6 m/s) and in a wide range of oil velocity (U_{SO} = 0.12 m/s to 0.65 m/s). In this case, oil droplets are dispersed in continuous water medium. At low velocity of oil, the dispersed oil phase occupies the upper portion of the pipe cross section as shown in Fig. 6.8a**.** Effect of valley on flow pattern is less at this velocity range because inertia dominates over the gravity.

- ***Dispersion of water in oil flow ($D_{W/O}$):*** This flow pattern is observed when water velocity is high (U_{SW} = 0.59 m/s to 1.12 m/s). Here water forms droplets and gets dispersed in continuous oil phase. The photograph of this flow pattern is shown in Fig. 6.8b. Amount of water dispersed in oil increases with increasing the water velocity.

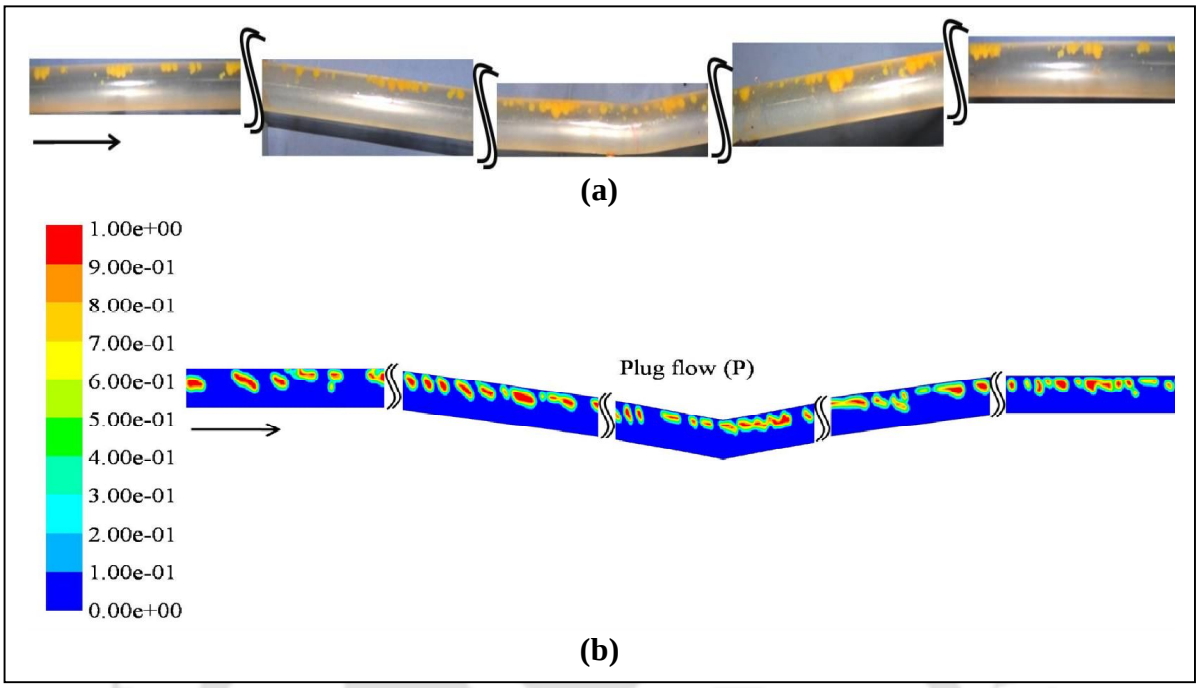

Fig. 6.3. Plug flow (P) at U_{SW} = 0.197 m/s, U_{SO} = 0.013 m/s**; (a)** Experimental image; **(b)** Simulated result

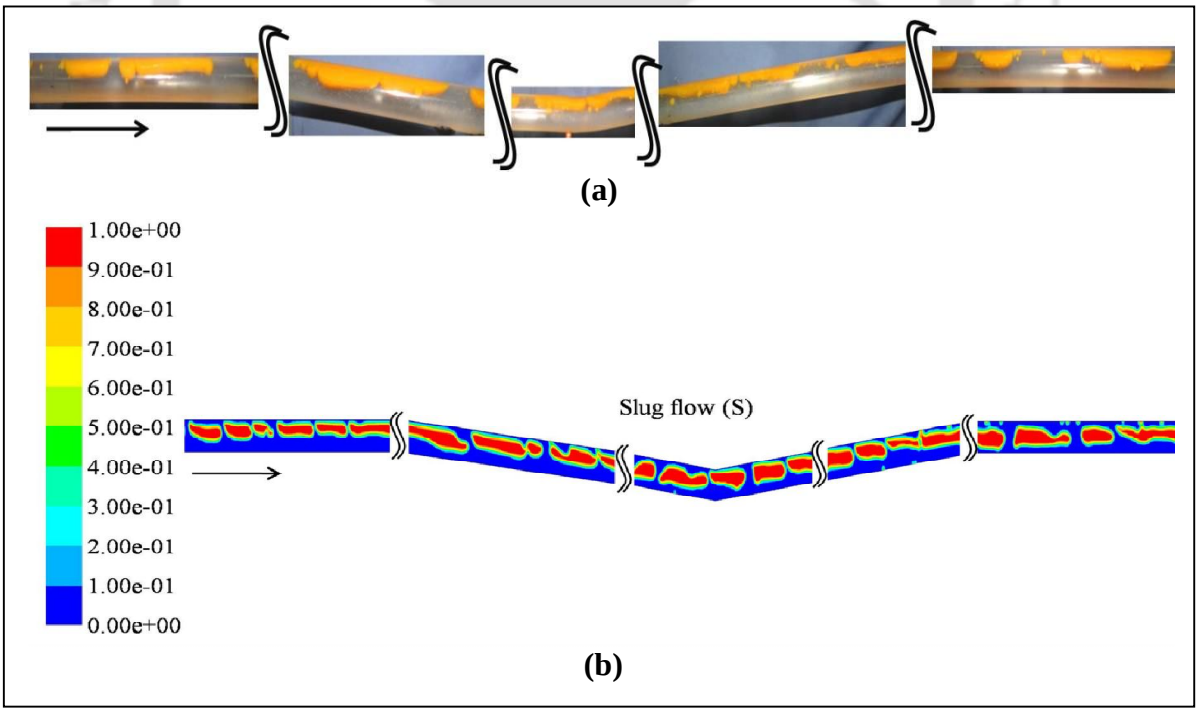

Fig. 6.4. Slug flow (S) at U_{SW} = 0.197 m/s, U_{SO} = 0.02 m/s**; (a)** Experimental image; **(b)** Simulated result

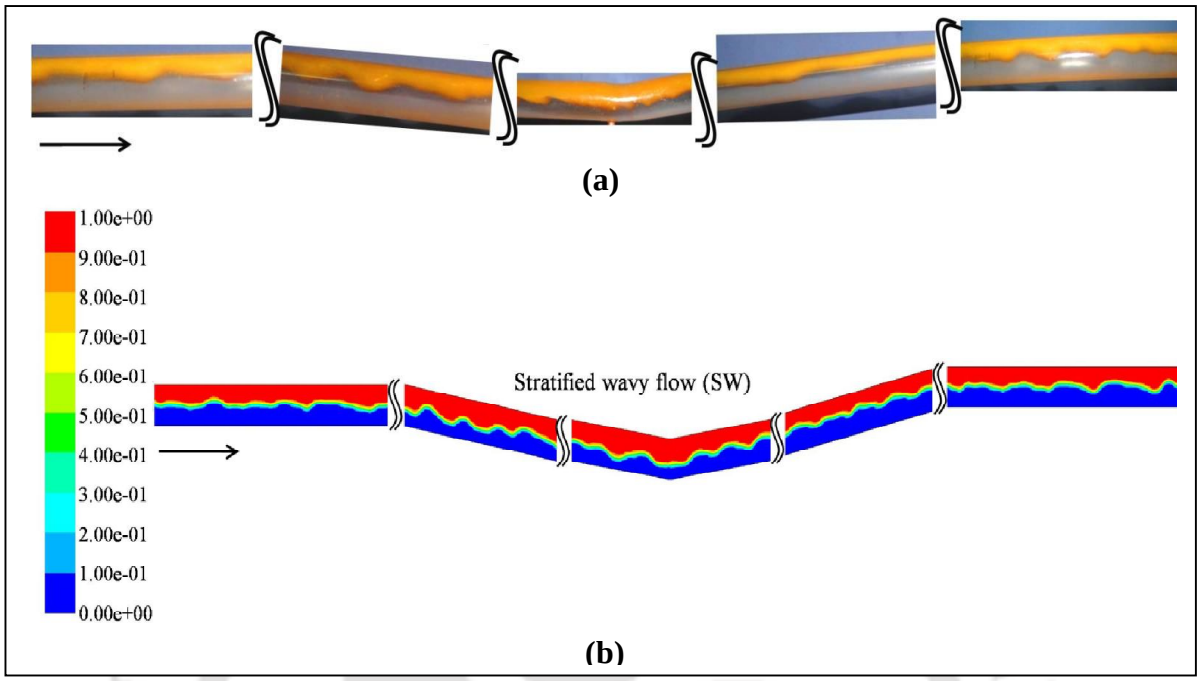

Fig. 6.5. Stratified wavy flow (SW) at U_{SW} = 0.164 m/s, U_{SO} = 0.07 m/s**; (a)** Experimental image; **(b)** Simulated result

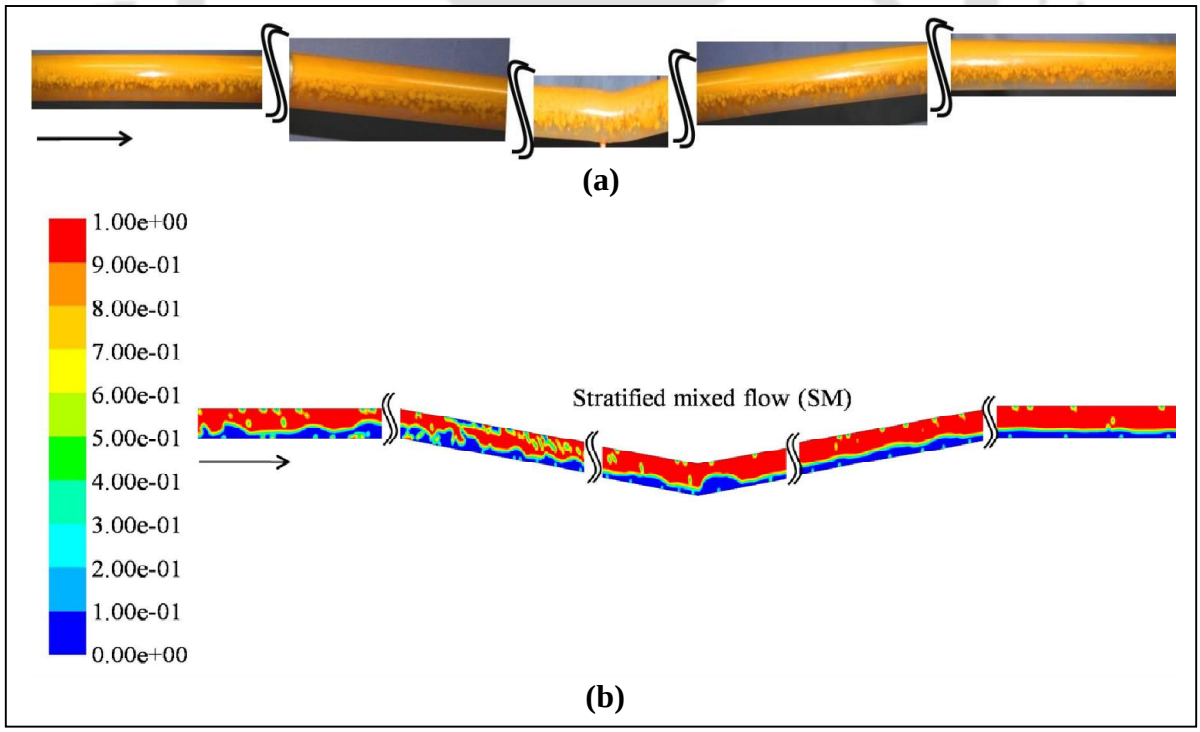

Fig. 6.6. Stratified mixed flow (SM) at U_{SW} = 0.132 m/s, U_{SO} = 0.3 m/s**; (a)** Experimental image; **(b)** Simulated result

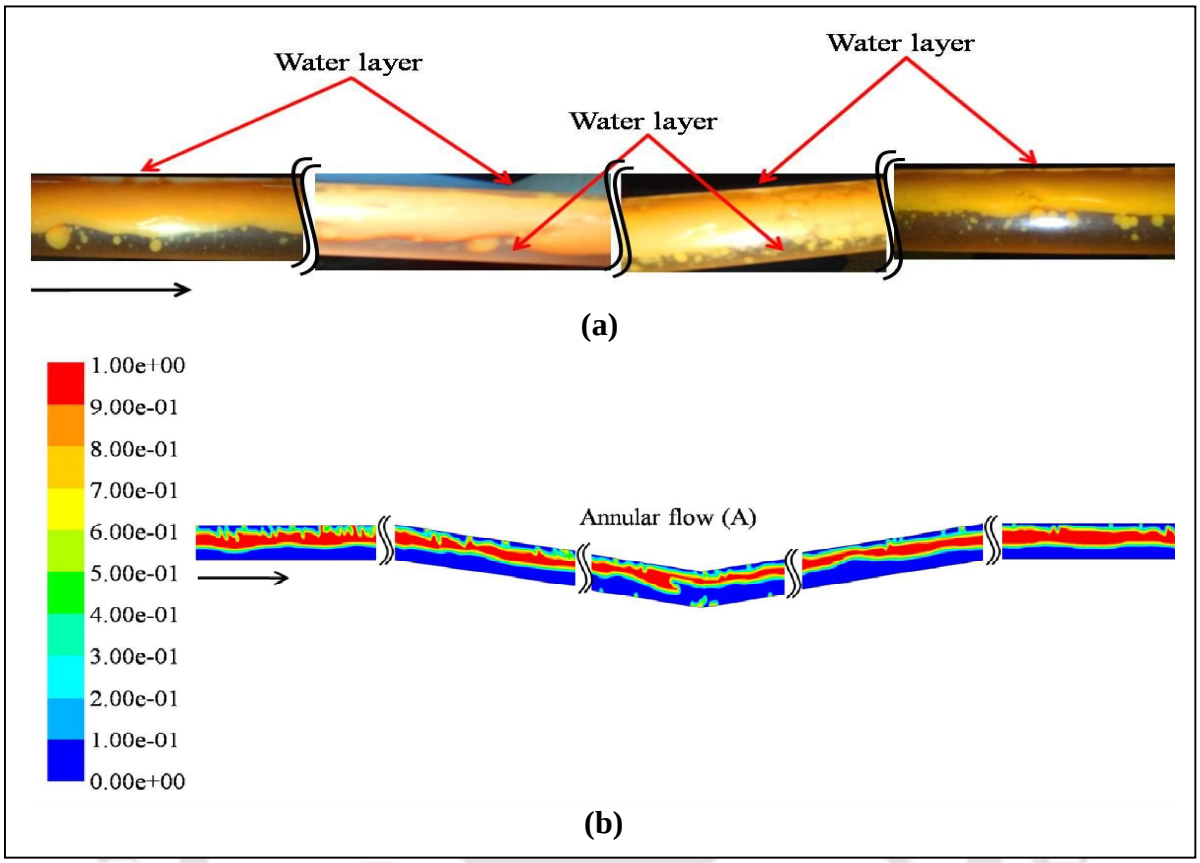

Fig. 6.7. Annular flow (A) at U_{SW} = 0. 4 m/s, U_{SO} = 0.4 m/s**; (a)** Experimental image; **(b)** Simulated result

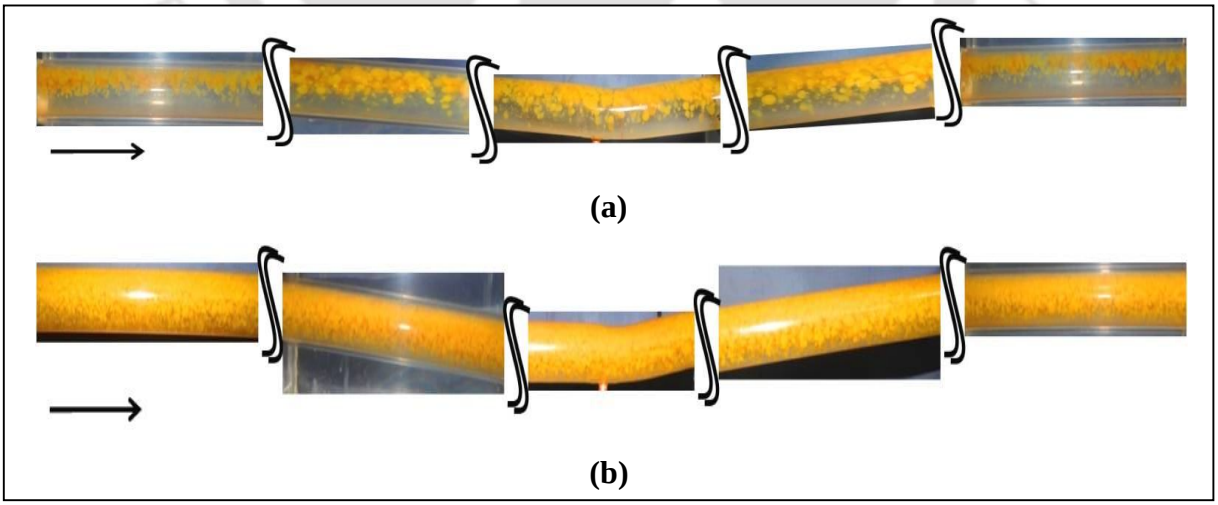

Fig. 6.8. Dispersed flow; **(a)** Dispersion of oil in water flow ($D_{O/W}$) at U_{SW} = 0. 7 m/s, U_{SO} = 0.21 m/s**; (b)** Dispersion of water in oil flow ($D_{W/O}$) at U_{SO} = 0.84m/s, U_{SW} = 0.40 m/s.

6.4.2 Flow pattern maps at different sections (US, DH, UH, DS) and a comparison among them

The flow patterns observed at four sections(US, UH, DH and DS) during aforementioned experiments are summarized in a graphical form using the superficial velocities of oil (U_{SO}) and water (U_{SW}) as coordinate axes, which is known as flow pattern map. For a better understanding, four flow pattern maps for four different sections are superimposed on each other in Fig. 6.9.

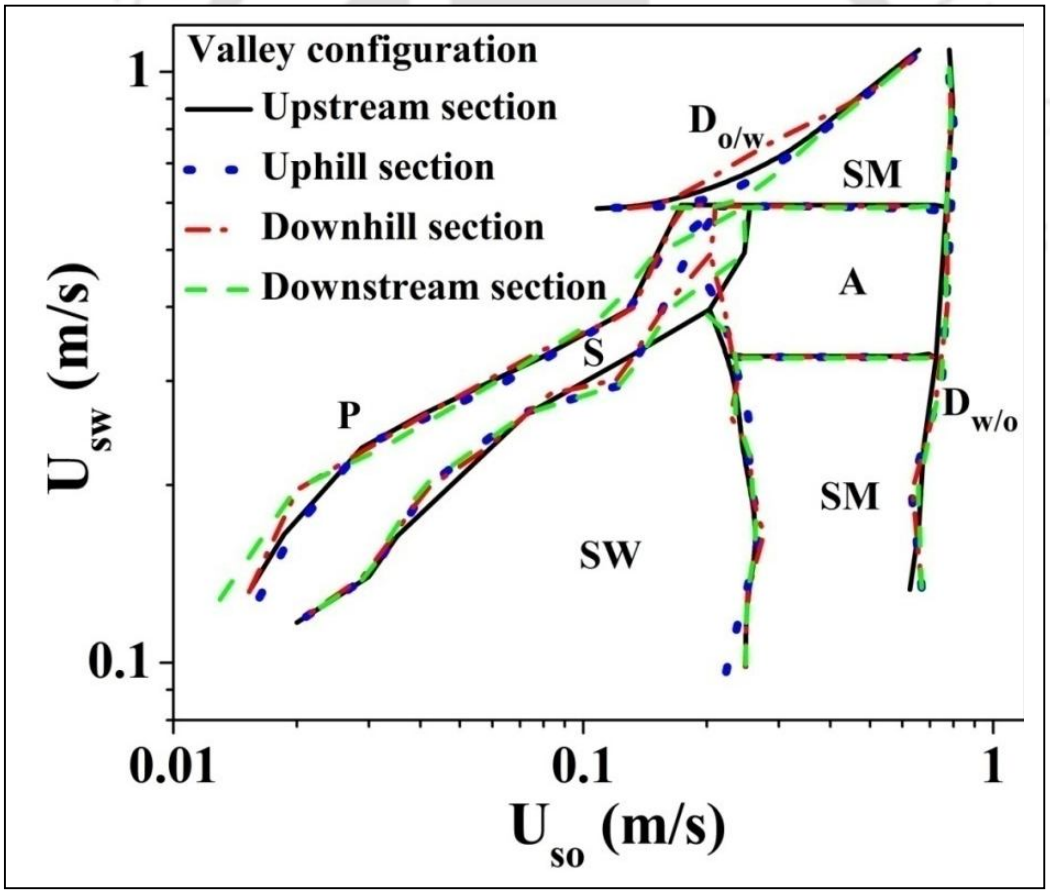

Fig. 6.9. Comparison of flow pattern maps observed at upstream, uphill, downhill and downstream sections of valley configuration

In the Fig. 6.9, solid black color line shows the transitions at upstream section, dotted blue color line shows the transitions at uphill section, red color dash dot line shows the transitions at downhill section and green color dashed line shows the transitions observed at downstream section. The salient features of the observations are described below.

- The transition boundaries of P to S, S to SW, SW to SM, SM to A and SM to $D_{W/O}$ are almost identical at all the four sections.
- A small variation is observed in the transition of slug to annular flow at downhill and uphill sections. At higher water velocities, slug flow occupies a larger area in upstream and downstream section as compared to the other sections (downhill and uphill). Downhill elbow accelerates the velocity at downhill section of valley configuration, which favors the coalescence of the consecutive slugs to form a continuous oil stream at center of the pipe. This phenomena leads to early transition of slug to annular flow at downhill and uphill section by overcoming the surface force and buoyancy force. Hence, the region of slug in the flow pattern map decreases as compared to upstream and downstream section.
- Similar deviations are also observed for the transition boundaries of $D_{O/W}$ to SM at uphill and downstream sections. This transition boundary is observed at higher oil velocity at these two sections.

From the above discussion, it appears that the influence of such small undulation on flow patterns is reasonably small.

6.4.3 Validation of simulated results

In order to validate the simulation, the results are compared with the experimental data of the present work. For this, oil volume fraction of plug, slug, stratified wavy, stratified mixed and annular flow has been simulated across the peak section and compared with the experimental result as shown in Fig. 6.10. Area average volume fraction of oil is calculated from simulation and considered as equivalent to the experimental volume fraction. The figure shows a good agreement between simulation and experiments with an average absolute error of 19.3%. Subsequently, experimental flow patterns are also validated by superimposing the simulated points on flow pattern map as shown in Fig. 6.11. Scattered data points represent simulated data while solid lines indicate the experimental transition boundaries observed at upstream section of valley configuration. Circled data points represent mismatching of simulated data in the flow pattern map. The results shown in Fig. 6.11 depict a good matching between the simulated and the experimental flow pattern except few.

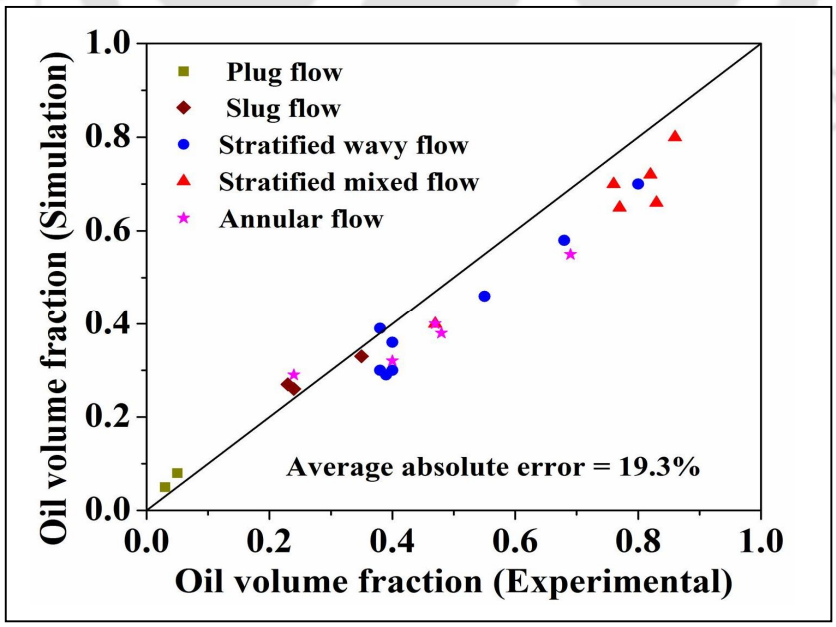

Fig. 6.10. Validation of oil volume fraction across the peak section

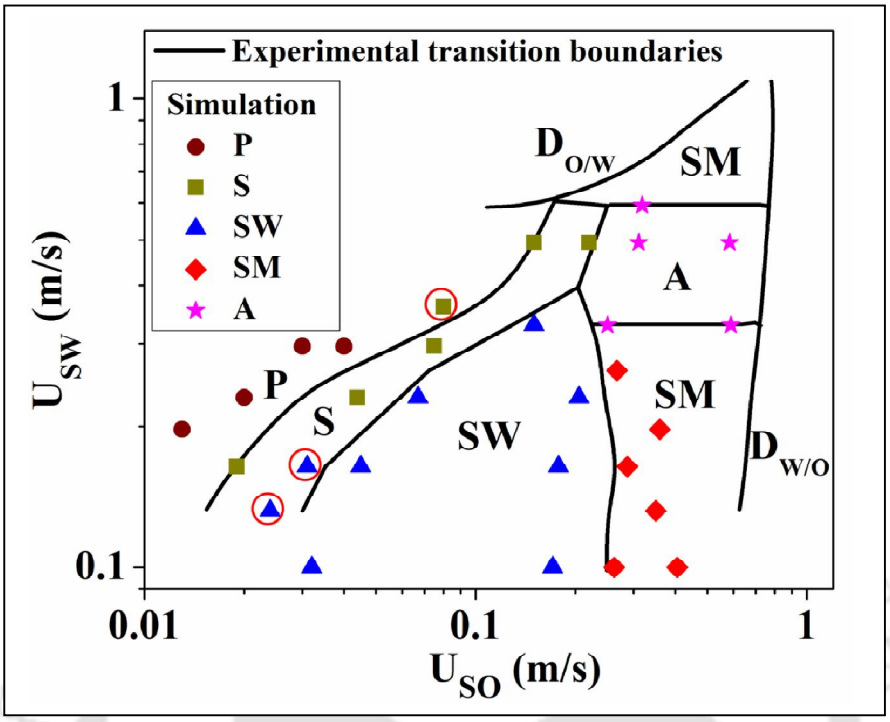

Fig. 6.11. Comparison of simulation results with experimental flow pattern map of present work (P - Plug flow, S - Slug flow, SW - Stratified wavy flow, SM - Stratified mixed flow, A - Annular flow, $D_{w/o}$ - Dispersion of water in oil flow, $D_{o/w}$ - Dispersion of oil in water flow)

6.5 Comparison with horizontal flow pattern map

To extract the effect of undulation on flow patterns, downstream section flow pattern map is compared with the horizontal flow pattern map. The comparison is shown in Fig. 6.12. Solid lines in Fig. 6.12 indicate the transition boundaries at downstream section of the valley configuration and different legends in the Fig. 6.12 represent different flow patterns observed in horizontal pipeline. Numerical numbers from 1 to 8 as shown in Fig. 6.12 represent the following different transition boundaries of horizontal flow pattern map:

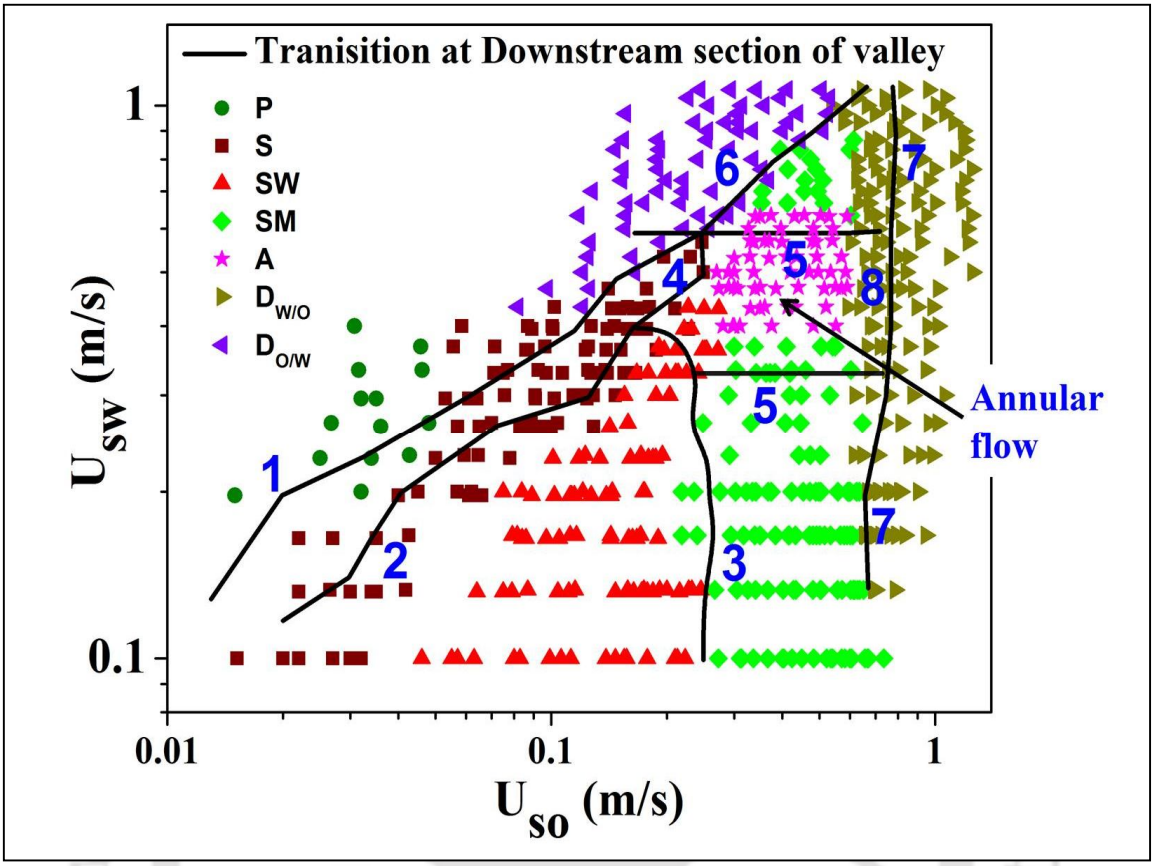

Fig. 6.12. Comparison of downstream flow pattern map of valley configuration with horizontal flow pattern map. (P - Plug flow, S - Slug flow, SW - Stratified wavy flow, SM - Stratified mixed flow, A - Annular flow, $D_{w/o}$ - Dispersion of water in oil flow, $D_{o/w}$ - Dispersion of oil in water flow)

1. Line 1 represents the transition boundary of plug to slug flow.
2. Line 2 represents the transition boundary of slug to stratified wavy flow.
3. Line 3 represents the transition boundary of stratified wavy to stratified mixed flow.
4. Line 4 represents the transition boundary of slug to annular flow.
5. Line 5 represents the transition boundary of stratified mixed to annular flow.
6. Line 6 represents the transition boundary of oil dispersed in water to stratified mixed flow.

7. Line 7 represents the transition boundary of stratified mixed to water dispersed in oil flow.
8. Line 8 represents the transition boundary of wispy annular to water dispersed in oil flow.

Fig. 6.12 shows that transition boundaries of downstream section slightly deviate from the horizontal flow pattern map. The transition of S to SW in undulated pipeline (no. 2) is shifted to lower oil velocities (≈0.02 m/s) than the horizontal one (0.044 m/s). As a result, the area under stratified wavy flow (SW) is increased in the present work. This deviation is due to the presence of uphill elbow in valley configuration, which enhances coalescing of oil slugs to form stratified wavy flow after this elbow. Transition of stratified wavy to stratified mixed (3) and is almost identical with horizontal flow pattern map. But stratified mixed to dispersion of water in oil transition (7) is shifted to a little bit higher oil velocity. It is due to the retarding effect of uphill elbow on fluid velocity as dispersed flow is an inertia dominated flow. As a whole stratified mixed region has acquired more area in the present flow pattern map. In downstream flow pattern map, annular flow is also observed in the range of U_{SW} = 0.33 to 0.6 m/s and U_{SO} =0.24 to 0.7 m/s. This velocity range is also in accord with the range reported in literature (Grassi et al. 2008; Poesio et al. 2012).

6.6 Comparison with literature

To understand the effect of viscosity on flow patterns, the experimental results of downstream flow pattern are compared with Mandal's (2007) work, where oil viscosity

is almost 90 times lower than the present work. The pipe geometry and operating conditions are same in both the works. The comparison is shown in Fig. 6.13. Scattered points in Fig. 6.13 depict the present experimental results of downstream section and solid lines represent the different flow patterns transition boundaries reported by Mandal (2007). To avoid the complexity in nomenclature of different flow patterns, dispersion of oil-in-water and water ($D_{O/W\ \&\ W}$) and three layer (TL) flow of Mandal (2007) are considered as dispersion of oil in water ($D_{O/W}$) and stratified mixed flow (SM) respectively in the present work.

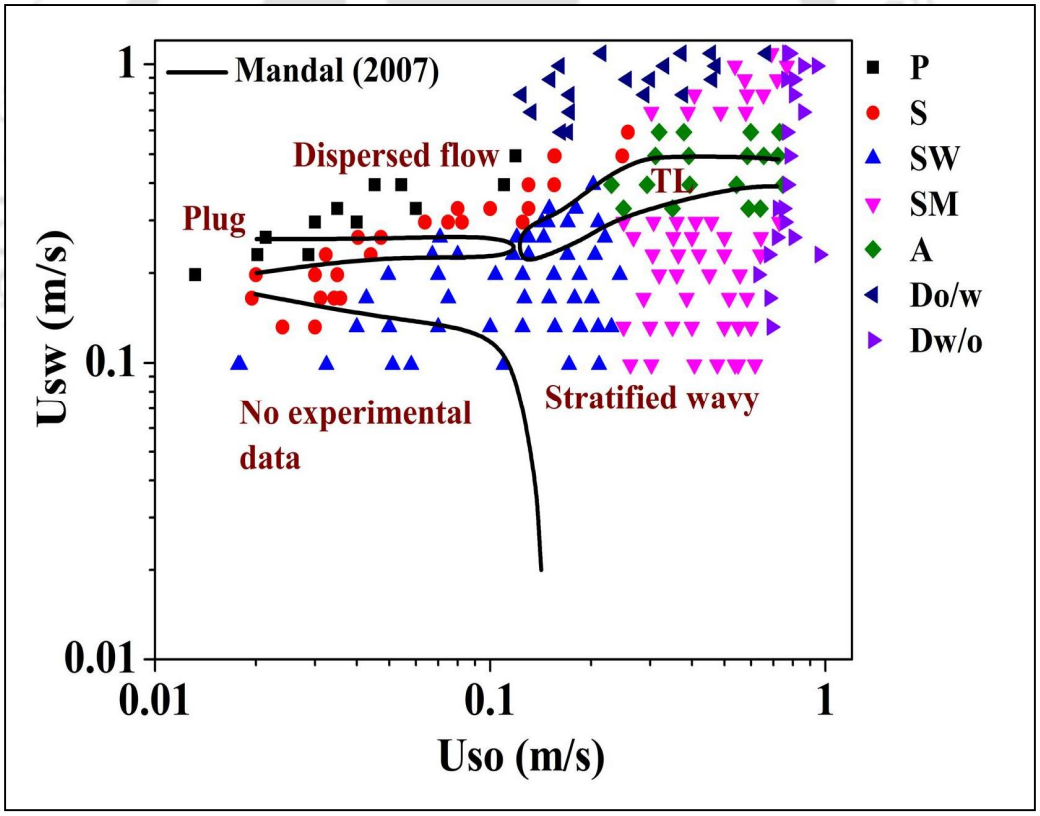

Fig. 6.13. Comparison of downstream flow pattern map of valley configuration (present work) with Mandals' (2007) flow pattern map. (P - Plug flow, S - Slug flow, SW - Stratified wavy flow, SM - Stratified mixed flow, A - Annular flow, $D_{w/o}$ - Dispersion of water in oil flow, $D_{o/w}$ - Dispersion of oil in water flow)

Usually, low viscous oils do not prefer slug, plug and annular flow (Abduvayt et al. 2006; Trallero et al. 1997; Russel et al. 1959). In the present work, slug and annular flow patterns (in valley) are observed and those are absent in less viscous oil and water flow (Mandal (2007)). The velocity span of stratified wavy flow reduces in the present work as compared to Mandal's (2007) as their oil viscosity is less. Similar observations are also noticed by comparing the present work with horizontal literature data (Al-wahaibi et al. 2011; Rodriguez et al. 2006; Raj et al. 2005). It indicates that the high viscous oil marginally reduces the velocity span of SW flow pattern as compared to low viscous oil. Similarly, higher viscosity fluids favor SM flow pattern as is evident from our experimental results and also from the literature (Wang et al. 2011; Bannwart et al. 2004) and annular flow (Sharma et al. 2011; Balakhrisna et al. 2010; Grassi et al. 2008). Comparison of upstream flow pattern map of Mandal (2007) and present work (at other sections) shows quite similar differences as discussed above, except minor deviation in velocity ranges for different flow patterns.

6.7 Conclusion

In the present study, flow patterns of viscous oil-water two-phase flow through undulated pipeline in valley configuration are successfully identified by visual, imagining and probe technique. Seven different flow patterns (viz., plug flow, slug flow, stratified wavy flow, stratified mixed flow, annular flow, dispersion of oil in water flow and dispersion of water in oil flow) have been observed at all the four sections. These flow patterns of all four sections are presented in the form of flow pattern maps and compared with each other. Comparison across the sections shows that small undulation (5°) has a marginal effect on the flow behavior of viscous oil-water mixture. VOF method successfully simulates plug, slug, stratified wavy, stratified mixed and annular flow except dispersion of both oil and water. Oil volume fraction validation showed 16.2% error between experimentation and simulation. Good agreement is observed when simulated data of flow patterns superimposed on experimental flow pattern map of the present study. Our observed flow pattern maps are compared with the literature to show the effect of undulation and effect of viscosity on flow patterns. The understanding on the effect of undulation on the hydrodynamics of two–phase flow would be helpful in industrial design such as, pipe network for oil transportation.

References

Abduvayt, P.,Manabe, R., Watanabe, T.,Arihara, N., 2006.Analysis of oil/water-flow tests in horizontal, hilly terrain, and vertical pipes. SPE Prod. Oper., SPE 90096, 123–133.

Al-Wahaibi, T.,Angeli, P., 2011. Experimental study on interfacial waves in stratified horizontal oil–water flow. Int. J. Multiphase flow 37, 930–940.

Balakhrisna, T.,Ghosh, S., Das, G., Das, P. K., 2010. Oil–water flows through sudden contraction and expansion in a horizontal pipe-phase distribution and pressure drop. Int. J. Multiphase flow 36, 13–24.

Bannawart, A. C., Rodriguez, O, M. H.,Carvalho, C. H. M. de, Wang, I. S.,Vara, R. M. O., 2004. Flow patterns in heavy crude oil-water flow. ASME 126, 184−189.

Fluent 6.3 User's Guide. Fluent Inc., Lebanon, USA, 2006.

Ghosh, S., Das, G., Das, P. K., 2010. Simulation of core annular downflow through CFD–A comprehensive study.Chem. Eng. Process. 49, 1222–1228.

Grassi, B.,Strazza, D.,Poesio, P., 2008.Experimental validation of theoretical models in two-phase high-viscosity ratio liquid-liquid flows in horizontal and slightly inclined pipes. Int. J. Multiphase Flow 34, 950–965.

Mandal, T. K., 2007. Some studies on Liquid–liquid slug flow. Ph.D. Thesis, IIT Kharagpur, India.

Poesio, P., Strazza, D. and Sotgia, G., "Two and three-phase mixtures of highly-viscous-oil/water/air in a 50 mm i.d. pipe," Appl. Therm. Eng. **49**, 41 – 47 (2012).

Raj, T. S., Chakrabarti, D. P., Das, G., 2005. Liquid-liquid stratified flow through horizontal conduits. Chem. Eng. Technol. 28, 899−907.

Rodriguez, O. M. H., Oliemans, R. V. A., 2006. Experimental study on oil-water flow in horizontal and slightly inclined pipes. Int. J. Multiphase flow. 32, 323–343.

Russell, T. W. F., Hodgson, G. W., Govier, G. W., 1959. Horizontal pipeline flow of mixtures of oil and water. Can. J. Chem. Eng. 37, 9–17.

Sharma, M., Ravi, P.,Ghosh, S., Das, G., Das, P. K., 2011. Hydrodynamics of lube oil–water flow through 180^{o} return bends. Chem. Eng. Sci. 66, 4468−4476.

Trallero, J. L.,Sarica, C., Brill, J. P., 1997. A study of oil/water flow patterns in pipes. SPE Prod. Fac., SPE 36609, 165−172.

Wang, W., Gong, J.,Angeli, P., 2011.Investigation on heavy crude-water two phase flow and related flow characteristics. Int. J. Multiphase flow37, 1156–1164.

Chapter 7

Conclusions and Future recommendations

In the present study, experiments have been conducted to study the hydrodynamics of liquid-liquid two-phase flow through an undulated pipe line (both in peak and valley configuration) by using lube oil and water as test fluids. Due to the complexity in understanding the physics of the oil-water in any pipe network, a simple horizontal geometry is chosen and studied the hydrodynamics prior to the investigation of viscous oil-water flow through undulated pipelines. All flow patterns except wispy annular flow are identified by visual and imaging technique while conductivity probe technique is used to detect the wispy annular configuration. Seven different flow patterns (viz., plug flow, slug flow, stratified wavy flow, stratified mixed flow, wispy annular flow, dispersion of oil in water flow and dispersion of water in oil flow) have been observed at all the four sections (Upstream, uphill, downhill and downstream). These flow patterns of all four sections are presented in the form of flow pattern maps and compared among them. Comparison across the sections shows that small undulation (5°) has a marginal effect on the flow behavior of viscous oil-water mixture.

Computational fluid dynamics study has also been conducted to predict different flow patterns of viscous oil-water two-phase flow through the undulated pipe. For this purpose, first simulation is carried out for a simple horizontal pipeline and validated with the experimental results. Then it is adopted for undulated pipeline. Based on the grid independent study 47037 (horizontal), 45682 (peak configuration), 50117 (valley configuration) numbers of cells are selected as optimum number of cells for simulation. Using VOF (volume of fluid) method with k-ε turbulence model, intermittent flow (viz., plug, slug) along with other separated flow patterns (viz., stratified wavy, stratified mixed

and wispy annular flow), and their transition boundaries are simulated successfully. Simulation results show a good agreement with experimental results in predicting of volume fraction, flow patterns and transition boundaries. Annular flow and its region is also simulated (not all the boundaries related to the wispy annular flow) with an appreciable accuracy. VOF also predicts the volume fraction, pressure and velocity profile of the separated flow. The present findings also reveal the ability of VOF to predict the hydrodynamics of viscous oil-water two-phase flow.

7.1 Conclusion

The key findings from the study are listed below:

i. Seven different flow patterns (viz., plug flow, slug flow, stratified wavy flow, stratified mixed flow, wispy annular flow, dispersion of oil in water flow and dispersion of water in oil flow) are identified during oil-water flow through undulated and horizontal pipeline.

ii. All the flow patterns have been observed in all four sections of an undulated pipeline (both peak and valley). However, the ranges of fluid velocities for a particular flow pattern differ from section to section.

iii. A conductivity probe has successfully been designed and developed for identifying the wispy annular flow in both the pipes (undulated and horizontal).

iv. The section wise flow pattern maps are developed and compared among them and also with literature data for understanding the effect of undulation and viscosity on hydrodynamics.

v. Comparison shows that small undulation (5°) has a marginal effect on the flow behavior of viscous oil-water mixture and higher viscosity favors wispy annular, slug and dispersed (water in oil) flow pattern.

vi. Comparison also shows that, high viscous oils marginally reduce the span of velocity ranges for SW flow pattern and favors stratified mixed flow pattern as compared to low viscous oils.

vii. The velocity span of wispy annular flow obtained in the present study is comparable with the reported literature data.

viii. Computational fluid dynamics study has been conducted to predict different flow patterns (intermittent and separated flow) and its transition, radial profile of oil volume fraction, total pressure and mixture velocity of viscous oil-water two-phase flow through a horizontal and undulated pipeline.

ix. Simulation result matches well with experimental results in prediction of area average volume fraction, flow patterns and respective transition boundaries.

x. Annular flow and its region are simulated with an appreciable accuracy.

7.2 Recommendations for future work

Based on the present study of hydrodynamics in an undulated pipeline, the following investigations are recommended for future study.

i. The work shown in the present study is confined to one type of pipe network. The work can be extended to study the hydrodynamics of oil-water in different pipe networks such as, road crossing, divergence network, etc.

ii. In the present work, only one single undulation (peak and valley) is used to study the effect of the undulation on flow patterns. It is recommended that, increase of undulations (viz., more number of undulated segments along the flow path) would give more disturbance/change to the observed flow patterns, which is more challenging for engineers to model such flow.

iii. The work can be extended for higher angle undulations using same liquid pair.

iv. To account for the effect of viscosity on flow patterns, the work can be extended to higher viscous oils.

v. Experiments for different diameters of pipe are recommended to account for the effect of various forces on flow patterns.

vi. The work can be extended for different pipe materials to understand the effect of wettability on flow patterns.

vii. An attempt is needed to develop a generalized pressure drop correlation for undulated system.

viii. Numerical simulation of dispersed flow patterns and pressure drop in pipe networks.

ix. The work can be extended to develop a correlation of interfacial height for stratified flows from experimentation and CFD simulation.

Outcome of the dissertation

List of publications

International Journals

1. **Anand B Desamala**, Anjali Dasari, Vinayak Vijayan, Bharat K Goshika, Ashok K Dasmahapatra and Tapas K Mandal. "CFD simulation and validation of flow pattern transition boundaries during moderately viscous oil-water two-phase flow through horizontal pipeline". *International Journal of Chemical, Nuclear, Metallurgical and Materials Engineering* 7 (2013), 72-77.
2. Anjali Dasari, **Anand B. Desamala**, Ashok Kumar Dasmahapatra and Tapas K. Mandal. "Experimental studies and PNN prediction on flow pattern of viscous oil-water flow through circular horizontal pipe". *Industrial & Engineering Chemistry Research* 52 (2013), 7975-7985.
3. Anjali Dasari, **Anand B Desamala**, Ujjal K Ghosh, Ashok K Dasmahapatra and Tapas K Mandal. "Correlations for Prediction of Pressure Gradient of Liquid-Liquid Flow through a Circular Horizontal Pipe". *Journal of Fluids Engineering* 136 (2014), 071302.
4. **Anand B. Desamala**, Ashok Kumar Dasamahapatra and Tapas K. Mandal. "Oil-Water Two-Phase Flow Characteristics in Horizontal Pipeline – A Comprehensive CFD Study". *International Journal of Chemical, Nuclear, Metallurgical and Materials Engineering* 8 (2014), 333-337.
5. **Anand B Desamala**, Ashok Kumar Dasmahapatra, and Tapas K Mandal. "An Appraisal of viscous oil-water two-phase flow through an undulated pipeline in peak configuration". Experimental Thermal and Fluid Science. **(Rebuttal submitted)**
6. **Anand B Desamala**, Ashok Kumar Dasmahapatra, and Tapas K Mandal. "Flow pattern investigation of viscous oil-water flow through an undulated pipeline in valley configuration by experiment and CFD simulation". International Journal of Multiphase Flow. (**under review**)

7. **Anand B Desamala**, Vinayak Vijayan, Anjali Dasari, Ashok K. Dasmahapatra and Tapas K. Mandal. "CFD simulation of flow pattern transition in viscous oil-water flow through a horizontal pipeline". Journal of Hydrodynamics. **(Under review)**

Conferences

1. **Anand B. Desamala**, Ashok Kumar Dasamahapatra and Tapas K. Mandal. "Oil-Water Two-Phase Flow Characteristics in Horizontal Pipeline – A Comprehensive CFD Study". *8th CUTSE International Conference*, Curtin University, Miri Sarwak Malaysia, 03-04 December 2013.
2. Anjali Dasari, **Anand B. Desamala**, Ashok K. Dasmahapatra and Tapas K. Mandal. "Correlation based Pressure Drop Prediction of visous oil-water two-phase flow through Horizontal Pipeline". Published in the proceedings of *65th annual session of the Indian Institute of the Chemical Engineers*, 27 - 30 December' 2012, Jalandhar, India.
3. V. Vijayan, **A. B. Desamala**, A. K. Dasmahapatra and T. K. Mandal., "Effect of an uphill elbow on interfacial wave encountered during the simultaneous flow of a pair of immiscible liquids through an undulated pipeline in its peak configuration" Published in the proceedings of *65th annual session of the Indian Institute of the Chemical Engineers*, 27 - 30 December' 2012, Jalandhar, India.
4. D. Anjali, **A. B. Desamala**, T. K. Mandal and A. K. Dasmahapatra. "Flow pattern of viscous oil-water flow: prediction by probabilistic neural network (PNN) and validation with experimental data". Published in the proceedings of *64th annual session of the Indian Institute of the Chemical Engineers*, 26 - 29 December' 2011, Bangalore, India.